ARL 64-150

THE BEHAVIOR OF DYNAMIC ELECTRIC ARCS

R. L. PHILLIPS

DEPARTMENT OF AERONAUTICAL AND
ASTRONAUTICAL ENGINEERING
UNIVERSITY OF MICHIGAN

SEPTEMBER 1964

Contract AF 33(615)-1326
Project 7065
Task 7065-01

AEROSPACE RESEARCH LABORATORIES
OFFICE OF AEROSPACE RESEARCH
UNITED STATES AIR FORCE
WRIGHT-PATTERSON AIR FORCE BASE, OHIO

FOREWORD

This Interim Technical Documentary Report was prepared by the Aircraft Propulsion Laboratory, Department of Aeronautical and Astronautical Engineering, The University of Michigan, on contract AF 33(615)-1326 for the Aerospace Research Laboratories, Office of Aerospace Research, United States Air Force. The work reported herein was accomplished on Task 7065-01, "Fluid Dynamics Facilities Research" of Project 7065, "Aerospace Simulation Techniques Research" under the cognizance of Capt. Ralph Prete of the Fluid Dynamics Facilities Laboratory, ARL. At The University of Michigan the project supervisor was Prof. J. A. Nicholls. This report covers work done during the period 1 October 1963 to 15 July 1964.

ABSTRACT

The thermal structure of an AC arc has been studied both experimentally and analytically. In order to provide a reasonable description of the manner in which the dynamic arc behaves as a circuit element, it is first necessary to solve the partial-differential equation that describes the energy-transfer processes within the arc column. In the idealized situation, where the arc is characterized by strict cylindrical symmetry and the electrodes have little effect on the positive column, certain limiting closed-form solutions have been obtained from the appropriate boundary-value problem. In the general case, the problem has been solved on a digital computer. In all cases, a simplified relationship between the electrical conductivity and the plasma temperature was assumed. The theoretically derived waveforms for electric-field strength and current bear a close relationship to those found by experiment. The latter results were obtained from a cascade-tube arc such as that employed by Maecker for his DC work. The present device was excited by 60-cps AC power, and rms currents up to 30 A were employed. Nitrogen, and argon were the working gases.

TABLE OF CONTENTS

LIST OF FIGURES

LIST OF FIGURES (cont.)

LIST OF FIGURES (cont.)

NOMENCLATURE

B	slope of linear approximation to electrical conductivity
$\vec{C}_s$	diffusion velocity of s^{th} species
C_p	specific heat at constant pressure
$\vec{E}$	electric field strength vector
E	axial (z) component of electric field strength
$\overline{E}$	normalized field strength in cascade analysis
E_n	normalizing factor for Kummer functions
F	energy density integral
h	enthalpy of arc gas (Section 2)
h	cell size in finite difference scheme
I	dimensionless arc current, dimensional in Section 2
I_o, I_1, I_m	DC or maximum values of I
$\vec{j}$	current density vector
K	boundary velocity of step-modulated arc
k	cell size in finite difference scheme
$k_1 \ldots k_6$	reaction rate coefficients
L	circuit inductance
ℓ	arc column length

M	number of cells in finite difference scheme
(M)	concentration of catalytic third body
m_s	mass of s^{th} species
N	number of cells in finite difference scheme
$(N_2), (N)$	molecular and atomic concentrations of nitrogen
n_s	particle number density of s^{th} species
P	static pressure
$\overline{P}_{out}, \overline{P}_{in}$	dimensionless power loss and input to arc
$\mathbb{P}$	pressure tensor
Q_{el}	joule heat addition
Q_{rad}	radiative heat loss
$\vec{q}$	generalized heat flux vector
R	tube radius
r	radial coordinate variable
r_o	time dependent arc radius
S	heat flux potential
S_1	cut-off value of S in electrical conductivity approximation
S_2	heat flux potential at tube wall
s	independent variable used in Section 3 and Appendix B

NOMENCLATURE (cont.)

T	temperature; also dependent variable in separation of variables scheme
t	dimensional time
U	dimensionless heat flux potential
U_m, U_o	DC or maximum values of U
$\vec{V}$	ordered mass velocity
V	scalar velocity (Section 2) and dimensionless heat flux potential
$\overline{V}$	normalized arc voltage
V_L	dimensionless voltage drop due to inductance
V_a	dimensionless total arc voltage
V_m	maximum circuit voltage
W	average dimensionless power input
W_o	velocity parallel to arc in cascade analysis
$\dot{w}$	mass flow through cascade device
X	dependent variable in separation of variables scheme
x	dimensionless radius in fixed boundary domain
y	dimensionless radius in fixed boundary domain
z	dimensionless axial variable

NOMENCLATURE (cont.)

β	separation constant and first root of Bessel function of first kind and zero order
Γ_s	net production of s^{th} species per unit volume per unit time
γ	phase angle appearing in constant radius arc analysis; also dummy variable
Θ	time constant of arc tube system
κ	thermal conductivity
$\overline{\kappa}$	"total" thermal conductivity
Λ	integral defined in Section 3
λ	thermal diffusivity
μ	separation constant defined in Section 3
ξ	independent variable used in Section 3
ρ	mass density (Section 2) and dimensionless arc radius
ρ_i, ρ_o	initial values of dimensionless arc radius
ρ_{dc}	DC value of dimensionless arc radius
σ	electrical conductivity
τ	dimensionless time variable
φ_n	orthonormal eigenfunctions
ω	radian frequency of arc current variation
$\omega\Theta$	effective AC arc frequency

1. INTRODUCTION

In recent years the increasing technological importance of the electric arc has motivated a quest for a better understanding of its phenomena. In the past, studies of the arc have been in the domain of physicists and electrical engineers (see (1) and (2) and their bibliographies). The advent of the ballistic missile, however, created the need for high temperature laboratory simulation of the re-entry environment and the aeronautical engineer quickly turned to the electric arc as a means of obtaining high enthalpy gas flows. Today dozens of organizations operate some type of gas-stabilized arc heater for either materials studies, hypersonic simulation, basic chemistry studies, or for use as a space propulsive device. In most applications the aim is to pass a stream of cold gas through and around a stabilized arc discharge thereby heating the flow to extreme temperatures. An excellent summary of the state of the technology (as of 1961) for this type of device is given in (3). It is evident upon reading (3) and similar articles that the development of the arc heater type of device has relied almost exclusively upon trial and error procedures. The complex interaction between the arc temperature field and the flow field surrounding it has made analysis of the problem especially difficult.

The present work was initiated in an attempt to understand some of the fundamental processes which occur in an arc type of gas heater,

Manuscript released by the author July 1964 for publication as an ARL Technical Documentary Report.

specifically one that uses an alternating current power supply. In (4) and (5) the details of this device, as well as some analytical investigations of its behavior are discussed. Before introducing the problems peculiar to dynamic arcs, however, it is instructive to consider the work that has been done on DC electric arcs.

At the outset it should be mentioned that the theory of the arc as developed here entirely disregards any phenomena that are due to the presence of electrodes. As is customary in studies of this sort only the quasi-neutral arc column is considered and, for most situations, this part of the discharge determines the operational characteristics of the whole arc. If the material properties of the arc gas are known, it is a simple matter to write an energy balance for the cylindrical arc column. This is known historically as the Elenbaas-Heller equation. Uhlenbusch (6) presents a summary of the various approaches that have been used to solve this resulting equation. In general, the theory of the cylindrically symmetric arc is firmly established and compares well with experiment. Even in the more difficult case of the DC arc where gaseous convection is important, considerable work has been done. To include the effects of convection one devises the simplest possible arrangement consistent with reality.

Imagine, for this purpose, an arc which is confined to a tube with well cooled walls and along whose axis gas is forced to flow. This arrangement is no mere fiction conceived for mathematical simplicity but it is actually utilized very successfully in some types of arc heaters. Its geometry is shown in Fig. 1. Entrance effects are allowed but the tube extends to infinity in the positive direction. Several investigators have studied the problem of the approach to the asymptotic column. That is the case where energy is transported both radially and axially until a fully developed profile is attained. There, all axial derivatives disappear and the arc is identical to the cylindrically symmetric column described above. Hence all analyses of the tube arc problem must eventually merge into an asymptotic column solution, such as those discussed in (6).

Skifstad (7), John (8), and Stine and Watson (9) have formulated tube arc problems with varying degrees of sophistication with the latter work showing particularly good agreement with experiment, (10). In fact, the apparent success of the method of Stine and Watson (9) indicates that the important processes occurring within a tube arc do not depend so much upon the phenomena of fluid dynamics as those of heat conduction. It will be shown that under certain conditions this is true for the AC arc as well.

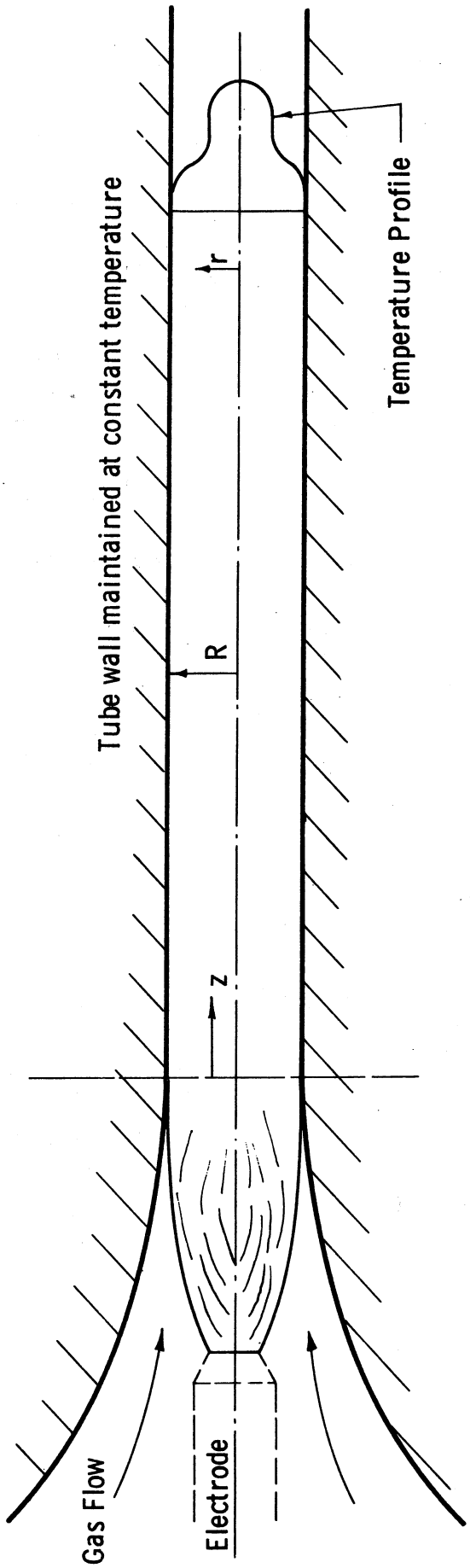

Figure 1. Coordinate System for the Tube Arc

The analytical description of the energy transfer processes in alternating current arcs is further complicated by the presence of the time variable. Most of the work on AC arcs has been done in connection with circuit breaker design, but nothing as comprehensive as that reported for DC arcs, (6)-(10), appears in the literature. There are no solutions at all for the problem of the approach to the asymptotic column and the cylindrically symmetric column has only been imperfectly examined. In short, the theory of the AC arc is not well established. Two noteworthy attempts at a theoretical treatment of the dynamic, cylindrical, positive column were reported about 25 years ago by Cassie (11) and Mayr (12). Both of these investigators formulated arc models where the radial variation of properties was not included or was integrated and not considered further. Cassie (11), for example, assumes an arc column within which the temperature is fixed and uniform in space and time, having constant per-unit-volume resistivity, power loss, and energy content. In order to obtain a variation in column conductance he invokes a variable arc radius. This leads to an ordinary differential equation with conductance as the dependent variable. Mayr (12), on the other hand, defines an "ersatz" arc gas whose transport properties exhibit a Gaussian dependence upon the radial variable. An integration over the arc

radius is then performed so that there remains only an ordinary differential equation for the arc conductance. If the assumption is made that the column energy loss per unit length is constant, it is possible to solve Mayr's equation for specified applied current or voltage variations. While the work of both Cassie and Mayr has had some limited usefulness for circuit breaker engineers, little insight into the detailed energy transfer processes which affect arc behavior has been gained.

From both theories there arises the notion of an arc time constant; that is, a typical time required for thermal re-adjustment. Because of the oversimplified nature of the Cassie and Mayr models, however, it is not possible to relate this time constant to any of the known conditions under which an arc is operating. In the present work it is shown how a theory can be developed which contains a time constant that is easily related to known conditions.

All subsequent attempts (see (13), (14), and (15)) to explain the nature of the dynamic arc are subject to the same objection put forth above; an integral approach is used to cast the inherently partial differential equations into a simple ordinary differential equation. The situation can be likened to a boundary layer theory based solely upon solutions of the Karman-Polhausen type with no knowledge of the exact profiles that exist.

In order to place the theory of the dynamic arc on a firmer footing the present investigation was initiated. A theory for the cylindrically symmetric dynamic arc has been formulated that considers the detailed structure of the column and that requires the solution of a set of non-linear partial differential equations. In two special cases, for a high frequency AC arc and for a DC arc which experiences a step function modulation in current, it was possible to obtain a closed form solution to the governing equations. In the general case, numerical solutions for the quasi-steady AC arc have been obtained with the aid of a digital computer. Only the AC arc that experiences thermal reignition was considered. Field intensified processes and glow discharge phenomena were not included. In all cases a simplified relationship between the electrical conductivity and the plasma temperature was assumed so that the dynamic behavior of an arc could be determined which is independent of any type of gas. Prior to this investigation no measurements had been made on AC arcs burning under well controlled conditions. The experimental results obtained by the writer from a specially constructed Maecker-like cascade arc show good agreement with the theoretically derived waveforms of electric field strength and current.

With the ability to predict the behavior of AC arcs burning under the conditions mentioned above, one can proceed to investigate questions of stability, circuit interaction, efficiency of energy transfer, etc.

2. THE FUNDAMENTAL EQUATIONS

2.1 The Conservation Equations

The equations needed to provide a description of the energy transfer processes within an electric arc, be it DC or AC excited, are the well established multi-component conservation equations. It is not intended to derive those equations here since they are exhaustively discussed in the literature (16), (17), and (18), and, except in cases where certain flux coupling terms may appear, there is no reason to doubt their applicability to the thermal arc. It is stipulated at the outset that no external magnetic fields will be applied to the region occupied by the arc column and, furthermore, the current carried by the arc will be small enough so that the self-magnetic field will be of no importance. Peters (19) has shown that an arc must carry several thousand amperes before the magnetic pressure induced thereby begins to be a significant fraction of the static pressure. This assumption is therefore not too limiting. A result of the above stipulations is that little new knowledge is gained from Maxwell's equations and that the conservation equations combined with a suitable form of Ohm's law suffice to describe the arc column properties completely. Furthermore, the effects of radiation, gas velocity, and finite reaction rates are included in the subsequent formulation only for the sake of temporary generality. In the analyses which follow, the neglect of radiation

and finite reaction rates are justified, while the effect of an ordered mass motion on the column properties is considered only for a highly idealized situation.

If one takes account of the foregoing remarks, the energy equation can be written as

$$\rho \frac{D}{Dt}\left(h + \frac{V^2}{2}\right) - \frac{\partial P}{\partial t} = -\nabla\cdot\vec{q} + Q_{el} - Q_{rad} \quad .$$

Here h is the weighted sum of the enthalpies of the constituent species, $\vec{q}$ is the generalized heat flux vector and Q_{el} and Q_{rad} are the joule heat and radiative loss terms, respectively. Of course, ρ is the overall density and D/Dt denotes the Eulerian derivative. The heat flux vector consists of an ordinary conduction term and several diffusion terms, most of which are quite negligible for the rather high pressures (one atmosphere and greater) being considered here. In fact, Cann (17), using the best available numbers for thermal and baro-diffusion coefficients, concludes that for many problems in arc physics these forms of energy transfer need not be considered. Thus the heat flux vector may be written as

$$\vec{q} = -\kappa\nabla T + \sum_s n_s m_s h_s \vec{C}_s$$

where κ is the ordinary thermal conductivity, $\vec{C}_s$ is the diffusion velocity peculiar to the s^{th} species (excluding baro-diffusion) and n_s, m_s, and h_s are the particle number density, mass, and specific enthalpy for a single component, respectively. An expression for the conservation of each species as well as the momentum equation is needed to complete the set of requisite equations. If Γ_s is the net change of species concentration per unit time, one finds

$$\frac{\partial n_s}{\partial t} + \nabla \cdot n_s (\vec{V} + \vec{C}_s) = \Gamma_s \quad .$$

While the consequences of a finite reaction rate (relaxation effects) would doubtless introduce some interesting effects into the present problem, the exclusion of such terms from the conservation equations will be justified. Since the present understanding of this "simplified" situation is far from complete, the inclusion of relaxation effects at this point would not be in order. Despite the fact that the momentum equation will be of little or no use in the ensuing discussion, it is included here for completeness:

$$\rho \frac{D\vec{V}}{Dt} = - \nabla \cdot \mathbb{P} \quad .$$

Here $\mathbb{P}$ is the usual pressure tensor which includes viscous as well as hydrostatic terms.

In addition to the conservation equations, a force-flux relationship generally known as Ohm's law (generalized or otherwise) is needed. In its most general form this equation includes a Hall effect term, an ion slip term, and a term accounting for electron inertia. In the present problem the simplest form of the expression will be employed; namely, that the current density is proportional to the electric field. The absence of a magnetic field obviates the need for the Hall and ion slip terms and electron inertia need be considered only if the frequency of the applied electric field is comparable to the so-called plasma frequency. This latter situation will never occur in the present study. Thus it is permissible to write simply

$$\vec{j} = \sigma \vec{E}$$

where the left member is the current density vector and is proportional to the electric field strength through the (scalar) transport property known as the electrical conductivity.

2.2 Equilibrium Times in a Thermal Plasma

It will be the purpose here to show that there is a range of external disturbance frequencies for which the usual assumptions of local thermodynamic equilibrium can be invoked in a study of the dynamic arc.

One could methodically evaluate the equilibrium assumption for a host of different gases but it will be sufficient to show that even for one gas the conditions can easily be met that validate the work to follow.

Nitrogen is chosen for an example, since for that gas the most is known about high temperature transport properties, reaction rate coefficients, and thermodynamic variables. In addition, much of the past work on arcs has been performed using nitrogen as the working fluid. In what follows, then, when it is necessary to relate the pertinent results to a specific gas, it will most often be nitrogen.

If one were to be completely precise in his investigation of the equilibrium times in a thermal plasma, he would begin by questioning whether or not there is sufficient time to locally establish a Maxwellian distribution for each species in the plasma (thereby permitting the assignment of a definite temperature to each component gas) and, furthermore, whether there is sufficient time for the species to interact so that a single temperature can be assigned to the mixture. In the arc plasma the electric field strengths are never very high (of the order of a few tens of volts per centimeter) so that there should be no tendency for the electron gas to be out of equilibrium with the atom-ion gas. This speculation is verified later.

In an alternating current arc the effect of the cyclical change in energy addition is felt first by the electrons through the alternating changes in imposed field strength. This change must in turn be transmitted to the more massive ion and neutral gases through elastic collisions between the species. Uhlenbusch (6), on the basis of a mean free path argument, estimates that the time required for the plasma to attain a unique temperature is given by

$$\tau_{eq} = M/n\nu qm \quad .$$

Here M is the mass of the constituent atoms (or ions), m is the electronic mass, n is the number density of the whole mixture, and ν and q are the electron collision frequency and Ramsauer cross section, respectively. For an atmospheric pressure plasma at about $10,000^{o}K$ the above expression yields a thermal equilibration time of the order of one microsecond.

At this point Uhlenbusch (6) and other writers have concluded that if external disturbances are applied with a frequency of less than about 10^5 cycles/second, one can legitimately assume that the gas is very nearly in thermodynamic equilibrium at all times. However, it seems that this conclusion cannot properly be reached without first considering the characteristic chemical times within a plasma. Most arcs do not operate in a state of full ionization (or even full dissociation in the

case of polyatomic gases) so that a change in the energy input to an arc will always result in a change in its chemical composition. Hence, some of the collisions between the electron gas and the heavy atom gas will be inelastic and the times required to establish local thermodynamic equilibrium can be longer than that predicted in (6).

For the reaction

$$\sum_{j}^{n} \nu_j' M_j \underset{\vec{k}_b}{\overset{k_f}{\rightleftharpoons}} \sum_{j}^{n} \nu_j'' M_j$$

Penner (20) and others show that the rates at which the various n participating quantities are created or destroyed are given by the following expression:

$$\Gamma_i = d(M_i)/dt = (\nu_i'' - \nu_i') k_f \prod_{j=1}^{n} (M_j)^{\nu_j'} + (\nu_i' - \nu_i'') k_b \prod_{j=1}^{n} (M_j)^{\nu_j''}$$

In the above (M_i) denotes the concentration of the i^{th} species, ν_i' and ν_i'' are the stoichiometric coefficients of the reactants and products, respectively, and k_f and k_b are the forward and backward reaction rate coefficients. For nitrogen, at temperatures up to $12,000^{o}K$ and a pressure of one atmosphere, the following reactions are the only ones of importance (21):

$$N_2 + M \underset{k_2}{\overset{k_1}{\rightleftharpoons}} N + N + M$$

$$N + N \underset{k_4}{\overset{k_3}{\rightleftharpoons}} N_2^+ + e$$

$$N + M \underset{k_6}{\overset{k_5}{\rightleftharpoons}} N^+ + e + M \quad .$$

Here e denotes the electron and M is some catalytic third body which acts as an energy carrier for the reaction. If the specific third body does not have too great an effect on the reaction rate coefficient, M may be considered to be any of the species in the mixture which exist at a given temperature level. For instance, at elevated temperatures there will be almost no molecular nitrogen so that for the last reaction listed above M could be atomic nitrogen, an ion, or an electron.

It is now possible to write a general expression for the time rate of change of concentration of each of the species listed above. This is not necessary, however, since the pertinent reactions are rather well compartmented as to temperature. That is, according to (21), only N_2 and N are present in any abundance if the pressure is one atmosphere or greater and the temperature is less than $6000^{\circ}K$. Hence, only the dissociation reaction is of any importance. For this, one can easily write

$$d(N_2)/dt = - k_1 (N_2)(M) + k_2 (N)^2(M)$$

$$d(N)/dt = 2k_1 (N_2)(M) - 2k_2 (N)^2(M)$$

Clearly the system presents some formidable mathematical difficulties and an exact solution would be quite hard to obtain. It will suffice, however, to gain only an order of magnitude knowledge about the slowest process in the above system of rate equations. The three body reactions will in general be the slowest so that an equilibration criterion can be conservatively based upon those processes.

According to Wray (22), the recombination of atomic nitrogen is slowest when the third body is N_2. Then for a small change in the concentration of N (and since it is assumed the recombination reaction dominates) one obtains from the general rate equations

$$d(N)/dt \cong - 2k_2 (N)^2(M) \quad .$$

Here k_2 corresponds to the nitrogen molecule and (M) is the total concentration. An approximate reaction time can be obtained by taking (M) to be approximately constant whereupon one finds

$$\tau_{ch} = \frac{1}{2k_2 (M)(N)_0} \left[\frac{(N)_0}{(N)_1} - 1 \right] \quad .$$

The bracketed expression represents a fractional change in (N) from the initial (equilibrium) value $(N)_0$. Using the numerical data from (21) with P = 1 atm., the reaction time, τ_{ch}, is found to be about 2×10^{-4} second for a 10% change in nitrogen atom concentration, when the initial temperature is $6000^{\circ}K$. These conditions are representative of the slowest reaction times in the arc column. Of course, the above approximation assumes a constant temperature process, but actually there must have been a slight decrease. The same analysis could be applied repeatedly until the final temperature in the cooling process were reached, but the characteristic time would probably still be of the order of a millisecond. At very low temperatures, however, the reaction rate would be quite slow, but the degree of dissociation would not be great enough to worry about.

A similar line of reasoning can be applied to the other reactions listed above and one concludes that an external disturbance frequency on the order of 1000 cps can easily be tolerated by a nitrogen arc without causing significant deviation from chemical equilibrium. In fact, the chemical time is easily seen to be the slowest equilibration time in the thermal plasma so that one can generally say that when it is small compared to disturbance times, local thermodynamic equilibrium prevails in the arc.

2.3 Energy Transfer by Radiation

It is quite simple to verify the assumption that for a wide range of conditions one can neglect the transport of energy by radiation compared to that carried by conduction and diffusion. One way to assess the importance of radiative transfer to the arc problem is to compute all of the relevant properties and then calculate the radiative flux which would result from this particular temperature distribution. The radiative properties of many gases are known well enough so that such a calculation can be carried out with confidence. If this computed radiation term is indeed small (as originally assumed), the correct temperature distribution is already in hand. Otherwise, one is confronted with a much more difficult problem.

In (23) it is shown that the radius of the arc plays a large role in determining when one may neglect radiative energy transport. This is understandable since the total radiated power depends upon a geometrical size and a larger arc radius implies a greater energy flux by radiation. Criteria can be developed by which one can be assured that radiation will not be of importance. This has been done in (23) and a summarizing figure therefrom is reproduced here as Fig. 2. The computation was made for nitrogen but similar results can be obtained for other gases. Maecker, in (24), shows that for argon, for

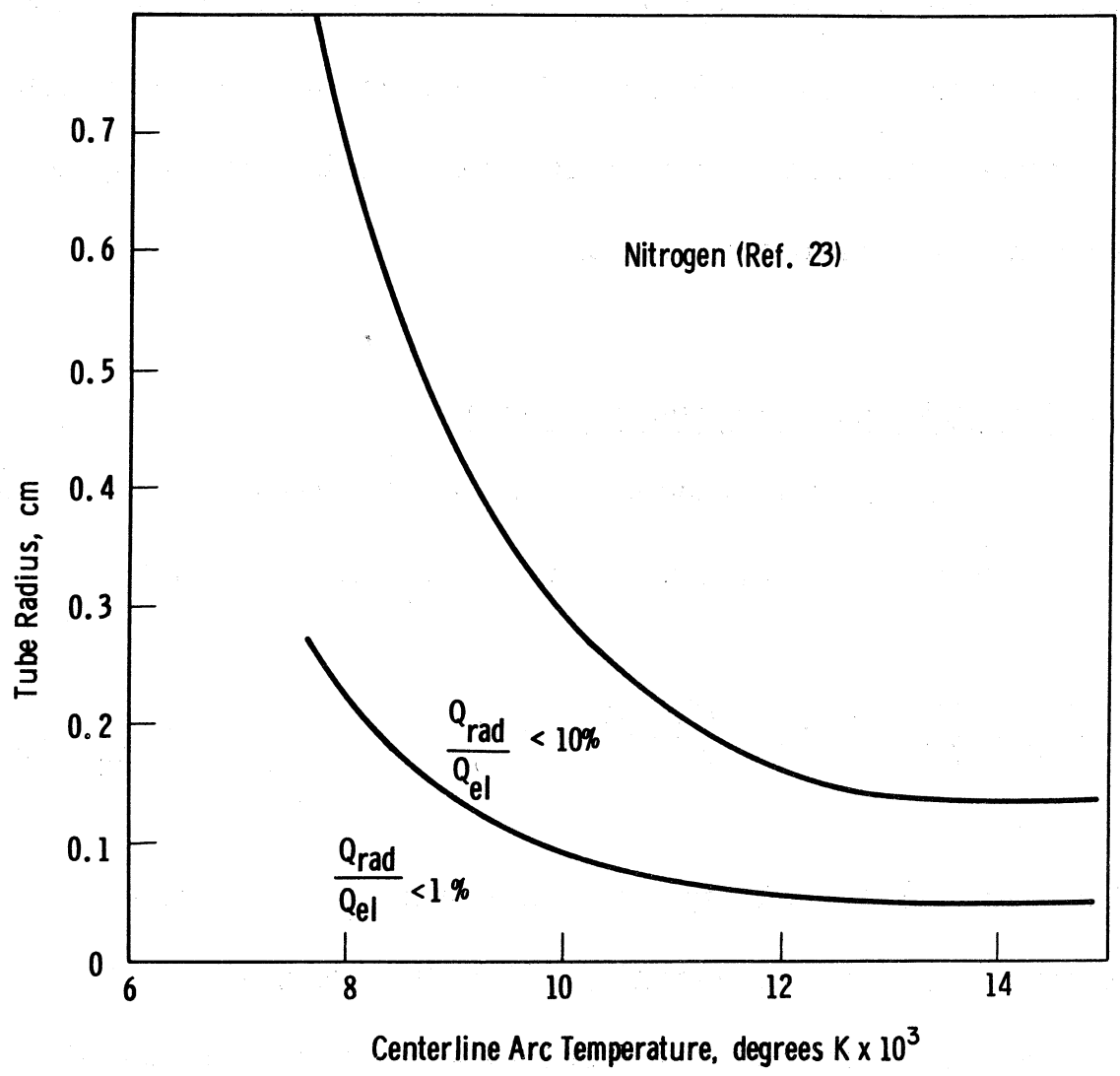

Figure 2. Map Showing Regions in the Tube Radius—Arc Temperature Plane Where Radiation is Negligible

example, the radiative energy transport is about 10% of the power input, even for a current of about 50 amps. The point is, that for a wide range of important conditions radiant energy transfer can be successfully neglected in an analysis of the arc column.

2.4 The Approach to the Asymptotic Column

If the simplifying assumptions which were discussed in the preceding paragraphs are incorporated in the energy equation, one obtains

$$\rho \frac{\partial}{\partial t}\left(h + \frac{V^2}{2}\right) + \rho\vec{V}\cdot\nabla\left(h + \frac{V^2}{2}\right) - \frac{\partial P}{\partial t} = -\nabla\cdot\left(-\kappa\nabla T + \sum_s n_s m_s h_s \vec{C}_s\right) + Q_{el} \quad .$$

The intent is to study the asymptotic arc column, or where there is no dependence upon the axial variable, z. Then the z components of the gradient operators in the above equation vanish and, since rotational symmetry is assumed, only derivatives with respect to the radial variable remain. Furthermore, the assertion that the change in the kinetic energy of the flow along the arc (no swirl or radial flow is assumed to exist) is trivial compared to the change in the static enthalpy of the arc gas is simple to justify. The arc gas typically has a temperature of the order of $10,000^{\circ}K$ whereas the flow velocity in the cascade device described previously is only a few feet per second everywhere. Hence

the Mach number of the flow is quite small. Furthermore, for large z, the convection term vanishes completely from the above equation since the axial derivative of the static enthalpy disappears in the asymptotic column.

It was mentioned earlier that no magnetic fields of any consequence are assumed to exist in the vicinity of the arc. Specifically, the currents are so low that self-magnetic fields can cause no noticeable pinching of the discharge. As is the case with most arcs, those presently being considered are presumed to operate in a constant pressure field, thereby allowing one to drop the $\partial P/\partial t$ term.

All of the above assumptions lead to the equations describing the time-varying asymptotic arc column. These are more fully developed in the following paragraphs.

2.5 The Working Equations

Having stated under what conditions the effects of radiation, convection, and chemical relaxation can be neglected, it is possible to specialize the energy equation and Ohm's law to strict cylindrical symmetry. From Faraday's law one can see that the electric field has only a z component. Since no magnetic field of consequence is present one can write

$$\nabla \times \vec{E} = 0 \quad ,$$

or, in cylindrical coordinates

$$\left(\frac{1}{r}\frac{\partial E_z}{\partial \theta} - \frac{\partial E_\theta}{\partial z}\right)\vec{e}_r + \left(\frac{\partial E_r}{\partial z} - \frac{\partial E_z}{\partial r}\right)\vec{e}_\theta + \left[\frac{1}{r}\frac{\partial}{\partial r}(rE_\theta) - \frac{1}{r}\frac{\partial E_r}{\partial \theta}\right]\vec{e}_z = 0 \quad .$$

Here $\vec{e}_r$, $\vec{e}_\theta$, and $\vec{e}_z$ are unit vectors in the respective coordinate directions. There is no θ-component of electric field and in the asymptotic column only derivatives with respect to r exist. Hence

$$\frac{\partial E_z}{\partial r} = 0$$

and the longitudinal electric field (denoted by E) is a function of time alone. The arc burns in a well cooled tube of radius R whose walls are maintained at a constant temperature, but which carries no current. This scheme is illustrated in Fig. 1. In line with other investigators the diffusive contribution to energy transfer is combined with the "frozen" thermal conductivity, κ, to give a total effective thermal conductivity, $\bar{\kappa}$. Dropping the pressure variation term from the energy equation (as discussed previously) one has

$$\sigma(T)[E(t)]^2 + \frac{1}{r}\frac{\partial}{\partial r}\left[r\left(\bar{\kappa}\frac{\partial T}{\partial r}\right)\right] = \rho(T)\frac{\partial h}{\partial t}$$

where $0 \leq r \leq R$, $T(R,t) = T_w$ and $t > 0$. In addition, Ohm's law becomes

$$E(t) \int_0^R 2\pi r\sigma(T)\, dr = I(t) \quad .$$

The energy equation has become simply a relation between the joule heat produced in the arc column, the energy transport by conduction, and the storage term, $\rho\partial h/\partial t$. The electric field strength is understood to have the spatially constant axial value mentioned above. In general, the transport properties σ and $\bar{\kappa}$ as well as the thermodynamic variables h and ρ depend upon both temperature and pressure. Here, however, there are no gradients in the pressure field so that only the temperature variations are of concern.

Finally, it should be mentioned that an equation describing an electric circuit should rightfully accompany the above set, but for the moment it is presumed that the arc burns in a current source, i. e., the arc impedance is small compared to the combined impedance of the rest of the circuit. It is only slightly more difficult to consider a circuit equation in conjunction with the column equations, but first there is much to be learned from the current source case. It is presumed, then, that the I(t) occurring in the Ohm's law expression has a simple cosine variation.

Unless one is willing to embark on a complete numerical program for the solution of these equations, it is necessary to make some simplifications. The temperature variation of the transport properties as well as the quadratic manner in which the electric field enters the problem introduce strong non-linearities. Some years ago Schmitz (25) introduced a transformation which has greatly simplified analytical investigations of arc problems. He defined the heat flux potential, S(T) by the relation

$$S(T) = \int_{T_{ref}}^{T} \bar{\kappa}\,(\alpha)\, d\alpha \quad .$$

Using S as the independent variable, instead of temperature, removes the troublesome thermal conductivity from the problem. However, one must be able to express all other thermodynamic and transport properties in terms of S since T is replaced everywhere by S as the dependent variable. The heat flux potential for nitrogen and argon is shown in Fig. 3. The pressure is one atmosphere and the data is due to Avco (26) and Marlotte (27).

There remains the problem of dealing with the electrical conductivity function. In Fig. 4 the electrical conductivity of nitrogen is shown as a function of S and it is seen that σ becomes non-zero quite

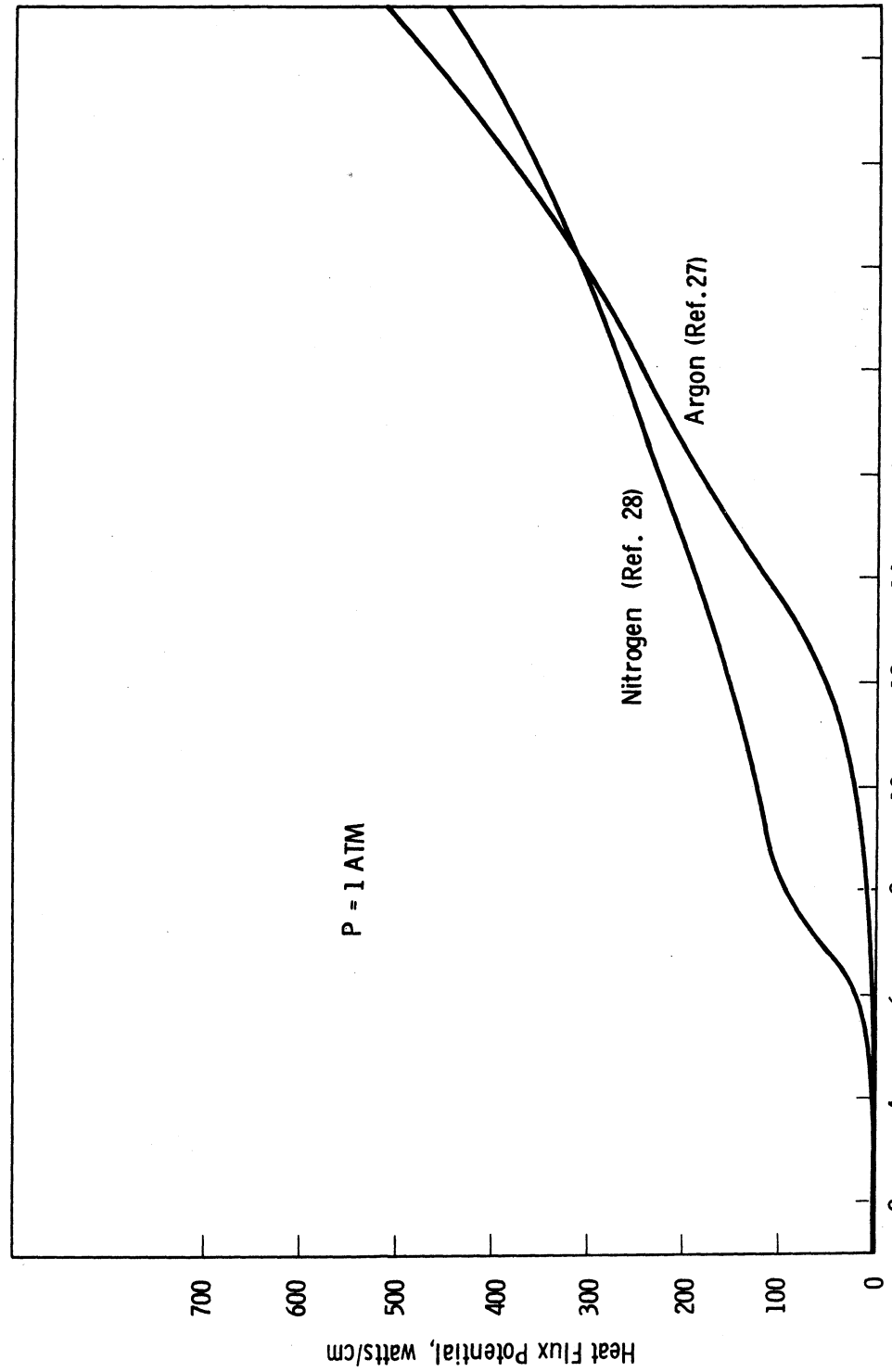

Figure 3. Temperature Dependence of Heat Flux Potential for Nitrogen and Argon

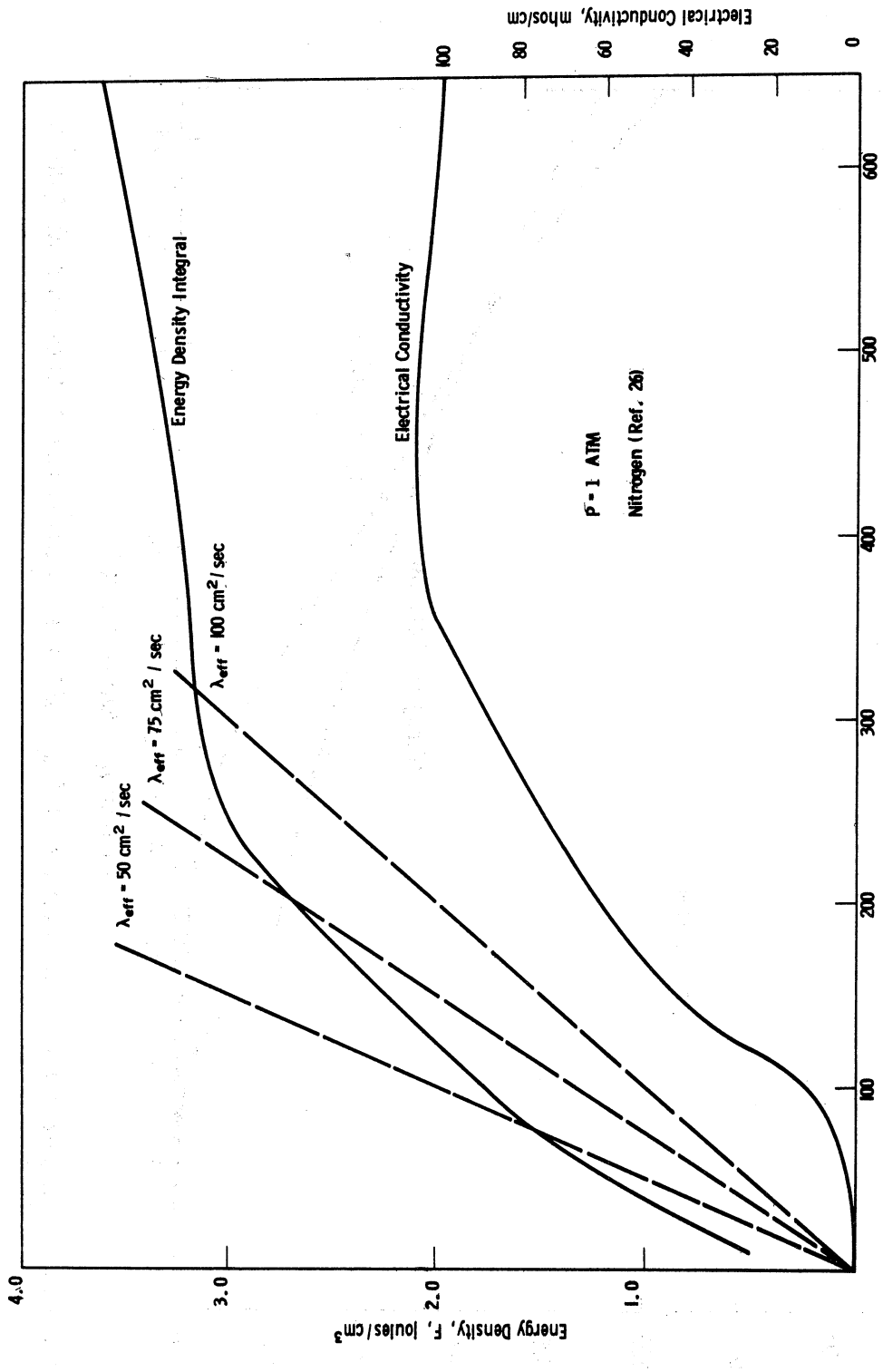

Figure 4. Electrical Conductivity and Energy Density Integral as a Function of Heat Flux Potential for Nitrogen

abruptly and rises sharply to rather large values. Looking for the simplest possible approximation to this behavior, while retaining its essential character, one turns again to the work of Schmitz (23). In his studies of direct current arcs Schmitz suggested that approximating the σ - S behavior by two straight lines might yield good results. In this scheme the electrical conductivity is assumed to be identically zero up to some cut-off value and then rise linearly with a best-fit slope to the highest value which occurs in the arc column. In this approximation S_1 is the heat flux potential when σ is "turned on" and B is the slope of the second straight line portion of the curve. Then

$$\sigma = 0 \quad , \quad S < S_1$$

$$\sigma = B\,(S - S_1) \quad , \quad S > S_1 \quad .$$

In what follows, this simple polygonal model will be employed for the electrical conductivity variation, in spite of one or two disadvantages which will be discussed later. Uhlenbusch (6) has described several analytical procedures which have been followed in the study of DC arcs and the interested reader can find there a good discussion of the various merits and demerits of these schemes. The straight line approximation has the particular advantage of allowing the governing equations to be fully non-dimensionlized so that they may be solved in general with no

reference to a particular gas. In addition, the sharp onset of electrical conductivity caused by this model introduces the notion of a conducting zone or arc radius, an extremely useful fiction. Most analytical models of electric arcs have required the knowledge of some sort of arc radius and here this position is automatically defined as the point where the local heat flux potential is equal to S_1, the cut-off value. It is to be noted, however, that the arc radius is a function of time for the AC arc. This fact introduces an interesting mathematical complication about which more will be said later.

Finally, in order that the proposed analysis not be tied to any specific gas with a unique set of thermodynamic and transport properties, it is necessary to modify the heat capacity term, $\rho\, \partial h/\partial t$. Toward this end it is convenient to introduce a new integral variable F, defined by the relation

$$dF = \rho dh = \rho\, C_p\, dT$$

or

$$F(T) = \int_{T_{ref}}^{T} \rho(\alpha)\, C_p(\alpha)\, d\alpha \quad .$$

This function can easily be computed for any T (and pressure) since high temperature thermodynamic properties are known with a reasonable degree of precision (28). Eventually, of course, this auxiliary function must be related to S, the chosen dependent variable. Since $\bar{\kappa}$, ρ, and C_p are all single valued functions of temperature, it is possible to prepare an F - S plot for any gas. The heat capacity term in the energy equation becomes

$$\rho(\partial h/\partial t) = F'(\partial S/\partial t) \quad ,$$

where F' is the local derivative with respect to S of the auxiliary function. Since $F' = \rho\, C_p/\bar{\kappa}$, the coefficient of the time derivative term is nothing more than the inverse of the instantaneous, temperature dependent, thermal diffusivity of the arc gas. Unlike most heat conduction problems this quantity is not strictly constant, but a glance at Figs. 4 and 5b indicates that for common gases like nitrogen and argon one can approximate their F - S behavior with one or two straight lines. In obtaining a linear fit to these curves one can weight his selection according to the average conditions which exist in a particular case.

A linear fit to the F - S curve implies that F' is a constant, which will be designated λ^{-1}. The energy equation can now be rewritten in the following simplified form:

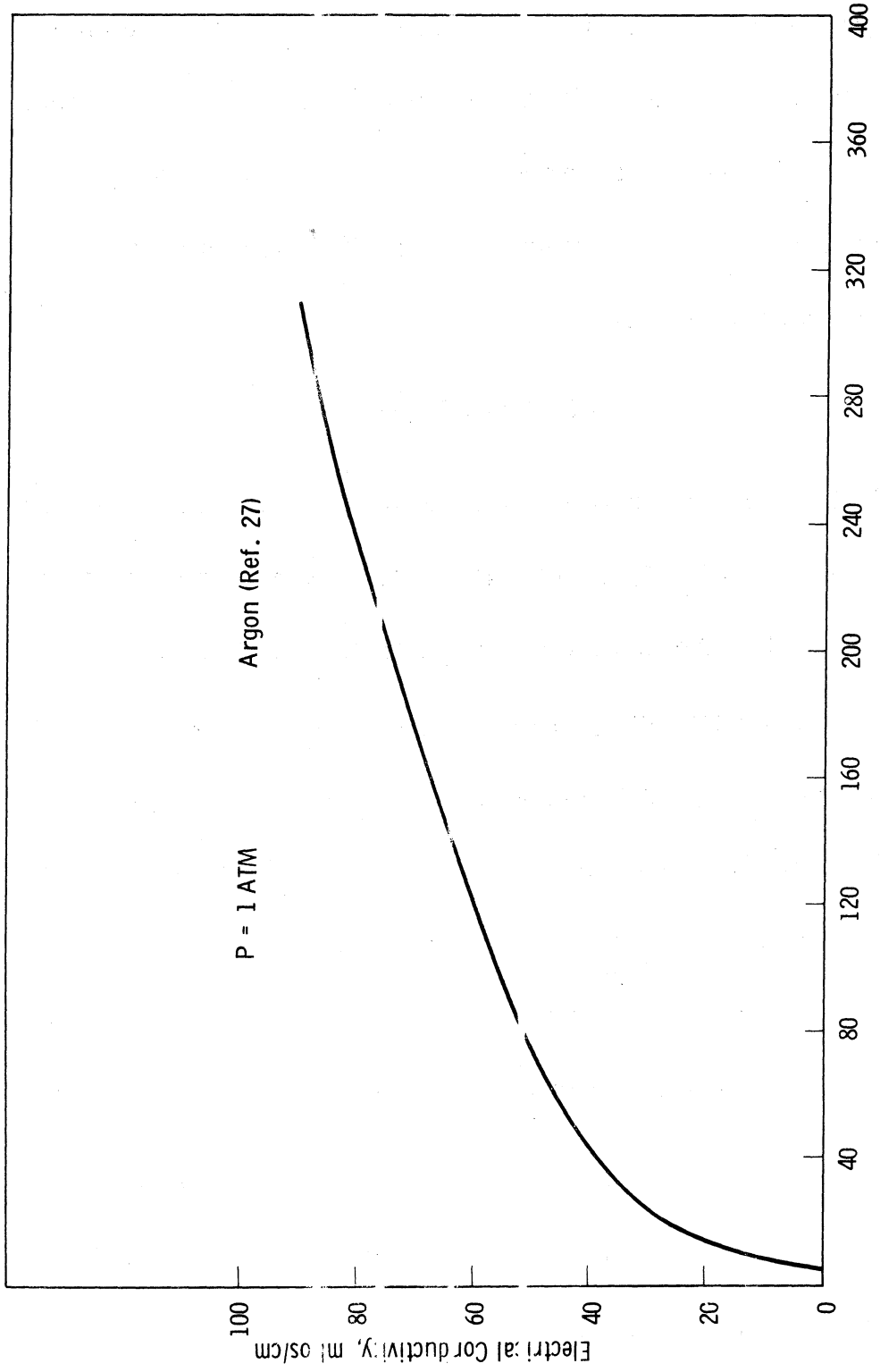

Figure 5a. Electrical Conductivity as a Function of Heat Flux Potential for Argon

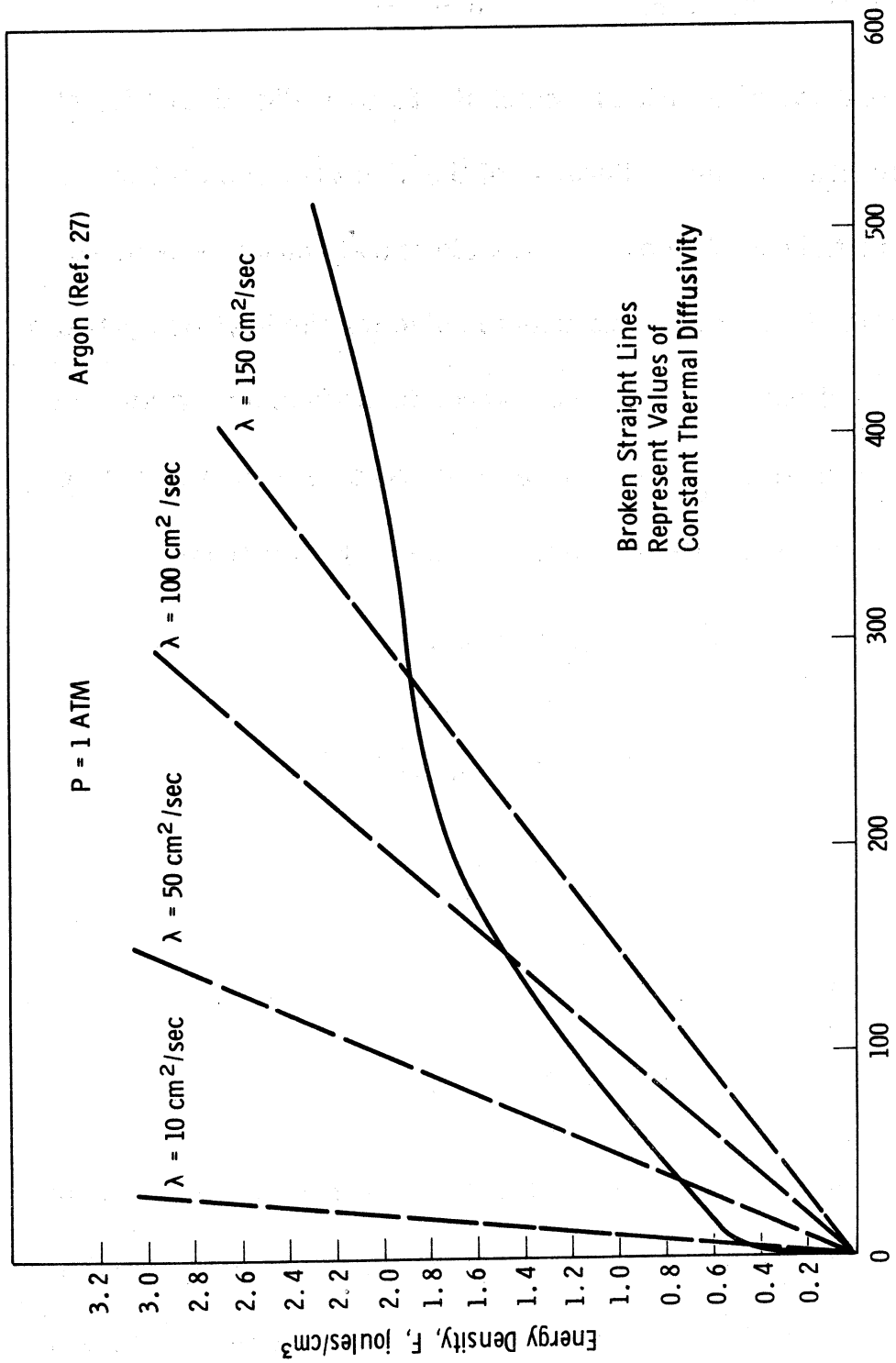

Figure 5b. Energy Density Integral as a Function of Heat Flux Potential for Argon

$$E^2 B(S - S_1) + \frac{1}{r}\frac{\partial}{\partial r}\left(r\frac{\partial S}{\partial r}\right) = \frac{1}{\lambda}\frac{\partial S}{\partial t} \quad , \quad (0 \leq r \leq r_o \quad , \quad t > 0)$$

$$\frac{1}{r}\frac{\partial}{\partial r}\left(r\frac{\partial S}{\partial r}\right) = \frac{1}{\lambda}\frac{\partial S}{\partial t} \quad , \quad (r_o \leq r \leq R \quad , \quad t > 0) \quad .$$

Here r_o is that radial location at which $S = S_1$ (see Fig. 6) and is, of course, a function of time. Because of the discontinuous coefficient introduced by the cut-off model for the electrical conductivity, there are two partial differential equations to solve for the heat flux potential. The solutions of both equations must agree in slope and magnitude at the moving boundary, $r_o(t)$ and there must be no heat sources within the region of interest. Hence the three auxiliary conditions

$$S_r(0, t) = 0$$

$$S(r_o^+, t) = S(r_o^-, t) = S_1$$

$$S_r(r_o^+, t) = S_r(r_o^-, t)$$

and, at the tube wall,

$$S(R, t) = S_2 \quad .$$

The plus and minus signs denote evaluation of the functions and their derivatives approaching the moving boundary from the outside and inside, respectively. It is the condition regarding continuity of slope that

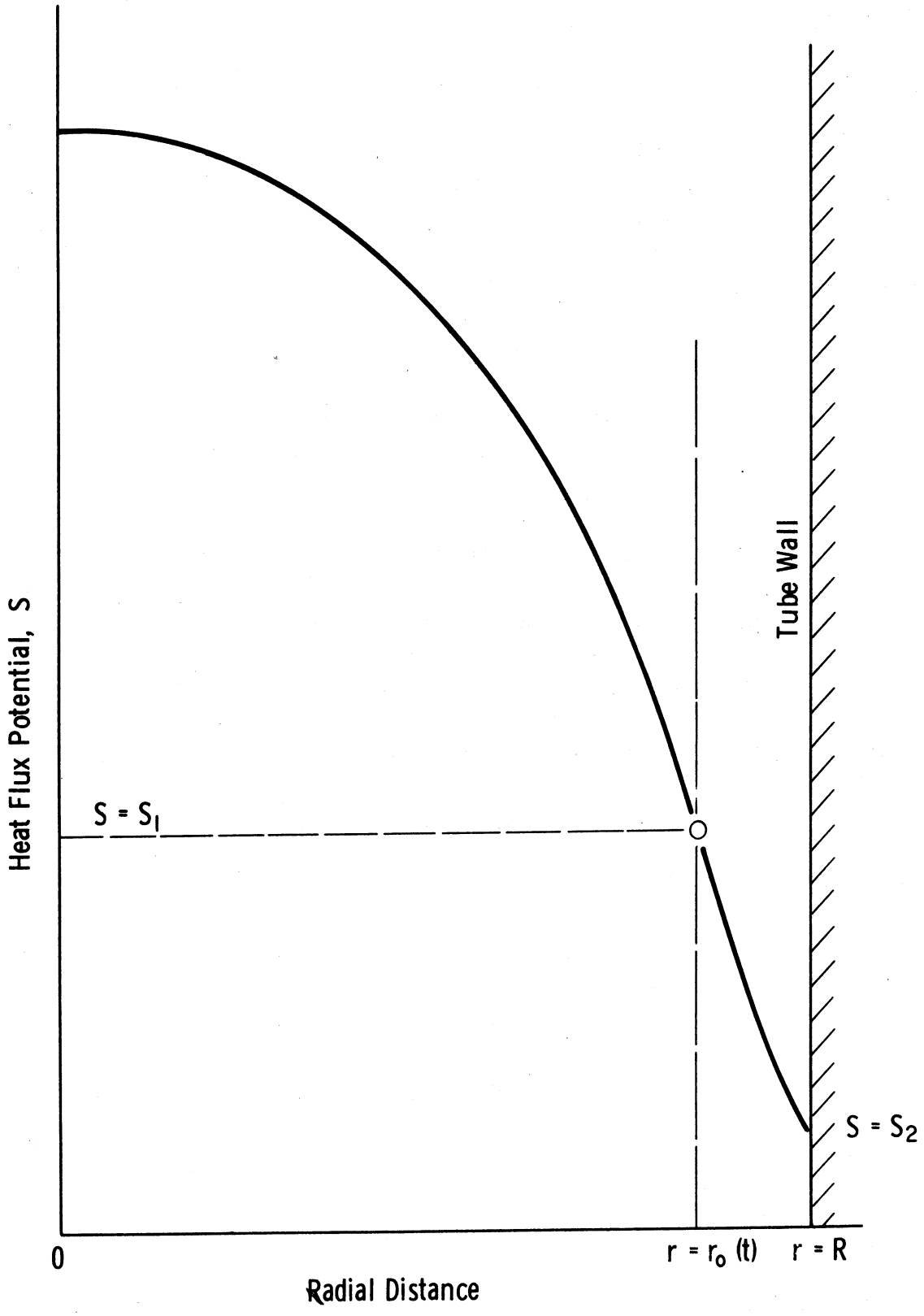

Figure 6. Coordinate System for the Cylindrically Symmetric Arc

determines the position of the conducting zone radius, which is unknown, a priori. In fact, if the problem is posed in the normal way, by specifying the current behavior, there are three dependent variables $S(r, t)$, $E(t)$, and $r_o(t)$. In order to make the problem determinate an additional equation is required. This is provided by Ohm's law,

$$2\pi BE(t) \int_0^{r_o(t)} r(S - S_1)\, dr = I(t)$$

The boundary value problem thus posed, while linear in the variable $S(r, t)$, presents a non-linear system by virtue of the moving boundary and the fact that the electric field strength occurs to the second power in the energy equation. Clearly, even with the simplifications which have been applied to the problem, it is still mathematically formidable. Even if the field strength, $E(t)$, and the boundary position, $r_o(t)$, are prescribed (thereby eliminating the need for some of the above equations), one still is confronted with a partial differential equation with variable coefficients, a class of equations that can prove most troublesome.

In order to arrive at a set of equations which are universal and apply to any gas, it is necessary to introduce several dimensionless variables. In addition, with a boundary that is free to move, it is

difficult to see what effect its motion will have on the evolution of the problem. The free boundary will therefore be fixed by an appropriate transformation. In order to eliminate the moving boundary a different transformation must be used for the conducting region than for the annular zone. For the inner region the following independent variable is introduced:

$$x = r/r_o(t) \quad , \quad 0 \leq r \leq r_o(t) \quad .$$

For the outer, annular zone it is proposed to fix the moving boundary by the transformation

$$y = (R - r)/[R - r_o(t)] \quad , \quad r_o(t) \leq r \leq R \quad .$$

The range of variation for both of these new independent variables is between zero and one but care must be exercised in forming derivatives with respect to these variables. The dependent variables are made dimensionless by the transformations

$$U = (S - S_1)/(S_1 - S_2) \quad , \quad 0 \leq r \leq r_o(t)$$

and

$$V = (S_1 - S)/(S_1 - S_2) \quad , \quad r_o(t) \leq r \leq R$$

where S_2 is the heat flux potential of the gas at the wall. Finally, one can introduce non-dimensionalizing factors for the moving radius, the

electric field strength and the current. These are

$$\rho(t) = r_o(t)/R \quad , \quad E = B^{1/2}\,(RE^*) \quad , \quad I = I^*/(S_1 - S_2)\,RB^{1/2} \quad .$$

Earlier, ρ was used to denote the gas density, but hereafter it will only refer to the dimensionless moving boundary and should cause no confusion. The starred quantities are the dimensional values and will not appear again except, perhaps, in some numerical examples. When the above variables are introduced into the boundary value problem two more transformations are strongly suggested. If one defines

$$\Theta = R^2/\lambda \quad , \quad \tau = t/\Theta \quad ,$$

where Θ is thetime constant for the heat conduction problem, it will be seen that a universal set of differential equations is obtained with the particular operating conditions of the arc contained solely within the current forcing function. The details of this transformation are described in Appendix A. The previously described dimensional boundary value problem becomes:

$$\left.\begin{aligned}
&\frac{1}{x}\frac{\partial}{\partial x}\left(x\frac{\partial U}{\partial x}\right) + \frac{1}{2}\frac{d\rho^2}{d\tau}\left(x\frac{\partial U}{\partial x}\right) + \rho^2 E^2 U = \rho^2\frac{\partial U}{\partial \tau} \quad , \quad 0 \le x \le 1 \quad , \quad \tau > 0 \\
&U_x(0,\tau) = 0 \quad , \quad U(1,\tau) = 0 \quad , \quad \text{plus initial condition} \\
&\left(\frac{\partial^2 V}{\partial y^2} - \frac{1}{\left[(1-\rho)^{-1} - y\right]}\frac{\partial V}{\partial y}\right) - \frac{1}{2}\left(\frac{1-\rho}{\rho}\right)\frac{d\rho^2}{d\tau}\left(y\frac{\partial V}{\partial y}\right) = (1-\rho)^2\frac{\partial V}{\partial \tau} \\
&0 \le y \le 1 \quad , \quad \tau > 0 \\
&V(0,\tau) = 1 \quad , \quad V(1,\tau) = 0 \quad , \quad \text{plus initial condition} \\
&U_x(1,\tau) = -\left(\frac{\rho}{1-\rho}\right) V_y(1,\tau)
\end{aligned}\right\} \quad (1)$$

and

$$2\pi\left[\rho(\tau)\right]^2 E(\tau)\int_0^1 x\,U(x,\tau)\,dx = I(\tau)$$

The non-linearity of the system, which was not obvious in its dimensional formulation, can now clearly be seen. In this new, fixed domain the differential equations have each acquired a term proportional to $d(\rho^2)/d\tau$. Since ρ is one of the dependent variables, the system is non-linear, even if the time dependence of the electric field is explicitly known. It is not strictly necessary, in fact, to consider E(t) as an unknown, but physically it makes more sense to specify the current carried by the arc and determine the resulting field strength. For

any specified current an arc will be thermally stable but only for certain variations of E(t) will this be true. It would even be possible, in fact, to assume an explicit temporal variation of the conducting zone radius and find the temperature profiles that would produce this variation. Then, however, all of the original equations could not be satisfied and one would have to be content with some non-constant tube wall temperature and/or variable tube diameter. Even the simplest temporal variation of ρ that one can devise proves to be too difficult to permit the solution of the boundary value problem. If $d(\rho)^2/d\tau$ is a linear function of τ, for instance, the partial differential equations have variable coefficients and, because of the second term in their left members, are not separable. Only when $d(\rho)^2/d\tau$ is either zero or any finite constant of either sign can a closed form solution to the above formulated boundary value problem be readily found. It is not immediately evident, however, that one can attach any physical significance to these solutions. Fortunately, it is possible to do so and these two situations, when $d(\rho)^2/d\tau = 0$ and when $d(\rho)^2/d\tau =$ constant, are discussed in detail in the following sections.

3. THE TRANSIENT BEHAVIOR OF DC ARCS

3.1 General Considerations

The system of dimensionless equations which was presented in the preceding section is capable of describing the dynamic behavior of all non-stationary arcs, provided that the original limitations imposed on the analysis are not violated. Thus the system should yield solutions which pertain to DC arcs (in the stationary state), AC arcs, and the transition from one DC discharge to another one burning under different conditions. The transient behavior of DC arcs has received considerable attention over the years for a number of reasons. Weinecke (29) attempted to measure the thermal conductivity of a nitrogen plasma by observing the variation in radius and temperature of a collapsing DC arc. He then employed numerical techniques to infer the transport property from the energy equation. Frind (30) and others have concerned themselves with transient arcs because they provide a means of assessing the relative merits of various gases which can be used as the atmosphere surrounding the contacts of high voltage, high power switchgear. If one measures the rate of decay of the conductance of an arc column which is composed of a certain gas, it is possible to predict its performance as a circuit breaking medium. Finally, the analytical treatments of dynamic arcs, (11) and (12), mentioned in the Introduction contain the notion of an arc column time constant which

cannot be immediately related to the properties of the arc gas or to the conditions under which it is burning. Nevertheless, these analyses, because of their great simplicity, have found favor among those engineers and scientists who have occupied themselves with switchgear problems. Therefore, several attempts have been made to obtain experimentally some typical values of this time constant so that the theories of Cassie (11) and Mayr (12) would be more quantitatively useful. The most recent work along this line is reported by Yoon and Spindle (31). There the scheme was to instantaneously apply a step function increase to the current flowing through a DC arc. The subsequent transient behavior of the electric field (arc voltage) was then monitored and the e-folding time was a measure of the arc time constant.

Most of the above mentioned investigators have interpreted their experimental results in the light of quite simplified analytical models, for instance, that of Mayr (12). It is felt that in what follows a more sophisticated description of the transient behavior of DC arcs is presented. The main improvement is seen to be that of providing a means of relating experimental observables to conditions actually prevailing in and around the arc. Such insight is denied by the spatially integrated models used previously. Additional improvements over past work will be indicated later.

If a DC arc suddenly receives a positive or negative step function modulation in current, the ensuing transient behavior will involve (with the model proposed previously) the difficulties associated with the moving boundary of the conducting zone of the arc. Thus, since the boundary position is a dependent variable of the problem, it is still not possible, even in this relatively simple case, to obtain a closed form solution to Eq. 1. It is, however, possible to obtain an approximate solution by specifying a boundary motion which is compatible with reality. If, in Eq. 1, the coefficient, $d\rho^2/d\tau$, is any positive or negative constant, a closed form solution can be obtained. Clearly, the specification of a boundary motion makes the set of equations, Eq. 1, overdetermined and some originally specified compatibility or boundary conditions must be relaxed. If one insists on continuity of heat flux at the moving boundary, the tube wall cannot have a constant temperature and/or position. The details of the boundary modifications are not too important, however, since the solution of the first differential equation gives the behavior of the arc proper and this is all one needs for comparison with experiment. The partial differential equation which applies to the annular region serves only to communicate to the arc (the conducting zone) that there is a fixed, cold wall in its vicinity, thereby determining the radius, $\rho(\tau)$. When $\rho(\tau)$ is known a priori the annular equation is no longer

essential. Thus one has simply

$$\left.\begin{aligned} &\frac{1}{x}\frac{\partial}{\partial x}\left(x\frac{\partial U}{\partial x}\right)+\frac{1}{2}\frac{d\rho^2}{d\tau}\left(x\frac{\partial U}{\partial x}\right)+\rho^2E^2U=\rho^2\frac{\partial U}{\partial \tau} \quad , \quad (0\leq x\leq 1 \quad , \quad \tau>0)\\ &U_x(0,\tau)=0 \quad , \quad U(1,\tau)=0 \quad , \quad d\rho^2/d\tau=\pm 4K\\ &2\pi\rho^2E\int_0^1 x\,U(x,\tau)\,dx=I \end{aligned}\right\}(2)$$

plus some initial condition. Here K is some arbitrary constant which represents the rate at which the conducting area increases or decreases. As in the more general formulation the current is some constant or specified function of time. The boundary motion equation can be integrated to give

$$\rho^2-\rho_i^2=\pm 4K\tau$$

if $\rho=\rho_i$ at $\tau=0$. Clearly, this approximate solution will not admit of any oscillatory behavior and is representative of only a temporally unidirectional process. There is a similarity here with the motion of the interface in a solidification or melting problem in an infinite or semi-infinite domain. There (see (32)) a closed form solution can be obtained only when the interface position is proportional to the square root of the time variable, whether the domain is a slab or is cylindrically symmetric.

The Eq. 2 can be solved by separation of variables, but first it is convenient to introduce the new variable $\xi = x^2$. Then one finds

$$\left.\begin{aligned} &\xi \frac{\partial^2 U}{\partial \xi^2} + (1 \pm K\xi) \frac{\partial U}{\partial \xi} + \frac{1}{4}\rho^2 E^2 U = \frac{1}{4}\rho^2 \frac{\partial U}{\partial \tau} \quad , \quad (0 \leq \xi \leq 1 \quad , \quad \tau > 0) \\ &\xi^{1/2} U_\xi (0, \tau) = 0 \quad , \quad U(1, \tau) = 0 \quad , \quad \rho^2 = \rho_i^2 \pm 4K\tau \\ &\pi \rho^2 E \int_0^1 U(\xi, \tau)\, d\xi = I \quad . \end{aligned}\right\} \quad (3)$$

If one assumes a solution of the form

$$U(\xi, \tau) = X(\xi) \cdot T(\tau) \quad ,$$

the following two ordinary differential equations are obtained:

$$\left.\begin{aligned} &\xi X'' + (1 \pm K\xi) X' + \mu^2 X = 0 \\ &T' + (4\mu^2/\rho^2 - E^2) T = 0 \\ &\xi^{1/2} X'(0) = 0 \quad , \quad X(1) = 0 \quad . \end{aligned}\right\} \quad (4)$$

In the above the primes denote differentiation with respect to the arguments and μ is a separation constant to be determined later. The first of these equations can be brought into a standard form known as Kummer's or the confluent hypergeometric equation. If one sets $s = \mp K\xi$, depending upon the direction of boundary motion, the following result is obtained:

$$sX'' + (1 - s)\, X' - \left(\frac{\mu^2}{\pm K}\right) X = 0$$

$$s^{1/2} X'(0) = 0 \quad , \quad X(\pm K) = 0$$

The general solution to this system can be found in many places, c. f. (33). For the equation

$$sX'' + (\gamma - s)\, X' - \alpha X = 0 \quad ,$$

when $\gamma = 1$ is an integer, the general solution contains four terms. They are discussed thoroughly in (33) or (34). In the present case $\gamma = 1$ and one of the terms in the general solution (a finite polynomial) vanishes identically. Two other terms will not appear here because of the condition of regularity at the origin which prevents a logarithmic term from being included. One is left, then, with a solution of the form

$$X(s) = C\, {}_1F_1(\alpha, 1; s)$$

where

$${}_1F_1(\alpha, 1; s) = 1 + \alpha \frac{s}{1 \cdot 1!} + \alpha(\alpha + 1) \frac{s^2}{2 \cdot 2!} + \ldots \quad .$$

The boundary condition $X(K) = 0$ implies that the non-trivial solutions of the Kummer equation are the eigenfunctions

$$X_n(s) = C\, {}_1F_1\left(\pm \frac{\mu_n^2}{K}, 1; s\right) \quad , \quad n = 1, 2, \ldots$$

where α has been replaced by the specific value, μ^2/K, and the eigenvalues are the roots of

$$ {}_1F_1\left(\pm\frac{\mu^2}{K}, 1; \pm K\right) = 0 \quad . $$

The second of Eq. 4 involves a specific current variation, i.e., the input function. From Ohm's law one finds that the electric field can be expressed as

$$ E = I/\pi\rho^2 \int_0^1 X(\xi)\cdot T(\tau)\, d\xi \quad . $$

Thus the T equation can be written as

$$ TT' + 4\frac{\mu^2}{\rho^2}T^2 = \frac{I^2}{\pi^2\rho^4\left[\int_0^1 X(\xi)\, d\xi\right]^2} \quad . $$

The above equation is non-linear as it stands but if T^2 rather than T is chosen as the dependent variable it can readily be solved. Recalling that $\rho^2 = (\rho_i^2 \pm 4K\tau)$, one finds the solution of the above equation to be

$$ T^2\left(1 + 4\frac{K}{\rho_i^2}\tau\right)^{\pm\frac{2\mu^2}{K}} - T_i^2 = \frac{2}{\pi^2\left[\int_0^1 X(\xi)\, d\xi\right]^2}\int_0^\tau \frac{I^2(\alpha)}{\rho^4}\left(1 \pm \frac{4K}{\rho_i^2}\alpha\right)^{\pm\frac{2\mu^2}{K}} d\alpha \qquad (5) $$

Then for any current variation which is compatible with the boundary motion the integral in Eq. 5 can be evaluated and the functional form of $T(\tau)$ thus obtained. This does not complete the problem, however, since a generalized Fourier series of the eigen-functions given above must be formed to accommodate an arbitrary initial distribution of temperature. To illustrate this procedure a DC arc upon which is imposed a positive step modulation in current will be considered.

3. 2 The Step Modulated DC Arc

Suppose a DC arc has been established which carries a dimensionless current I_o. By some means it is possible to instantaneously increase the current to a new value, I_1. Since the arc cannot immediately adjust its thermal structure to correspond to this new current, the voltage drop (electric field strength) increases at the outset. The increased heating due to the higher field strength raises the temperature and with it the electrical conductivity. Gradually, for a fixed current, the field strength decreases and the arc reaches a new steady state condition corresponding to the DC current I_1. This process is illustrated in Fig. 7. Then consider the solution of Eq. 3 when $\rho^2 = \rho_o^2 + 4\,K\tau$ and

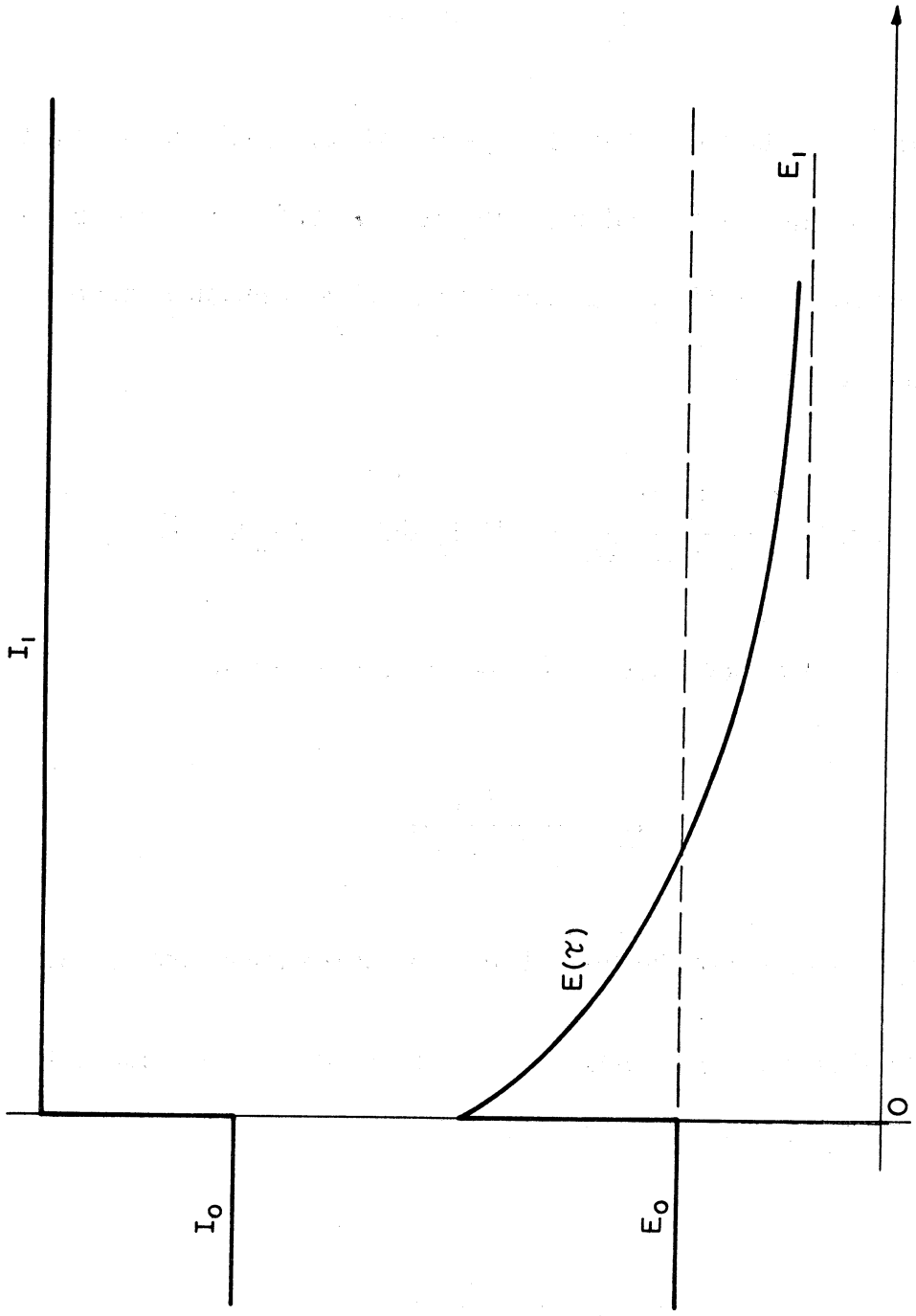

Figure 7. Schematic Behavior of the Electric Field and Current in a Step-Modulated DC Arc

$$I = I_o \quad , \quad (\tau \leq 0)$$

$$I = I_1 \quad , \quad (\tau > 0) \quad .$$

The initial distribution of heat flux potential can easily be obtained from Eq. 1 by setting the time derivatives to zero and solving the resulting set of ordinary differential equations. This solution is denoted by $U_o(x)$ and is given by

$$U_o(x) = \frac{J_o(\beta x)}{\beta J_1(\beta) \ln (1/\rho_o)} = U_o J_o(\beta x) \qquad (0 \leq x \leq 1) \quad ,$$

where ρ_o is found by specifying $I = I_o$ and using the relation

$$I_o = \frac{2\pi}{\beta} \frac{\rho_o}{\ln (1/\rho_o)} \quad .$$

Here β is the first zero of the Bessel function of the first kind, $J_o(x)$.

When the direction of boundary motion is positive, the solution to the Kummer equation is

$$X_n(s) = {}_1F_1\left(\frac{\mu_n^2}{K}, 1; s\right)$$

or, by Kummer's first theorem,

$$X_n(\xi) = e^{-K\xi}\ {}_1F_1\left[\left(1 - \frac{\mu_n^2}{K}\right), 1; K\xi\right] \quad .$$

The integral in Eq. 5 can easily be evaluated to yield

$$T^2 = \frac{I_1^2\left(1 + \frac{4K}{\rho_o^2}\tau\right)^{-\frac{2\mu_n^2}{K}}}{2\pi^2 K\rho_o^2\left(\frac{2\mu_n^2}{K} - 1\right)\Lambda^2}\left[\left(1 + \frac{4K}{\rho_o^2}\tau\right)^{\frac{2\mu_n^2}{K} - 1} - 1\right] + U_o^2\left(1 + \frac{4K}{\rho_o^2}\tau\right)^{-\frac{2\mu_n^2}{K}} \qquad (6)$$

where T_i^2 has been replaced by U_o^2 in order to satisfy the condition at $\tau = 0$. In addition, Λ represents the integral

$$\int_0^1 e^{-K\xi}\ {}_1F_1\left[\left(1 - \frac{\mu_n^2}{K}\right), 1; K\xi\right] d\xi \quad .$$

From Slater (33) one finds that this integral can be evaluated to yield

$$\Lambda = e^{-K}\ {}_1F_1\left[\left(2 - \frac{\mu_n^2}{K}\right), 2; K\right] \quad .$$

It is interesting to note that one obtains a power law character for the time solution rather than the familiar exponential behavior. The solution

to Eq. 2, then, has the form

$$X(s) \cdot T(\tau) = C_n \cdot {}_1F_1\left(\frac{\mu_n^2}{K}, 1; s\right) \cdot T(\tau)$$

with $T(\tau)$ being given by the square root of Eq. 6. Now according to Sturm-Liouville theory the Kummer functions can be shown to form an orthogonal set in the internal $0 \geqq s \geqq - K$ with respect to the weight function e^{-s}. Furthermore, a normalizing factor can be found that permits the formulation of an orthonormal set. Changing to a positive s interval and using Kummer's first theorem allows one to find the normalizing factor, E_n, from

$$E_n^2 = \int_0^K e^{-s} \left\{ {}_1F_1\left[\left(1 - \frac{\mu_n^2}{K}\right), 1, s\right] \right\}^2 ds \quad .$$

Thus, one can form the orthonormal set

$$\varphi_n(s) = E_n^{-1} e^{-s} {}_1F_1\left[\left(1 - \frac{\mu_n^2}{K}\right), 1; s\right] \quad .$$

Finally, the coefficients, C_n, are found by means of the orthonormal properties of the $\varphi_n(s)$ and from the initial distribution of heat flux potential, $J_0(\beta x)$. (The magnitude, U_0, of the initial distribution has been absorbed in the $T(\tau)$ function.) One obtains

$$C_n = E_n^{-1} \int_0^K J_o(\beta\sqrt{s/K}) \cdot {}_1F_1\left[\left(1 - \frac{\mu_n^2}{K}\right), 1; s\right] ds \quad .$$

The complete solution of Eq. 3 for the case of a step modulated arc can now be written as

$$U(\xi, \tau) = \sum_{n=1}^{\infty} C_n \cdot T_n(\tau)\, e^{-K\xi}\, {}_1F_1\left[\left(1 - \frac{\mu_n^2}{K}\right), 1; K\xi\right] \cdot E_n^{-1} \qquad (7)$$

and, as indicated earlier, the μ_n are found from

$${}_1F_1\left[\left(1 - \frac{\mu_n^2}{K}\right), 1; K\right] = 0 \quad .$$

In order to obtain numerical results from Eq. 7, a series of μ_n, C_n, and E_n must be computed, the number depending upon the accuracy desired. Unfortunately, it does not seem to be possible to obtain a closed form for either the coefficients, C_n, or the normalizing factor, E_n. In addition, a tabulation of the roots, μ_n, has apparently only been made for the first eigenfunction, μ_1, (33). Thus, in what follows, only the first term in the series Eq. 7 will be considered in order to obtain a rough idea of the behavior of the solution. If K is small, this one term series will yield nearly the exact solution to Eq. 3 since, from

Slater (33), one finds that Kummer functions have the following asymptotic behavior as $\alpha \to \infty$:

$$ {}_1F_1(\alpha, \gamma, z) \sim \Gamma(\gamma)\, e^{z/2} (kz)^{1/2} \left|\frac{1-\gamma}{2}\right| \cdot J_{\gamma-1}(2k^{1/2} z^{1/2}) \left\{1 + O(|k|^{\sim \nu})\right\} $$

In the present case $\alpha = 1$, $k = \mu_n^2/K - 1/2$, and $\nu = 1/2$ so that one finds:

$$ {}_1F_1\left[\left(1 - \frac{\mu_n^2}{K}\right), 1; K\xi\right] \sim e^{K\xi/2} J_o(2\mu_n \xi^{1/2}) \left\{1 + O(K^{1/2})\right\} \quad , \qquad K \to 0 $$

In the limit $K = 0$ the Kummer function is identical to the initial Bessel function distribution. Also, for $K = 0$, all coefficients, C_n, for $n > 1$ vanish identically. Thus for K close to zero, (slow boundary motion) the one term series will be a good approximation to a more exact evaluation of Eq. 7, since the Kummer function and Bessel function profiles nearly coincide for K small.

Retaining only the first term in Eq. 7 results in the expression

$$ U(k, \tau) = e^{-Kx^2} \, {}_1F_1\left[\left(1 - \frac{\mu_1^2}{K}\right), 1; Kx^2\right] \cdot T_1(\tau) $$

where

$$T_1(\tau) = \left\{ \frac{I_1^2 \left(1 + \frac{4K}{\rho_o^2}\tau\right)^{-\frac{2\mu_1^2}{K}}}{2\pi^2 K \rho_o^2 \left(\frac{2\mu_1^2}{K} - 1\right) \Lambda^2} \left[\left(1 + \frac{4K}{\rho_o^2}\tau\right)^{\frac{2\mu_1^2}{K} - 1} - 1 \right] + U_o^2 \left(1 + \frac{4K}{\rho_o^2}\tau\right)^{-\frac{2\mu_1^2}{K}} \right\}^{\frac{1}{2}}$$

and μ_1 is the first eigenvalue of the system. With the above equation and Ohm's law the variation in electric field strength with τ can be computed, a value which could easily be compared with experiment.

The behavior of the centerline heat flux potential (x = 0) and the electric field strength is shown in Fig. 8 and 9, respectively. Initial conditions corresponding to $\rho_o = 0.8$ were chosen and values of K = .416 and .441 were used to compute U (o, τ). These boundary velocities correspond to $(1 - \mu_1^2/K) = -3.0$ and -2.8, respectively. As this parameter goes to negative infinity there is no boundary motion and one can show that for the present situation the boundary velocity is effectively zero when $(1 - \mu_1^2/K) \cong -4.0$. One thing to note is that the higher the value of K (rapid boundary motion) the smaller the rate of temperature rise. This is evident from the way in which the $d\rho^2/d\tau$ term enters the original differential equation, Eq. 2. For $d\rho^2/d\tau > 0$ that term will

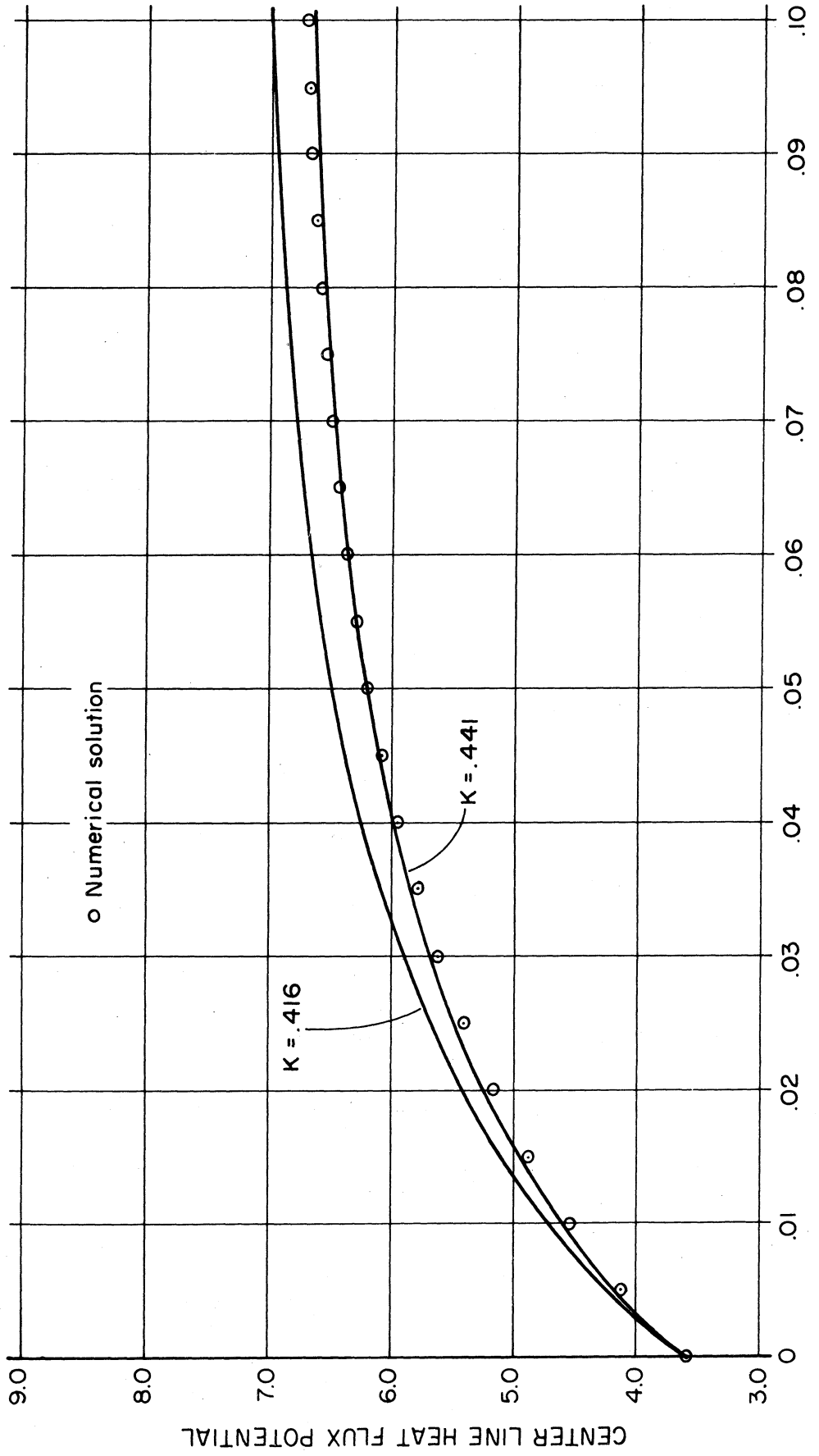

Figure 8. Behavior of the Centerline Heat Flux Potential of a Step-Modulated DC Arc

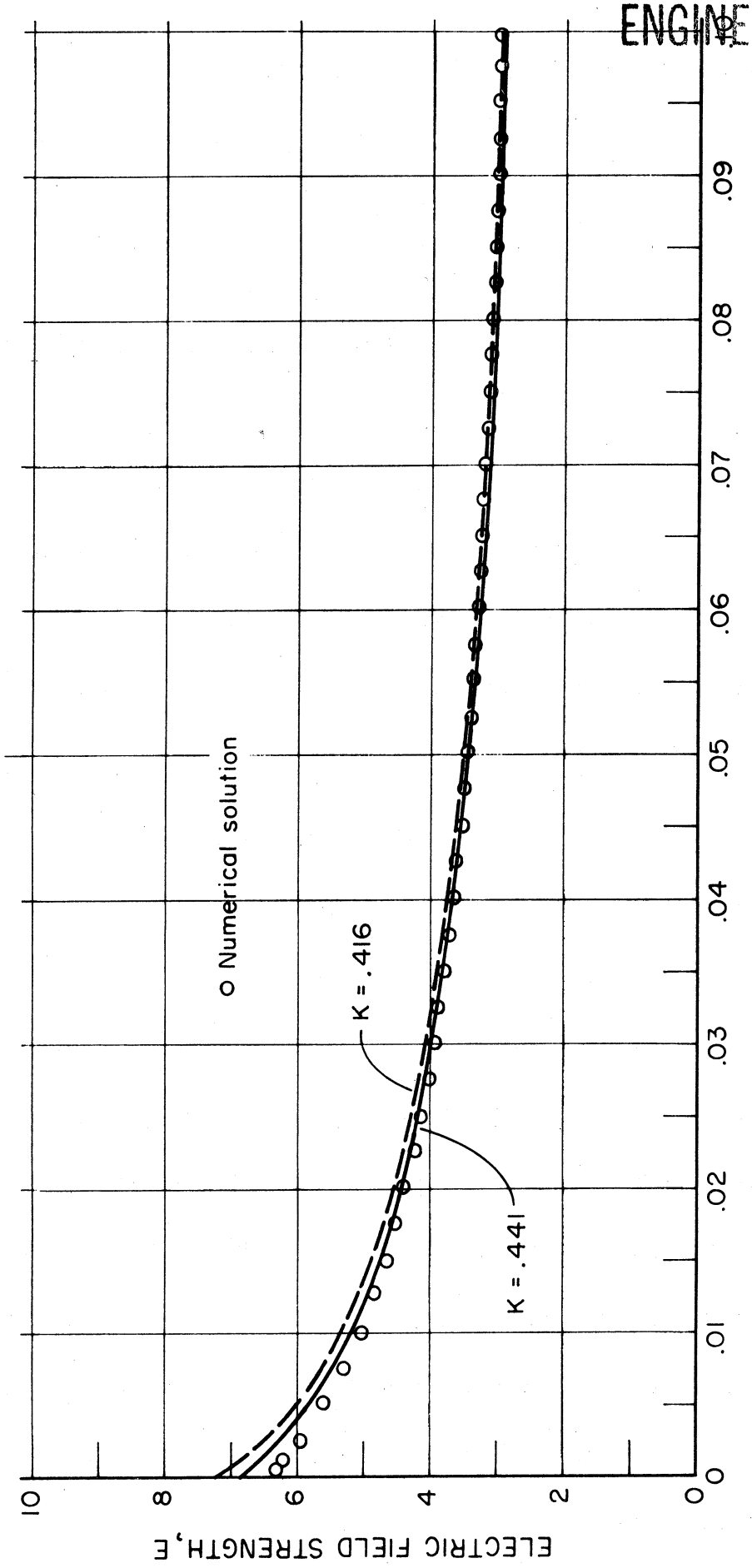

Figure 9. Behavior of the Electric Field Strength in a Step-Modulated DC Arc

make a negative contribution to the energy equation since $\partial U/\partial x$ is negative for all $x > 0$. Thus, the advancing boundary has the effect of slowing the rate of temperature rise. Included in the Figs. 8 and 9 are the results of an exact solution of the complete boundary value problem posed earlier. This solution was obtained on a digital computer and will be discussed later in more detail. For the present, however, it will be sufficient to point out that for a proper choice of K the approximate solution given here corresponds satisfactorily to the "exact" theoretical result. The value K = . 441 provides a reasonable linear approximation to the ρ^2 vs. τ curve which was obtained from the numerical computation.

Finally, a word about time constant determination from transient arc behavior is in order. Yoon and Spindle (31) and others define the time constant as that point where the falling $E(\tau)$ curve intersects the original value E_0 on the way toward approaching E_1. This time constant is then related to an analysis (Mayr (12)) wherein a constant radius arc with constant energy losses is postulated. According to the present work, the time constant determined in this way is too low, by perhaps a significant factor. It is suggested that measured arc time constants that have been interpreted in terms of cruder, constant radius models could be re-evaluated in terms of a more sophisticated model,similar to the one presented herein.

4. THE CONSTANT RADIUS AC ARC

In the preceding section it was mentioned that the boundary motion specified by $d\rho^2/d\tau = \pm 4K$ is quite unsuitable for application to oscillatory arc phenomena. Since alternating current arcs comprise an extremely important part of the technology of gaseous discharges, it behooves one to search for a specified boundary motion that could apply to a quasi-steady, oscillatory column. An appeal to physical intuition can be quite useful in determining the conditions under which this might be possible.

As noted previously, Eq. 1 merely describes a very sophisticated heat conduction problem with a constant thermal diffusivity, λ. As in any time unsteady conduction problem the diffusivity is a measure of the speed with which temperature changes can be effected when either a boundary condition or an internal heat generation function is altered. Then, since the conducting zone radius is defined simply as the locus in the time-space plane of a fixed temperature, its position and rate of change of position must depend in some way upon the thermal diffusivity.

Physically, the conducting zone radius reaches extreme values in the AC arc when conditions are such that there is no tendency to raise or lower the temperature on either side of its immediate position, or when, locally, there is no net heat flux across the boundary.

When this situation occurs, there is an inflection point in the heat flux potential profile at the zone boundary. This is easily seen from the differential equations. At x = 1 the first of Eq. 1 becomes

$$\frac{\partial}{\partial x}\left(x\frac{\partial U}{\partial x}\right)\Bigg|_1 + \frac{1}{2}\frac{d\rho^2}{d\tau}\left(\frac{\partial U}{\partial x}\right)_1 = 0$$

since both U and $\partial U/\partial\tau$ vanish at x = 1. Then, when ρ has an extremum, $d\rho^2/d\tau = 0$ and

$$\frac{\partial}{\partial x}\left(x\frac{\partial U}{\partial x}\right)\Bigg|_1 = 0 \quad .$$

Thus, since the boundary position is thermally determined, it is reasonable to expect that under some conditions the motion of the conducting boundary will be small and unimportant. Specifically, if the external conditions which are imposed upon the arc (the current function) are changed so rapidly that the arc cannot readily adjust to these changes there will be little overall variation with time in the structure of the arc. Even if the changes are not rapid but the arc is thermally "slow", the result again will be that there is only a slight temporal variation in arc properties. The parameter that is a measure of these relative rates of change is the product of the circular frequency, ω, of the current waveform and the pseudo-time constant of the arc-tube system,

$\Theta = R^2/\lambda$. When this product is large, implying either ω or Θ is large, one expects the arc to be operating under the conditions described above; namely, there is almost no change in the arc structure. It is not yet possible to say, however, just how large is "large".

There is more than just intuition to stimulate the type of reasoning described above. Analyses by von Engel and Steenbeck (35), Rompe and Weizel (36), Frie (37), and Uhlenbusch (6), of the linearly modulated DC arc have all indicated that as the applied frequency of the disturbance is increased, the magnitude of the deviations from the DC condition becomes vanishingly small. Frie (37), indicates, in fact, that the perturbation to the conducting boundary position decreases as $(\omega\Theta)^{-3/2}$ while centerline temperature perturbations die out only as $(\omega\Theta)^{-1}$. All of these analyses treat the case of a DC arc, operating at a given point on its characteristic, and upon which is superimposed a small (linear) AC signal. It is possible to obtain, in most cases, a closed form solution to this problem and the four authors cited above have done this with varying degrees of sophistication. They all indicate, however, that as $\omega\Theta \to \infty$ the arc essentially stagnates and retains a fixed temperature distribution with no consequent change in its conductance. Thus, in the infinite frequency limit the arc should look like an ohmic resistor with a positive voltage-current characteristic.

One is led, then, to make the following conjecture: at a suitably large value of $\omega\Theta$ one can neglect altogether the influence of the moving boundary on the determination of arc structure. That is, the conducting zone pulsates only so slightly that the arc essentially has a constant radius. This can only be strictly true in the limit as $\omega\Theta \to \infty$ but it is assumed that for other "large" values of $\omega\Theta$ the approximate solution to the energy equation obtained by this simplification will closely resemble reality. It is shown in the sequel how this assumption can be substantiated a posteriori and also how a "large" $\omega\Theta$ can be defined.

If it is presumed that there is effectively no boundary motion then $d\rho^2/d\tau = 0$ in Eq. 1. As indicated earlier, this makes it possible to obtain a closed form solution. Actually, this corresponds to the case $K = 0$ in the previous section but it will be more convenient to rework the problem with slightly different notation.

Under the assumptions made above the governing equations become

$$\left.\begin{aligned} &\frac{1}{x}\frac{\partial}{\partial x}\left(x\frac{\partial U}{\partial x}\right) + \rho^2 E^2 U = \rho^2 \frac{\partial U}{\partial \tau} \quad , \quad (0 \leq x \leq 1 \quad , \quad \tau > 0) \\ &U_x(0,\tau) = 0 \quad , \quad U(1,\tau) = 0 \quad , \quad \text{plus initial condition} \\ &2\pi\rho^2 E \int_0^1 x\, U(x,\tau)\, dx = I_m \cos(\omega\Theta\tau) \end{aligned}\right\} \qquad (8)$$

where the sinusoidal current waveform has been specified. Again, since the boundary motion is known, there is no need for either the annular differential equation or the remaining boundary and compatibility conditions. It is convenient to use for the initial conditions the properties of a DC arc that is carrying a current, I_m, equal to the peak value of the AC current level. It is possible to solve Eq. 8 by the method of separation of variables. Assuming a solution of the form

$$U(x, \tau) = X(x) \cdot T(\tau)$$

allows one to obtain the following ordinary differential equations:

$$X'' + \frac{1}{x} X' + \beta^2 X = 0$$

$$X'(0) = 0 \quad , \quad X(1) = 0$$

$$T' - (E^2 - \beta^2/\rho^2)\, T = 0$$

Here β is a separation constant to be determined by the boundary conditions on X(x). The first equation is easily solved to yield the Bessel function solution

$$X(x) = C J_0(\beta x)$$

where application of the condition $X'(0) = 0$ has demanded the exclusion of the second solution, $Y_0(x)$. Upon applying the second boundary

condition one finds that for non-trivial solutions

$$J_o(\beta) = 0 \quad \text{or} \quad \beta = \beta_n \quad , \quad n = 1, 2, 3, \ldots \quad .$$

Thus the separation constant assumes the values of the zeros of the Bessel function. From Ohm's law

$$E = \frac{I_m \cos(\omega\Theta\tau)}{2\pi\rho^2 \int_0^1 x\, X(x) \cdot T(\tau)\, dx} \quad ,$$

and the T equation can be arranged in the form

$$TT' + \frac{\beta^2}{\rho^2} T^2 = \frac{I_m^2 \cos^2(\omega\Theta\tau)}{4\pi^2\rho^4 \left[\int_0^1 x\, X(x)\, dx\right]^2} \quad .$$

As in the case of the transient DC problem, the time equation is non-linear but if $T^2(\tau)$ is chosen as the dependent variable it can readily be solved. It will be convenient to absorb the constant, C, into the initial conditions, so one obtains the result

$$\int_0^1 x\, J_o(\beta x)\, dx = \frac{1}{\beta} J_1(\beta) \quad .$$

Finally,

$$T^2 \exp\left(\frac{2\beta^2\tau}{\rho^2}\right) = \frac{\beta^2 I_m^{\,2}}{2\pi^2\rho^4 J_1^{\,2}(\beta)} \int_0^{\tau} \exp\left(\frac{2\beta^2\alpha}{\rho^2}\right) \cos^2(\omega\Theta\alpha)\, d\alpha + T_i^{\,2} \qquad (9)$$

The initial conditions for this problem are those which prevail for a DC arc carrying a current I_m. This solution was obtained in the previous section but it will be fruitful to rederive it here in more detail.

In the DC arc all time unsteady terms vanish, leaving one with

$$\frac{1}{x}\frac{d}{dx}\left(x\frac{dU}{dx}\right) + \rho^2 E^2 U = 0 \quad , \quad (0 \leq x \leq 1)$$

$$\left.\frac{dU}{dx}\right|_0 = 0 \quad , \quad U(1) = 0$$

$$\frac{d^2V}{dy^2} - \frac{1}{[(1-\rho)^{-1} - y]}\frac{dV}{dy} = 0 \quad , \quad (0 \leq y \leq 1) \qquad (10)$$

$$V(0) = 1 \quad , \quad V(1) = 0$$

$$\left.\frac{dU}{dx}\right|_1 = -\frac{\rho}{1-\rho}\left.\frac{dV}{dy}\right|_1 \quad , \quad 2\pi\rho^2 E \int_0^1 x\, U(x)\, dx = I_m$$

Since the solution to the first equation must be well behaved at the origin one finds

$$U(x) = U_m J_o (\rho E x)$$

But, since this function must vanish at x = 1, the requirement for a non-trivial solution is $\rho E = \beta$, the first zero of the Bessel function. Subsequent roots are not considered since the solution cannot assume negative values. Using the compatibility condition allows one to obtain the solution to the annular equation in the form:

$$V(y) = U_m \beta J_1(\beta) \ln \left[\frac{1 - (1 - \rho) y}{\rho} \right] .$$

The edge of the conducting zone can be found by noting that at y = 0, V = 1. Thus,

$$U_m = \frac{1}{\beta J_1(\beta) \ln (1/\rho)}$$

Ohm's law yields the relation,

$$I_m = 2 \pi \rho U_m J_1(\beta)$$

and, upon combining this with the expression for U_m above, one obtains the following relation between arc current and conducting zone radius:

$$I_m = \frac{2 \pi}{\beta} \frac{\rho}{\ln (1/\rho)} .$$

Notice that when there is no boundary motion (as in the DC case) it is possible to solve the complete problem exactly and a unique value of ρ can be determined. It should be possible, therefore, at the high frequency limit of the AC arc ($\omega\Theta \to \infty$) to similarly determine a unique radius for the conducting zone. This follows from the presumption that for large values of $\omega\Theta$ there will again be no boundary motion. Henceforth the value of ρ which applies to the DC arc will be denoted by ρ_{dc} while the AC value will have no subscript.

Since the initial distribution of heat flux potential is identical to the first eigen-function of the present boundary value problem, there is no need to form a generalized Fourier series for the representation of the time varying distribution. The first Fourier coefficient is simply unity and all others are identically zero.

The integral in Eq. 9 is easily evaluated to yield

$$T^2 = \frac{I_m^2}{8\pi^2\rho^2 J_1^2(\beta)}\left\{\left[1 + \cos\gamma\cos\left(2\omega\Theta\tau - \gamma\right)\right] - \left(1 + \cos^2\gamma\right)\exp\left(\frac{-2\beta^2\tau}{\rho^2}\right)\right\}$$

$$+ T_i^2 \exp\left(\frac{-2\beta^2\tau}{\rho^2}\right) \quad . \tag{11}$$

Here an auxiliary angle, γ, has been introduced and is defined by

$$\tan \gamma = (\omega\Theta)\rho^2/\beta^2 \quad .$$

At $\tau = 0$ the DC solution holds, $T = T_i$, $U(x) = U_m J_o(\beta x)$, and $T_i = U_m$. The two terms involving exponentials in Eq. 11 represent the transient transition from the initial DC arc to the quasi-steady AC column. Since the transient part of the solution is of no interest, let $\tau \to \infty$ and obtain the desired expression. Thus, one can find

$$U(x, \tau) = \frac{I_m J_o(\beta x)}{2\sqrt{2}\,\pi\rho J_1(\beta)} \left[1 + \cos\gamma \cos(2\omega\Theta\tau - \gamma)\right]^{1/2} \qquad (12)$$

Now it was mentioned earlier that the above solution would be expected to apply to the situation where the conducting boundary motion is slight and consists of a small oscillation about some mean value. One would not necessarily expect that mean value to be ρ_{dc} so the solution is not complete until a proper AC radius has been defined. Since this solution is valid only when $\omega\Theta$ is large, the radius corresponding to the infinite frequency limit is the most logical one to choose. For large $\omega\Theta$, $\gamma \to \pi/2$, $\cos\gamma \to 0$, and Eq. 12 becomes

$$U(x) = \frac{I_m}{2\sqrt{2}\,\pi\rho J_1(\beta)} J_o(\beta x) \quad .$$

It is convenient to refer all quantities to their DC counterparts so the above may be rewritten as

$$U(x) = \frac{\sqrt{2}}{2} \frac{U_m}{(\rho/\rho_{dc})} J_o(\beta x)$$

One sees that were it not for the difference in conducting radii the heat flux distribution of the high frequency limit AC arc would be the RMS value of the corresponding DC column. As it is, by analogy with the DC solution, one finds the radii to be related by

$$\frac{\rho}{\ln \rho} = \frac{\sqrt{2}}{2} \frac{\rho_{dc}}{\ln \rho_{dc}} \quad .$$

From Eq. 12, the expression for the time varying heat flux potential, it is possible to obtain the electric field waveforms which correspond to this high frequency arc. With the help of Ohm's law it is not difficult to obtain the expression:

$$E = \sqrt{2} \frac{\beta}{\rho} \frac{\cos(\omega\Theta\tau)}{[1 + \cos\gamma \cos(2\omega\Theta\tau - \gamma)]^{1/2}} \qquad (13)$$

which, of course, applies only for the assumed cosine current waveform. Again, notice that as $\omega\Theta$ becomes very large, implying that $\cos\gamma \to 0$, the denominator in the above expression becomes unity and the column appears to behave as though it were a fixed composition (ohmic) resistor.

That is, the voltage waveform precisely follows the current input and is directly proportional to it. It appears that the electric field is independent of the current or power level, normally indicated by the magnitude of I_m. It must be remembered, however, that the power level enters Eq. 13 through the arc radius, ρ.

Since it is still not known for how low a value of $\omega\Theta$ the present analysis is valid, it is instructive to plot Eq. 13 for an arbitrary range of values of the frequency parameter. Since the electric field strength is an easily measured observable of AC arcs it is possible to compare the results of this analysis with some carefully taken experimental results. In Fig. 10 the electric field waveform is plotted for values of $\omega\Theta = 0.5,\ 1.0,\ 1.5,\ 2.0,\ 5.0,\ 10.0$, and 100.0. A value of $\rho^2 = 0.64$ was chosen in order to compute the angle γ but it does not really matter what number is used as long as a wide enough range for $\omega\Theta$ is chosen. That is, it would be just as easy, in the present case, to absorb the factor ρ^2/β into the definition of the time constant Θ so that γ would be a function of this new value alone. Since $\Theta\tau$ is the original dimensional time, the arguments of the cosine functions in Eq. 13 are simply the radian measure of position in the cycle. By plotting Eq. 13 for values of γ from zero to $\pi/2$ one obtains all possible shapes that can be assumed by the electric field waveform.

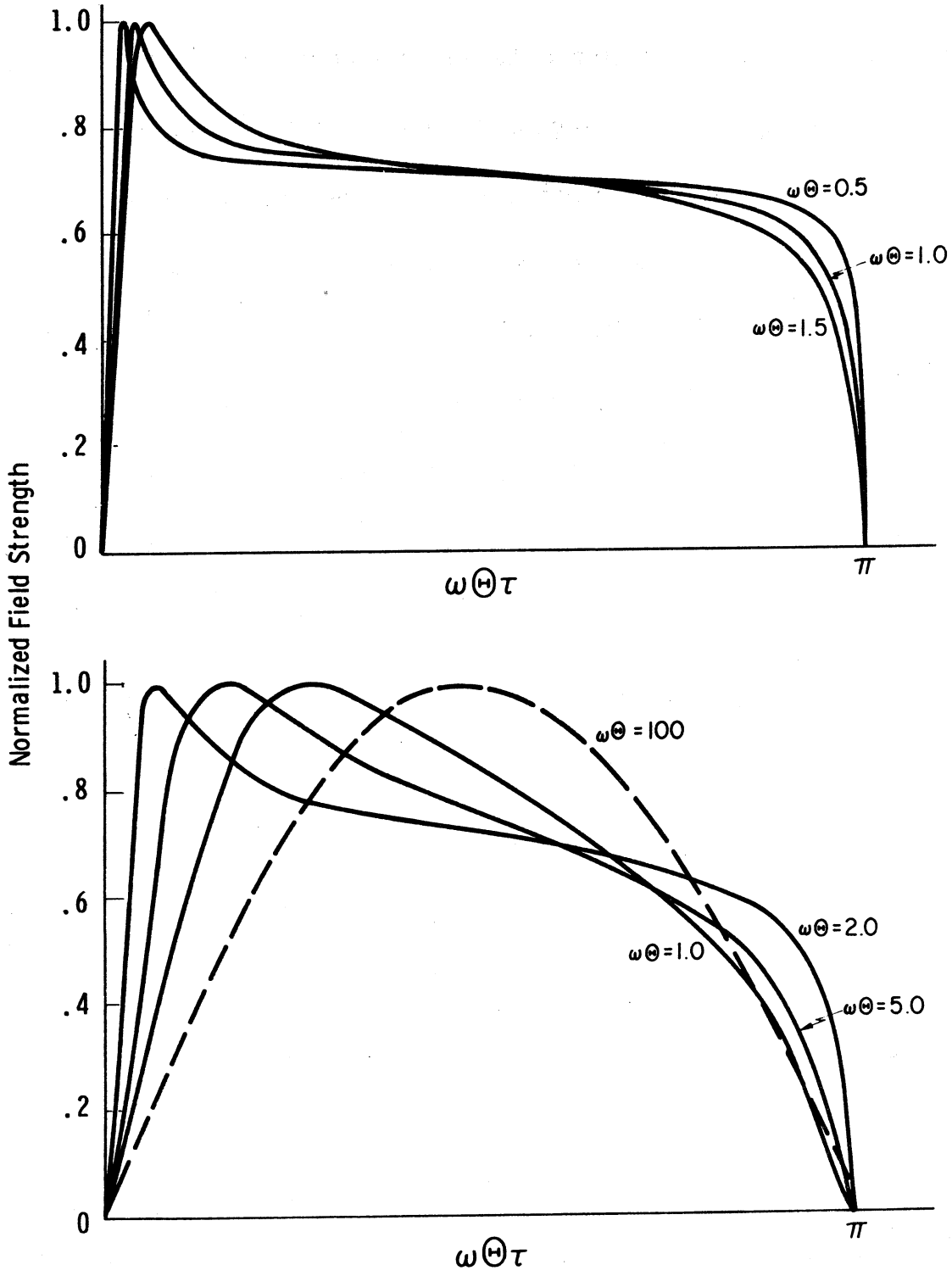

Figure 10. Electric Field Waveforms for a Constant Radius AC Arc

In Section 6, experimentally obtained electric field waveforms indicate that any analysis of the AC arc column must be capable of predicting two important features that are characteristic of small values of $\omega\Theta$. Shortly after the point of current zero passage, a large voltage spike appears which is known as the reignition peak. The voltage then drops sharply to a low plateau level, remains nearly constant for much of the half-cycle, and then rises slightly to a second peak before falling to zero at the next current zero passage. This second voltage spike is called the extinction peak. The value of $\omega\Theta$ at which these features occur is certainly less than 5 and probably close to unity.

A glance at Fig. 10 indicates that none of the analytically derived waveforms bear the proper resemblance to reality. The reignition peaks are too low relative to the plateau values to be realistic and an extinction peak never develops. It would, of course, be quite surprising if there were good agreement between experimentally obtained waveforms and those given by this simple analysis. For low values of $\omega\Theta$ one concludes that the moving radius must be included in a meaningful analysis of the AC column. Also, the value of $\omega\Theta$ at the lower limit of applicability of the analysis is certainly greater than five but just how much greater can only be determined by comparison with an exact solution of Eq. 1. Such a solution has been obtained and is discussed in the next section.

The results shown in Fig. 11 compare the variation of centerline heat flux potential for the "exact" arc and the "approximate" arc (Eq. 12) for $\omega\Theta = 100$ and $\rho_{dc} = .80$. The agreement is excellent indicating that 100 is a "large" value of the frequency parameter. A similar comparison is shown in Fig. 12 for the same ρ_{dc} and $\omega\Theta = 10$. Here the agreement is satisfactory but not as good as in the first case. A glance at Fig. 13 indicates why there begins to be a discrepancy between the two solutions. Shown there is the variation in $\rho(\tau)$, starting from a DC state and decaying to a quasi-steady AC value. For $\omega\Theta = 100$, the radius undergoes only a 1/2% oscillation about its mean value while the central heat flux potential has about a 5 1/2% variation. For $\omega\Theta = 10$ the oscillations are 7% and 40%, respectively so that the moving boundary has more than a second order effect in that case.

In the next section it is shown that a numerical solution to the exact Eq. 1 can be obtained and the low values of $\omega\Theta$, which correspond to those easily obtained in the laboratory, can be examined. In addition, it will be possible to say something about the time relationships between processes (heat generation, heat loss, etc.) that occur within the column, as well as the temporal variation in arc structure.

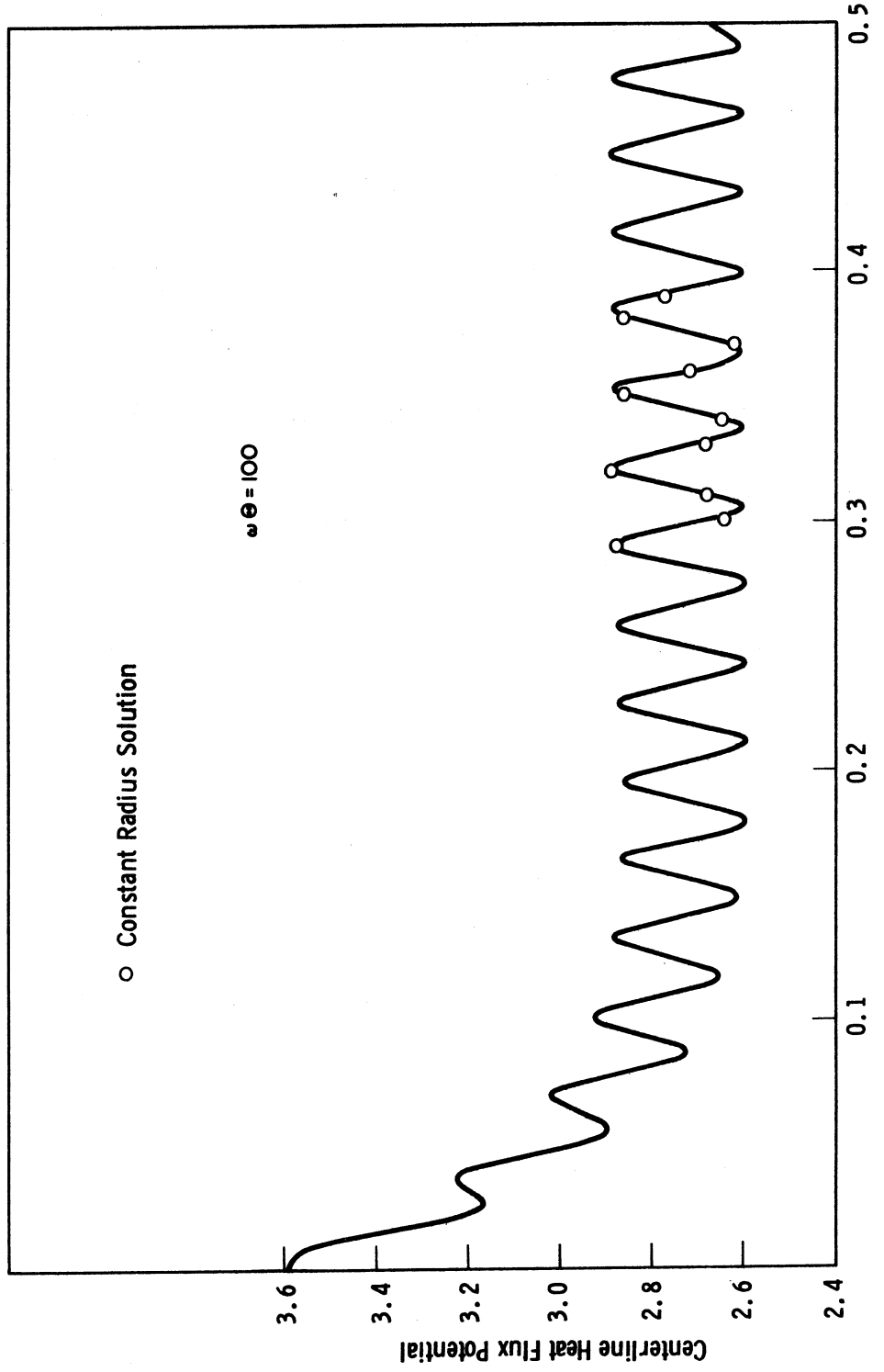

Figure 11. Comparison of Centerline Heat Flux Potential Behavior Obtained from the Constant Radius Model and from Numerical Computation, $\omega\Theta = 100$

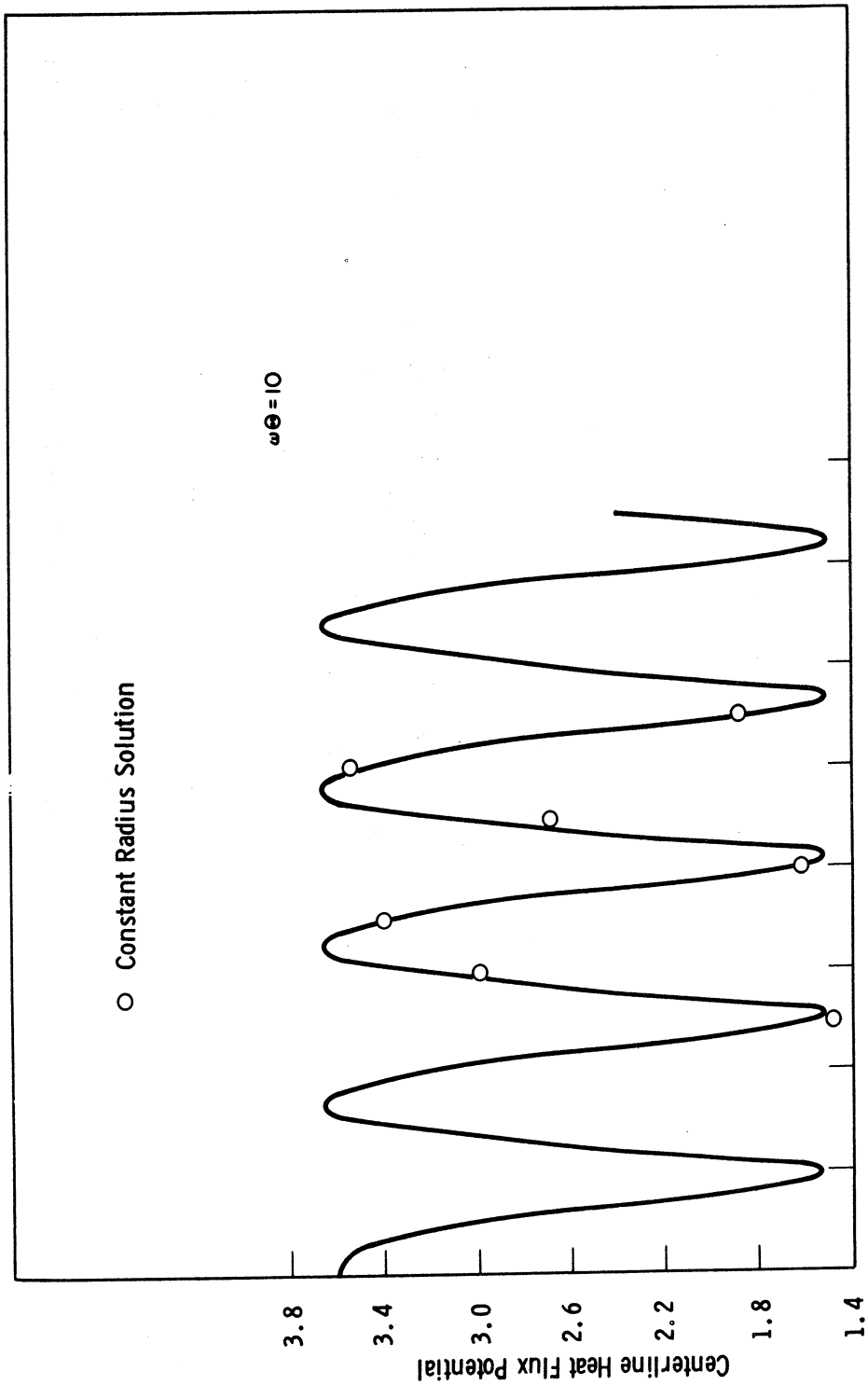

Figure 12. Comparison of Centerline Heat Flux Potential Behavior Obtained from the Constant Radius Model and from Numerical Computation, $\omega\Theta = 10$

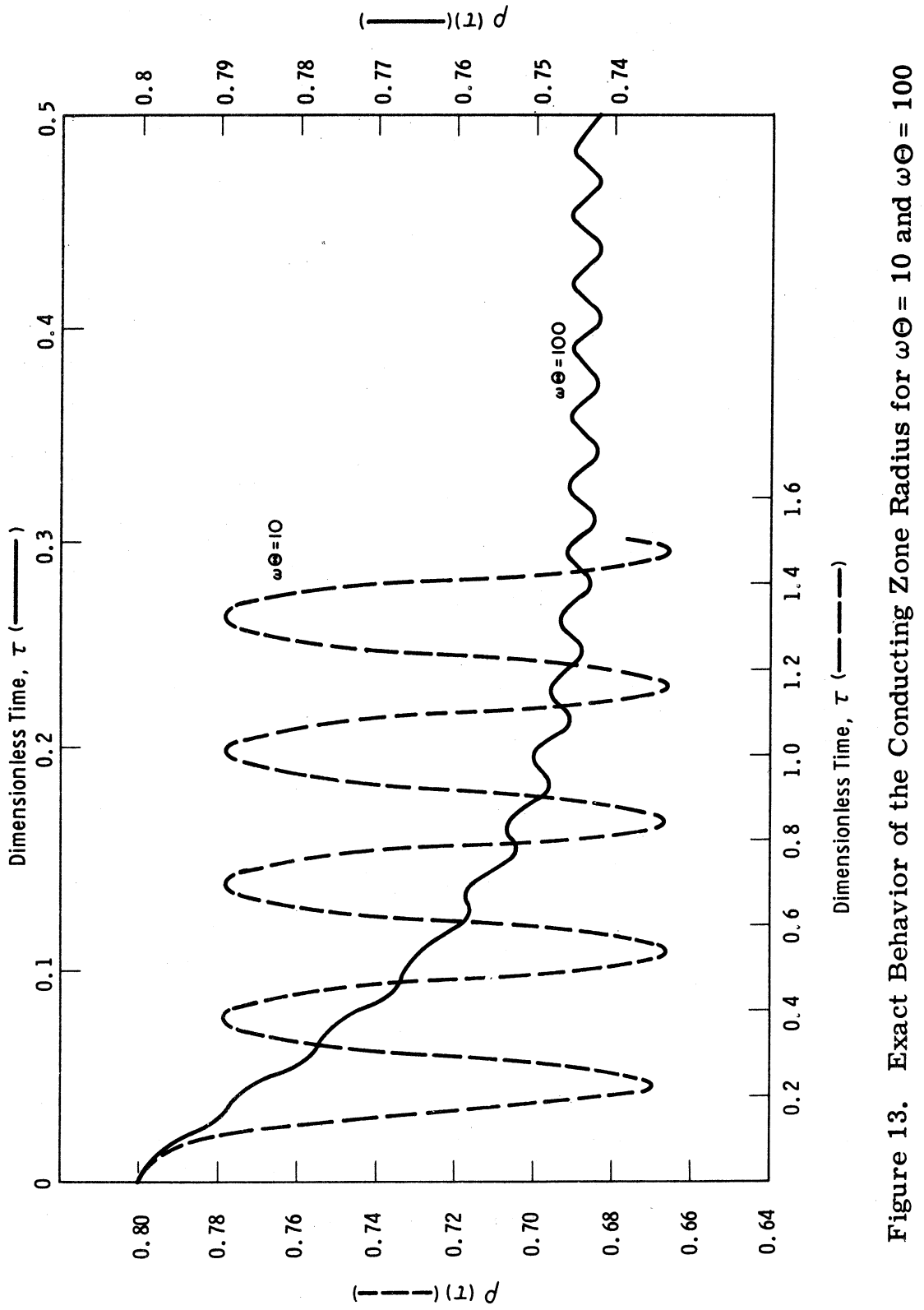

Figure 13. Exact Behavior of the Conducting Zone Radius for $\omega\Theta = 10$ and $\omega\Theta = 100$

5. THE NUMERICAL SOLUTION OF THE BOUNDARY VALUE PROBLEM

5.1 The Finite Difference Method

Except for the two special cases treated in the preceding sections, it has not been possible to find an analytical solution to the boundary value problem posed in Section 2. It was decided, therefore, to attempt to solve the system numerically for an AC positive column which receives a perfect sine wave of current from some imaginary power supply. Of course, the equations are capable of describing the processes occurring within any dynamic arc, but herein attention will be focused primarily on the AC column.

The art of solving partial differential equations by numerical techniques has been described in many recent books c. f. Forsythe and Wasow (38), Fox (39), and it is generally agreed that obtaining stable, accurate solutions economically and efficiently is troublesome. The technique adopted here is closely related to that used to obtain solutions to partial differential equations on analog computers. There one first applies a finite difference scheme to the space-like variables, leaving a series of ordinary differential equations to be solved in the usual way on an analog computer. This procedure is described in many places among which are (40), (41), and (42); the latter paper being a

very elegant treatment of the general procedures to be followed as well as the errors incurred by the application of finite differences. Fox (39) also mentions this procedure and suggests that one might try solving the resulting ordinary differential equations on a digital rather than analog computer by some simple forward integration technique such as the Runge-Kutta method. The accuracy is not better than that obtainable with an analog solution, but it is usually simpler to implement the digital process. Fox also gives a stability criterion that should be satisfied by the cell size of the finite difference scheme together with the step size for the time integration, but the experience of the writer has shown it to be too optimistic. In all cases it was necessary to use a step size that was considerably smaller than that given by Fox's criterion.

Finite difference schemes as applied to tabular data are discussed in many books on numerical analysis, typical of these is (43). Basically the idea is to examine the first, second, and higher order differences that exist between a given piece of data and its tabular neighbors and determine an approximate expression for the derivatives that exist at that point or close nearby. Fundamentally, there are forward, backward, and central difference schemes, with the essential differences between them being the direction that one proceeds from a tabular point to examine the differences between it and its neighbors. By using the

first order central difference method a rather high degree of accuracy can be obtained without the expense of undue mathematical sophistication.

Consider Fig. 14 where the coordinate system for the finite difference scheme is illustrated. It is presumed that the values of U and V at a particular time are known only at discrete stations (or in finite cells) in their respective spatial domains. The finite difference scheme consists of finding an interpolating polynomial that passes through the point in question and through an arbitrary number of neighboring points, depending upon the degree of accuracy desired. Then, first and second (partial) derivatives can be formed at each station and the partial differential equations are cast into a series of ordinary differential equations, equal in number to the prescribed number of cells.

From (43) or its equivalent one finds that the first and second derivatives at a point in the difference table, say, U_m, can be approximated in the first order central difference scheme by

$$\left.\frac{dU}{dx}\right|_m = \frac{1}{2\Delta x}(U_{m+1} - U_{m-1}) + O[(\Delta x)^2]$$

$$\left.\frac{d^2U}{dx^2}\right|_m = \frac{1}{(\Delta x)^2}(U_{m-1} - 2U_m + U_{m+1}) + O[(\Delta x)^2]$$

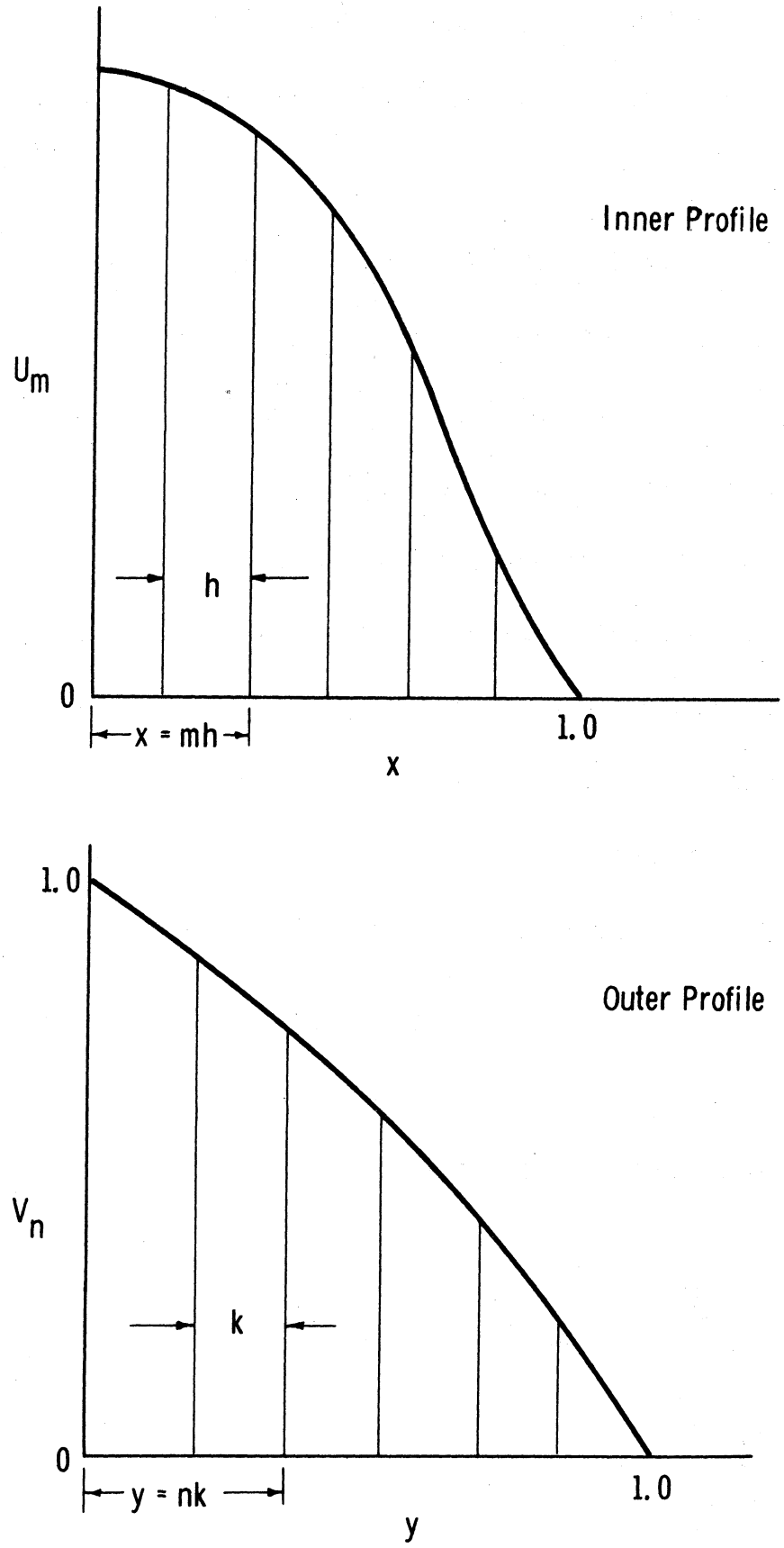

Figure 14. Coordinate System for the Finite-Difference Scheme

where U_{m+1} and U_{m-1} are the tabular values on the positive and negative side of U_m, respectively. The cell size is denoted by Δx and is related to the spatial coordinate by $x = m(\Delta x)$. At a boundary station it is easy to see that one can encounter difficulty, for fictitious cells are introduced. Often, at the boundaries, one switches to a forward or backward difference scheme giving the same degree of accuracy (second order in this case) in order to circumvent the introduction of a fictitious tabular value. There are manipulations that can make this unnecessary, however, and, in the present case, it has been found that the fictitious tabular values can be eliminated to yield needed additional relations that account for the moving boundary. Finally, it should be noted that at the axis of symmetry some additional manipulation is required since $U_x \to 0$ as $x \to 0$. By L'Hôpital's rule

$$\lim_{U_x,\, x \to 0} \left(\frac{1}{x}\frac{\partial U}{\partial x}\right) = \left.\frac{\partial^2 U}{\partial x^2}\right|_{x=0} ,$$

so that

$$\left[\frac{1}{x}\frac{\partial}{\partial x}\left(x\frac{\partial U}{\partial x}\right)\right]_{x=0} = \frac{4}{(\Delta x)^2}(U_1 - U_o) .$$

One can now proceed to prepare the set of equations in Eq. 1 for solution by the finite difference technique. For the inner, conducting

region let x = mh so that 1 = Mh, with M being the chosen number of cells. At m = 0 the special result above enables one to obtain

$$\frac{4}{h^2}(U_1 - U_o) + \rho^2 E^2 U_o = \rho^2 \frac{dU_o}{d\tau} \quad . \tag{14}$$

Otherwise, one finds

$$\frac{1}{h^2}(U_{m-1} - 2U_m + U_{m+1}) + \frac{1}{2mh^2}(U_{m+1} - U_{m-1}) + \frac{m}{4}\frac{d\rho^2}{d\tau}(U_{m+1} - U_{m-1}) +$$

$$\rho^2 E^2 U_m = \rho^2 \frac{dU_m}{d\tau} \tag{15}$$

$$m = 1, 2, \ldots, (M - 1) \quad .$$

The boundary condition $U(1,\rho) = 0$ gives the relation, $U_M = 0$ and, of course, the U_m are functions of τ only. Including the special case for m = 0, the above set provides M equations. So far, (M + 2) unknowns have been introduced, U_o through U_m as well as $\rho(\tau)$ and $E(\tau)$.

For the annular region let y = nk, 1 = Nk, and obtain

$$\frac{1}{k^2}(V_{n-1} - 2V_n + V_{n+1}) - \frac{(V_{n+1} - V_{n-1})}{2k[(1 - \rho)^{-1} - nk]} - \frac{n}{4}\frac{d\rho^2}{d\tau}\left(\frac{1 - \rho}{\rho}\right)(V_{n+1} - V_{n-1})$$

$$= (1 - \rho)^2 \frac{dV_n}{d\tau} \tag{16}$$

This equation holds for n = 1, 2, . . . , (N - 1) since both V_o and V_N are known from the boundary conditions. Thus (N - 1) more equations

and unknowns are introduced by consideration of the non-conducting zone. Two more equations are evidently required to make a determinate set. One of these is provided by Ohm's law (in which Simpson's rule is used to evaluate the integral) and the other must result from the compatibility condition for the derivatives at the moving boundary. Since $V_N = 0$, one can apply Eq. 16 at y = 1 (or n = N) and obtain

$$\frac{2}{k}\left[(V_{N+1} - V_{N-1}) + 2V_{N-1}\right] - \left(\frac{1-\rho}{\rho}\right)\left(1 + \frac{1}{2}\frac{d\rho^2}{d\tau}\right)(V_{N+1} - V_{N-1}) = 0 \quad .$$

The fictitious variable V_{N+1} appears in this equation but this is of no concern since it is the difference $(V_{N+1} - V_{N-1})$ which is of importance. With this difference term one can calculate the slope $\partial V/\partial y$ at y = 1. By rearranging the above expression one finds

$$\left.\frac{\partial V}{\partial y}\right|_{y=1} = \frac{1}{2k}(V_{N+1} - V_{N-1}) = -\frac{2V_{N-1}/k^2}{\left[\frac{2}{k} - \frac{1-\rho}{\rho}\left(1 + \frac{1}{2}\frac{d\rho^2}{d\tau}\right)\right]} \quad . \tag{17}$$

Similarly, at x = 1, Eq. 15 gives the result

$$\frac{2}{h}\left[(U_{M+1} - U_{M-1}) + 2U_{M-1}\right] + \left(1 + \frac{1}{2}\frac{d\rho^2}{d\tau}\right)(U_{M+1} - U_{M-1}) = 0 \quad .$$

Finally,

$$\left.\frac{\partial U}{\partial x}\right|_{x=1} = \frac{1}{2h}(U_{M+1} - U_{M-1}) = -\frac{2U_{M-1}/h^2}{\left[\frac{2}{h} + \left(1 + \frac{1}{2}\frac{d\rho^2}{d\tau}\right)\right]} \quad . \tag{18}$$

One can now apply the compatibility condition which Eq. 17 and 18 must obey and find

$$\left(1 + \frac{1}{2}\frac{d\rho}{d\tau}^2\right) = \frac{2}{hk}\left(\frac{\frac{U_{M-1}}{h} - \frac{\rho}{1-\rho}\frac{V_{N-1}}{k}}{\frac{1-\rho}{\rho}\frac{U_{M-1}}{h^2} + \frac{\rho}{1-\rho}\frac{V_{N-1}}{k^2}}\right) . \tag{19}$$

The condition $\rho = 1$, which could only occur for infinite current, will never arise. Thus, by suitable manipulation of the boundary conditions, an explicit ordinary differential equation for the boundary motion has been obtained. The original partial differential equations have been reduced to (M + N) ordinary differential equations for (M + N + 1) variables. The additional equation is the integral relation furnished by Ohm's law. The set is, of course, still badly non-linear and recourse to numerical techniques is necessary.

There are many methods available for solving the initial value type of ordinary differential equation (or set of equations) but for the present problem it was found to be convenient to use the Gill modification of the Runge-Kutta technique (43). This method has the advantages of requiring no starting solution (only initial values are needed), the step size may be changed at will anytime during the computation, and it is inherently stable. In addition, the fourth order technique, which

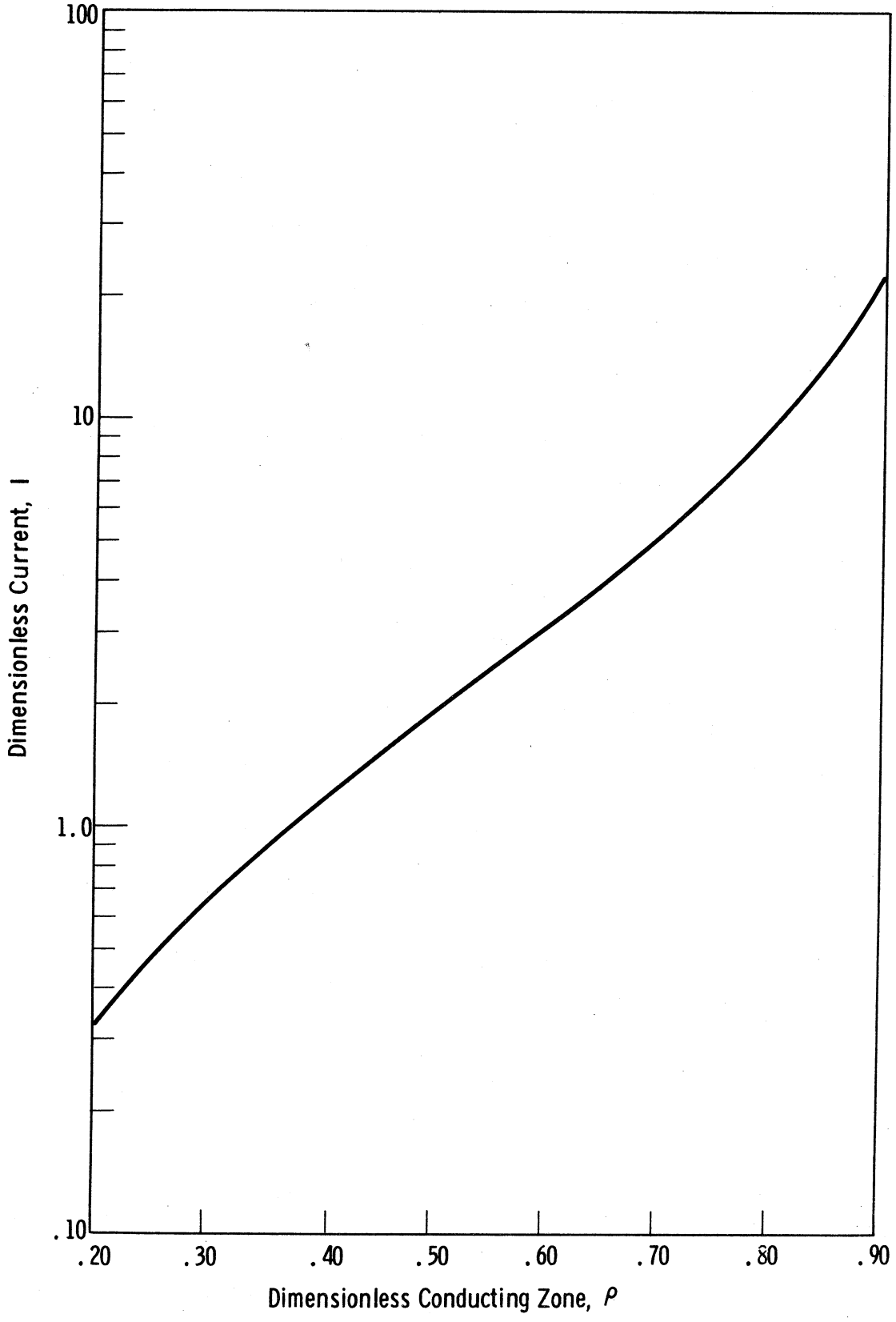

Figure 15. Dimensionless Current vs. Conducting Zone Radius for the DC Arc

was used herein, has an error at each step that is proportional to only the fifth power of the step size.

Ohm's law and Eq. 14, 15, 16, and 19, were programmed for solution on The University of Michigan IBM 7090 digital computer wherein the Runge-Kutta method is included as a library sub-routine. The MAD language (Michigan Algorithmic Decoder) was used in programming this problem and it was presented to the computer in as general a way as possible so that changes in the program could easily be made by varying only data cards in the input deck. For initial conditions it was convenient to use the structure of a DC arc carrying a dimensionless current I_m. For the AC arc a cosine variation of current is assumed to begin at $\tau = 0$ and I_m then becomes the peak value of current. Actually, it is more convenient to assign an initial value of ρ and calculate the resulting value of I_m from the DC solution. The relation between the conducting radius and I_m is shown in Fig. 15. It is seen that neither an infinite nor zero value of current can be tolerated in the present approximation to the AC arc problem so that care must be taken in the numerical computation to insure that cumulative errors do not cause ρ to vanish. In addition to the parameter I_m (or its equivalent ρ), one must specify the product $\omega\Theta$ which is needed in the expression

$$I = I_m \cos(\omega\Theta\tau) \quad .$$

This is sufficient information to permit computation of all the V_n, U_m, ρ and E for each instant of time. Usually, the transient period between the DC arc and the quasi-steady AC solution is of no interest and the solution is carried out far enough in time to insure the establishment of a steady state. The balance of this section will be concerned with the steady state AC arc which carries a perfect cosine wave of current. Furthermore, except for one or two special cases, only $\omega\Theta$ will be varied over a significant range, I_m being held constant.

Besides the temperature distribution and electric field strength there are other quantities associated with the arc which are useful in interpreting its behavior. These are the instantaneous power input and the instantaneous power transferred to the tube walls. These two variables can easily be computed according to the finite difference scheme. The heat entering the tube walls is given in dimensional variables as

$$2\pi R \frac{\partial S}{\partial r}\bigg|_R = P_{out} \text{ (watts/cm)} \quad .$$

With the transformations and dimensionless variables introduced earlier, one can bring this expression into the form

$$\frac{P_{out}}{(S_1 - S_2)} = \frac{2\pi}{(1 - \rho)} \frac{\partial V}{\partial y}\bigg|_{y=0} \quad .$$

Upon evaluating the above derivative in finite difference terms one obtains

$$\overline{P}_{out} = \frac{2\pi}{k(1 - \rho)} \cdot \frac{(V_1 - 1)}{\left[1 + \frac{k}{2}(1 - \rho)\right]} \quad .$$

where the bar denotes non-dimensionalization with respect to $(S_1 - S_2)$. The dimensionless power delivered to the arc is easily found to be

$$\overline{P}_{in} = E(\tau) \cdot I(\tau) \quad .$$

Finally, there are one or two situations where it is fruitful to consider the arc as a circuit element, in which case the current can no longer be specified. Thus an additional unknown is added to the system, but a circuit equation can also be written. The circuit which has been chosen is easily represented and is also commonly used. It is presumed that the arc burns in series with a pure inductance of L henries and a power supply which generates a voltage, $V_m \sin \omega t$. The circuit equation can be written as

$$V_m \sin \omega t + L \frac{dI^*}{dt} + E^* \ell = 0 \quad ,$$

where ℓ is the effective length of the arc (positive column) and the asterisks denote dimensional quantities. In dimensionless form one obtains

$$\frac{dI}{d\tau} = -\omega\Theta\left(\frac{V_m}{V_L}\right)\left(\sin\omega\Theta\tau + \frac{V_a}{V_m}E\right) \tag{20}$$

Here

$$V_L = \omega LRB^{1/2}(S_1 - S_2) \quad \text{and} \quad V_a = \frac{\ell}{RB^{1/2}},$$

which are two additional parameters to be specified when necessary.

The accuracy of the finite difference scheme has not been thoroughly investigated but a comparison of some numerical results for large $\omega\Theta$ with the closed form solution presented earlier shows close agreement. For this comparison the boundary velocity was set to zero in the numerical computation so that the same problem was solved in both cases, i. e., analytically and numerically. In addition, a computation using fewer cells (4 rather than 6) was tried for a particular problem ($\omega\Theta = 3$) and no appreciable effect on the numerical result was observed.

5. 2 Numerical Results and Discussion

From Fig. 15 one finds that for $\rho_{dc} = 0.8$, $I_m = 9.4$. Depending upon the particular type of gas and constrictor size for which one

desires physical results, this could represent current levels from a few amps to perhaps 100 amps. With this parameter fixed, $\omega\Theta$ has been varied between 1 and 100. Furthermore, N = M = 6 in all cases. Rather than deluge the reader with dozens of curves, only the most representative of the numerical results is presented and discussed. Three sets of data corresponding to high, intermediate, and low frequencies are scrutinized.

In Figs. 16, 17, and 18 are shown the pertinent variables for a high frequency column, $\omega\Theta = 100$. The applied current waveform is common to all three figures in order to facilitate comparison with the forcing function of the problem. At this frequency the closed form solution obtained earlier agrees well with the exact solution, as shown in the preceding section. In addition to the arc current, Fig. 16 shows the variation of $U_0(\tau)$, the centerline heat flux potential and the conducting zone radius, $\rho(\tau)$. The oscillation frequency for U_0 and ρ is about twice the fundamental, a fact also indicated by the approximate solution. Since the frequency is so high that the arc displays an Ohmic type of behavior, the power input to the column varies as $I^2(\tau)$. The heat flux potential and other thermally determined variables react not primarily to the current, but to the power input. Thus, the sine squared behavior of the heat flux potential and $\rho(\tau)$. The power input

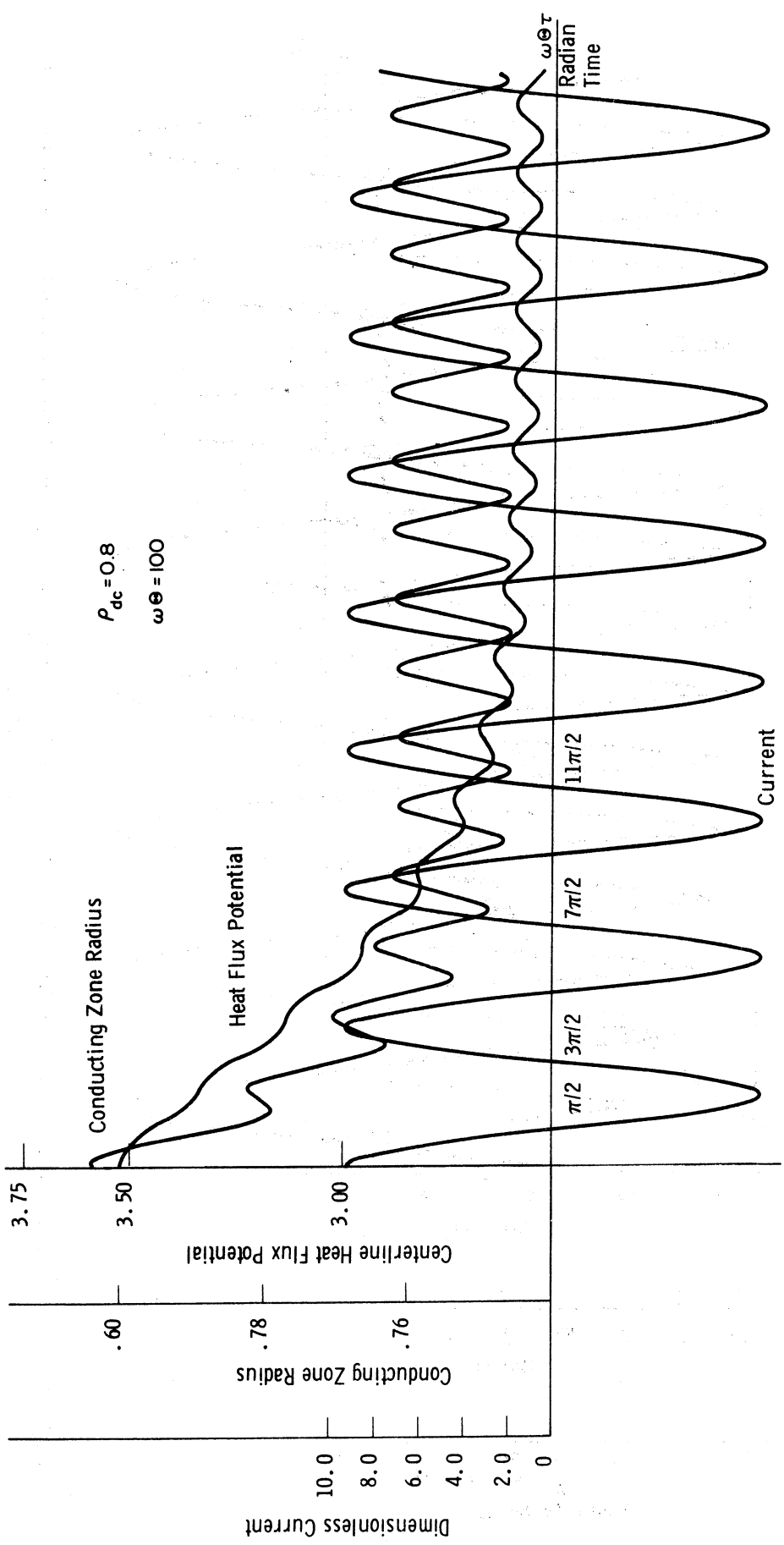

Figure 16. Theoretical Waveforms of Centerline Heat Flux Potential, Conducting Zone Radius, and Dimensionless Current for $\omega\Theta = 100$

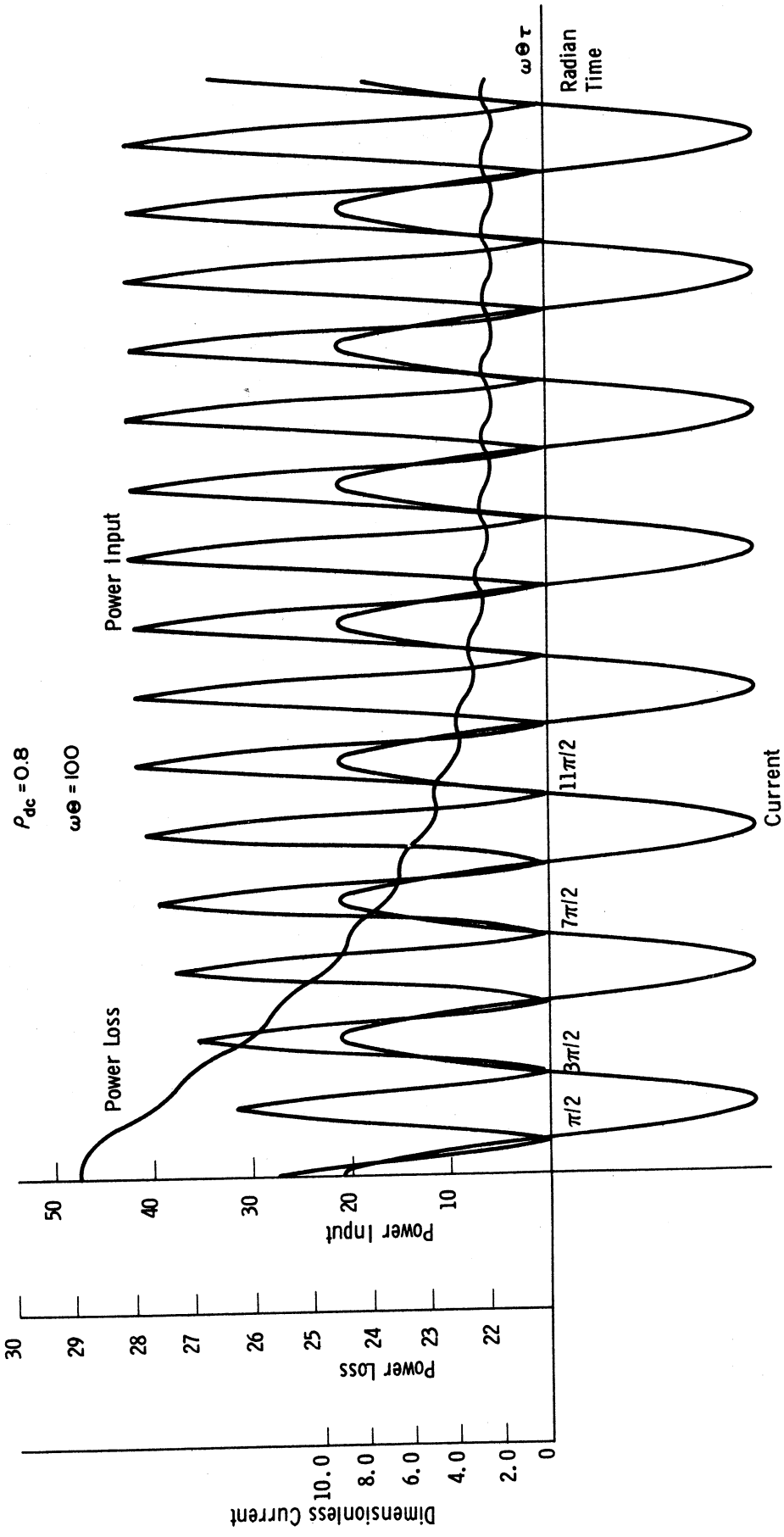

Figure 17. Theoretical Waveforms of Power Input, Power Loss, and Dimensionless Current for $\omega\Theta = 100$

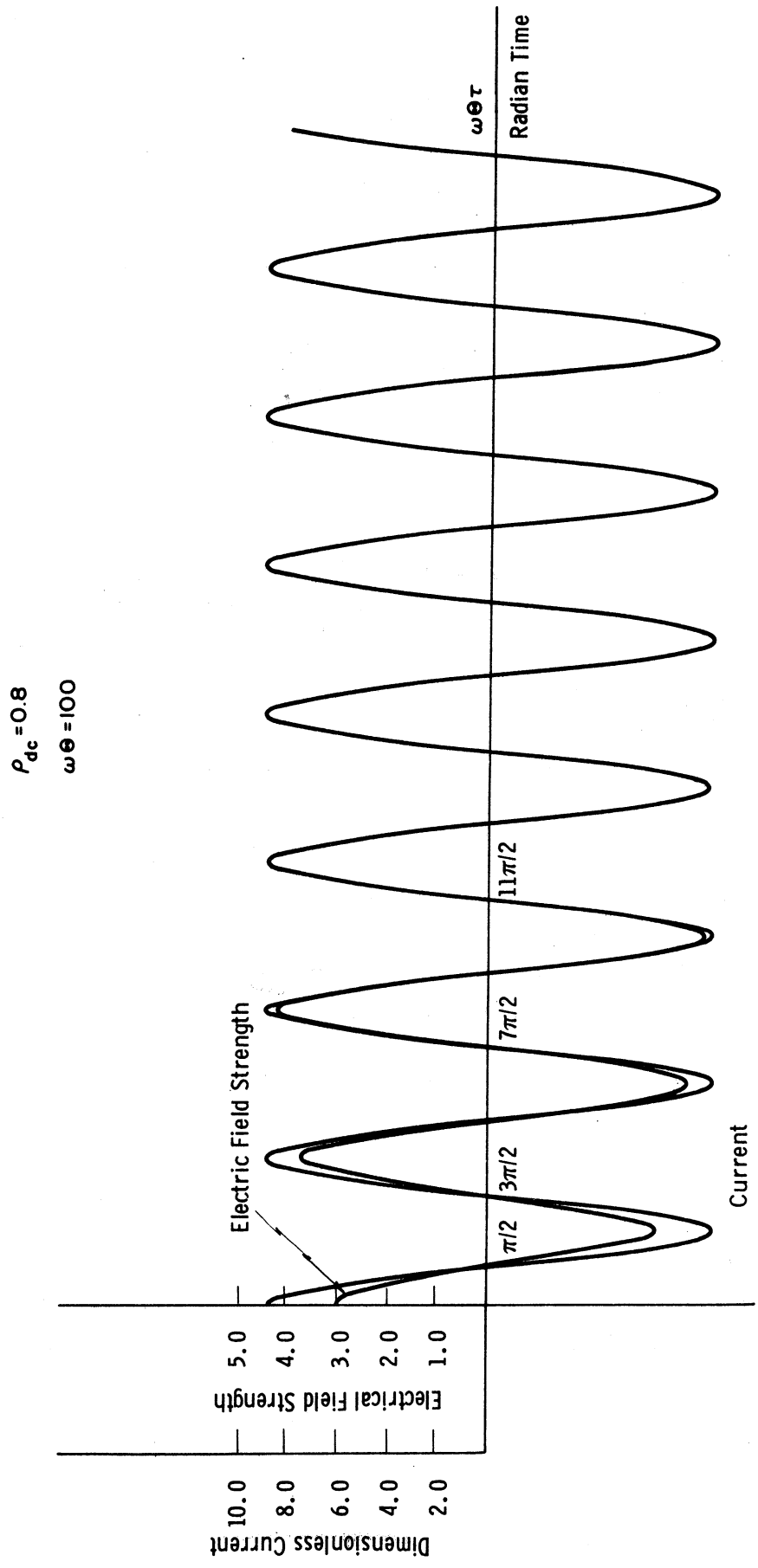

Figure 18. Theoretical Waveforms of Electric Field Strength and Dimensionless Current for $\omega\Theta = 100$

behavior is shown in Fig. 17 and clearly has a sine squared character. The power lost to the tube walls, also shown in Fig. 17, departs only slightly from a mean value that is nearly equal to the average power input to the column. If $\omega\Theta$ were infinite, there would be no temporal variation at all in the power loss behavior; it would be precisely equal to the average power input. In Fig. 18 the electric field variation is shown along with the current, and the expected proportionality between the two quantities is evident. In general, the power is nearly in phase with the applied current and all of the thermal and thermally determined variables lag the power input by about 90^{o}. The sole exception is the arc radius, which lags the power input by about 130^{o}. This is reasonable since the conducting zone radius must lag somewhat the centerline temperature variation.

At lower effective frequencies (lower $\omega\Theta$) the entire character of the arc changes. Since the thermal properties can follow the externally applied variations more faithfully, there are large changes in the heat flux potential, conducting zone radius, and other variables. There no longer exists the proportionality between the applied current and the arc voltage that one finds at higher $\omega\Theta$. In fact, the arc voltage

waveform assumes quite an unusual shape due to the large, non-linear changes in thermal conditions which occur. Furthermore, the waveforms of the thermal variables begin to resemble fully rectified sine curves, rather than the pure sine curves (of twice fundamental frequency) that occur at higher frequencies.

The waveforms of the variables of interest for an arc having an $\omega\theta$ of 5 are shown in Figs. 19, 20, and 21. The centerline heat flux potential, the arc radius, $\rho(\tau)$, and the applied current are shown in Fig. 19. There is initially a rapid fall-off in both $U_o(\tau)$ and $\rho(\tau)$ as the current is modulated away from the DC value. When the current reverses, however, and approaches a negative maximum, the heat flux potential quickly rises to a level which even exceeds the DC value. This is possible because the arc is not losing energy as fast as it is gaining it, as for the stationary discharge. On the other hand, the conducting zone radius never quite reaches its DC magnitude, indicating that the higher overall temperature (and the concomitant higher conductivity) allows the arc to carry the same current with a smaller radius. Notice the rectified sine wave behavior, referred to above, that is manifested by both $U_o(\tau)$ and $\rho(\tau)$. This results because the current waveform (actually power) can be closely followed by the arc, except at the zero passage points where a cusped behavior is in

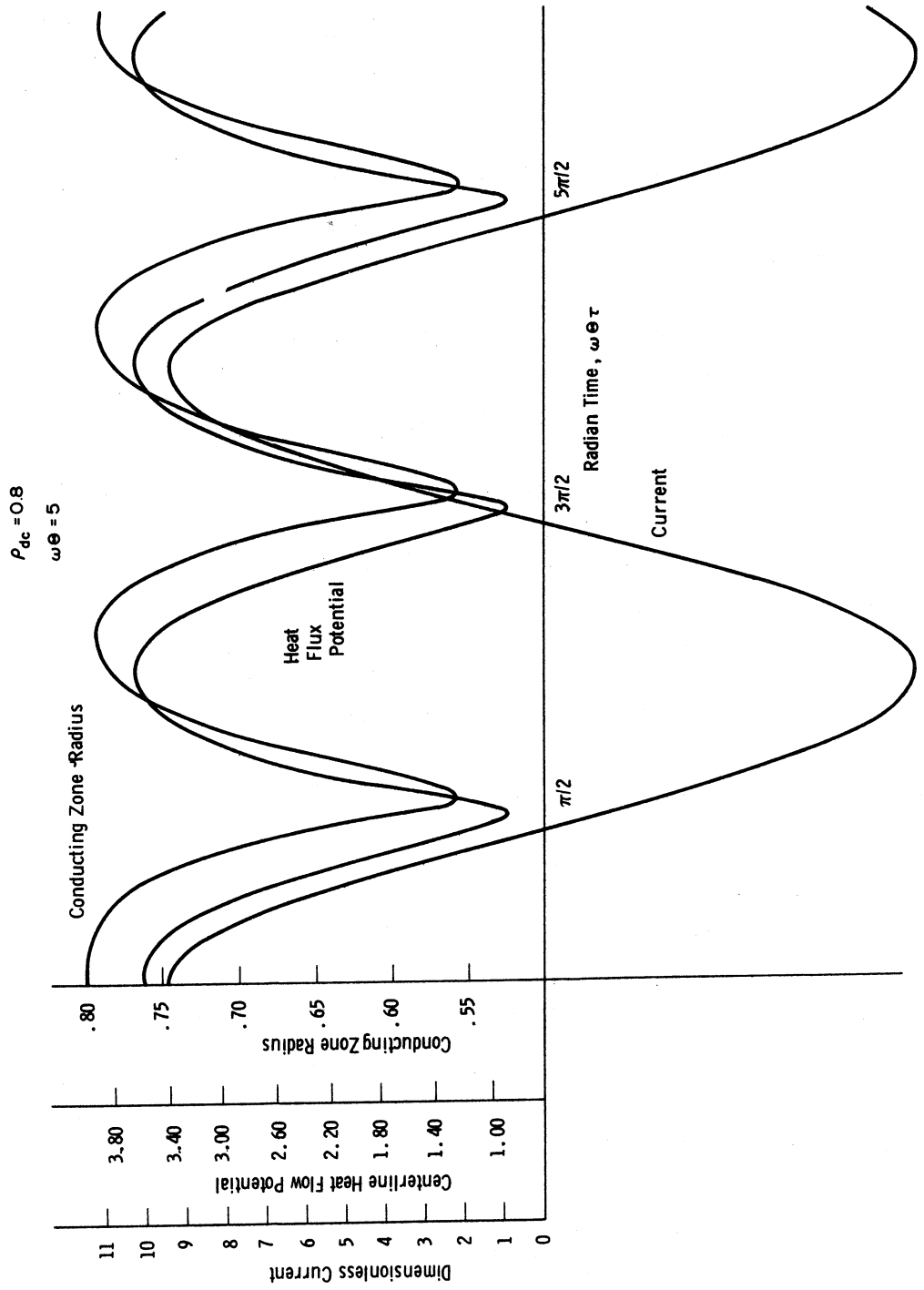

Figure 19. Theoretical Waveforms of Centerline Heat Flux Potential, Conducting Zone Radius, and Dimensionless Current for $\omega\Theta = 5$

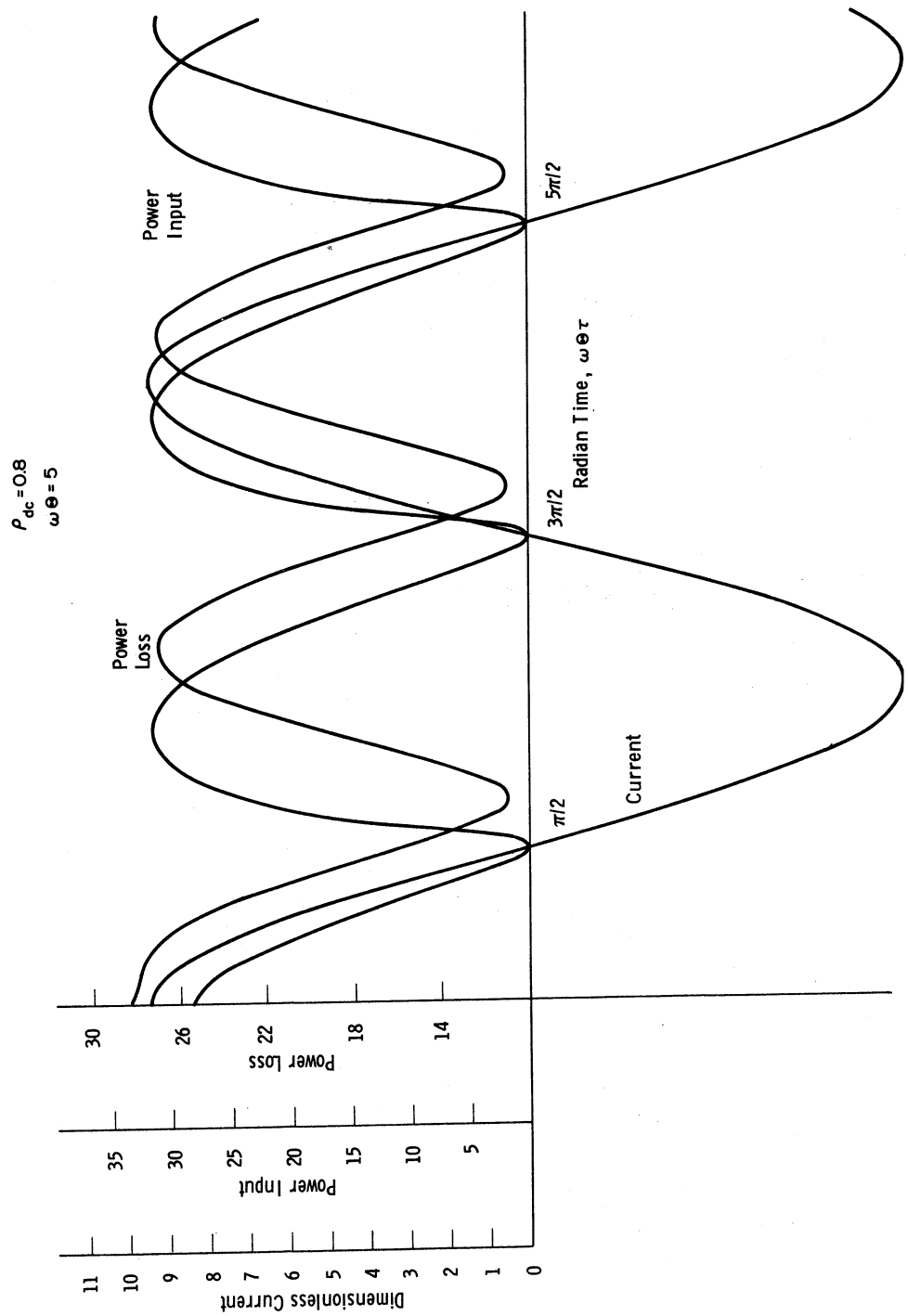

Figure 20. Theoretical Waveforms of Power Input, Power Loss, and Dimensionless Current for $\omega\Theta = 5$

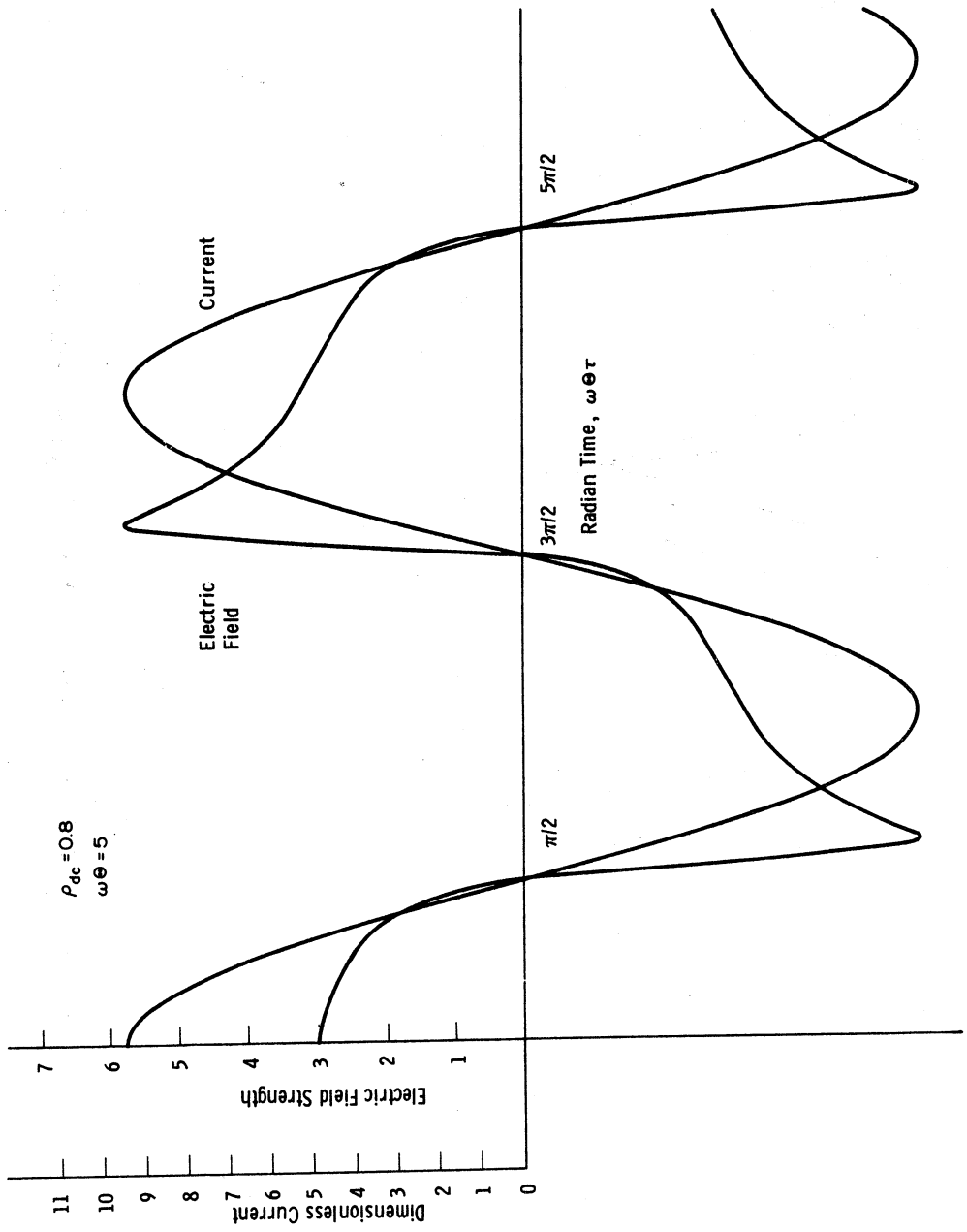

Figure 21. Theoretical Waveforms of Electric Field Strength and Dimensionless Current for $\omega\Theta = 5$

evidence. Of course, the thermal variables must always have a positive sign so there must be a rapid reversal in behavior as the current changes direction.

The power input and loss waveforms are shown in Fig. 20, with the rectified behavior again occurring. There is a marked asymmetry to the power input waveform and one notices that it reaches a maximum well before (leads) the current. The reason for this behavior will be explained shortly. Notice first, however, the lag in power loss with respect to the heat generation function, the phenomenon that accounts for the temperature overshoot mentioned above.

In Fig. 21 the electric field waveform displays a sharply rising behavior, immediately following the current zero passage. Physically, this obtains from the arc having lost considerable energy (and having gained resistance) during the interval when the current was low. The small time constant indicates that the arc stores energy poorly and rapidly loses the qualities of a good conductor of electricity. Since the current is specified, the force (electric field) required to produce this electron flux becomes large and remains so until sufficient energy has been added to significantly increase the column conductance. Since the power input depends upon the product of E and I, its asymmetric character is easily understood. It must lead the current by a

considerable amount, for the electric field reaches its peak at nearly the beginning of a cycle, about 90^{o} before the current. Note, also, that the strong departure of the $E(\tau)$ waveform from a sine curve indicates the presence of harmonics higher than the fundamental. This suggests some interesting speculations on the power factor of an AC arc, a subject to be discussed later.

Finally, consider the characteristics of a low frequency arc, as depicted in Figs. 22, 23, and 24. Here, $\omega\Theta = 1.0$, a value close to that obtained in the laboratory for an argon arc. The rectified sine curve behavior is even more pronounced than in the previous case, as seen from the cusped nature of the centerline heat flux potential in Fig. 22. In the same figure is shown $\rho(\tau)$; one notices immediately the broad maximum that is exhibited. Since the conducting boundary position is determined by a special heat flux equilibration (as described earlier), the broad peak indicates that over a large portion of the half cycle of heating an inflection point in the profile resides at $x = 1$. Close to the point of zero current passage, however, the conducting zone radius changes very rapidly, drops to a sharp minimum, and then rises quickly to a nearly constant value for the next half-cycle. From another point of view, the small value of $\omega\Theta$ used for these calculations implies that the DC characteristic (the E-I curve) can be rather faithfully

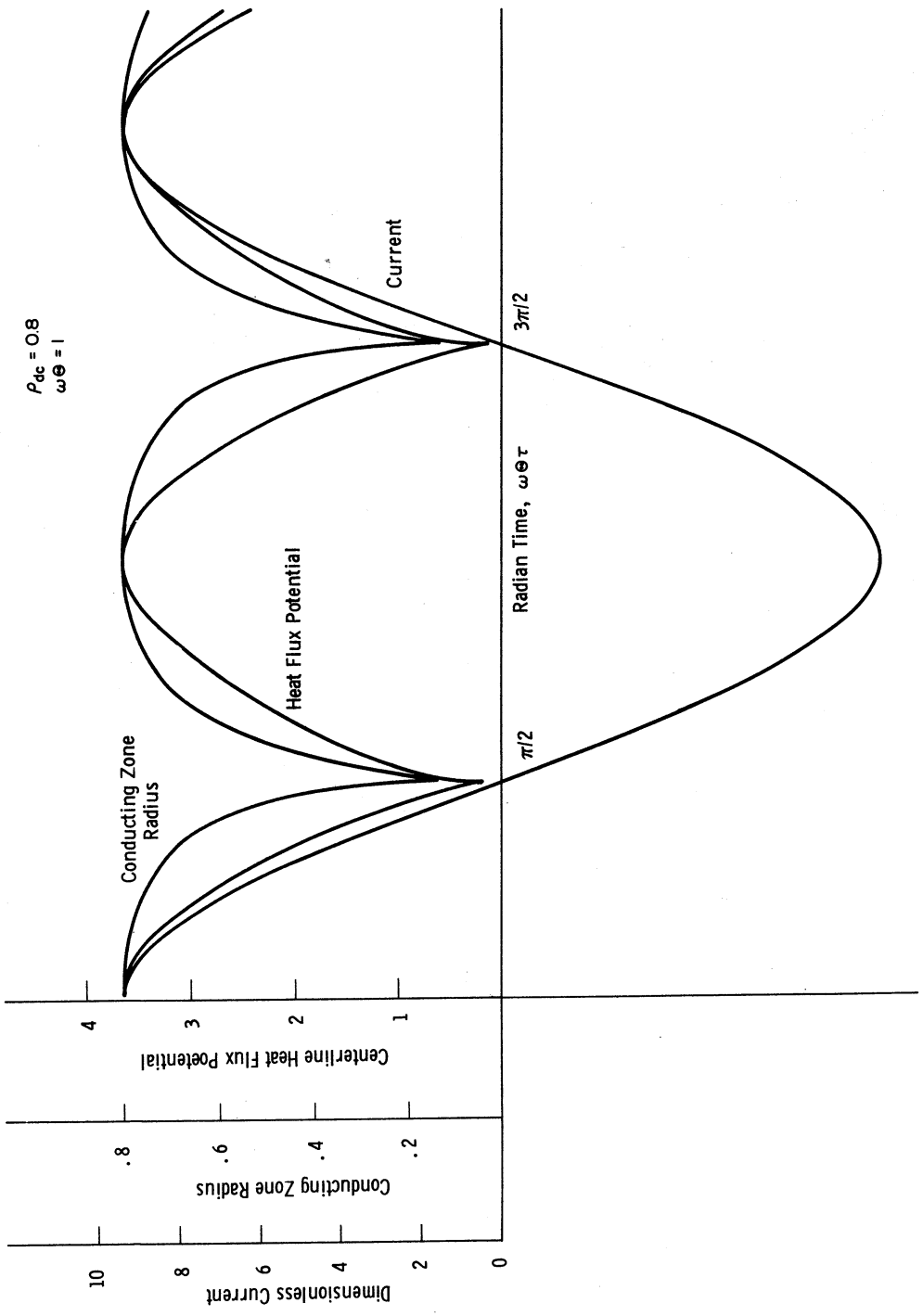

Figure 22. Theoretical Waveforms of Centerline Heat Flux Potential, Conducting Zone Radius, and Dimensionless Current for $\omega\Theta = 1$

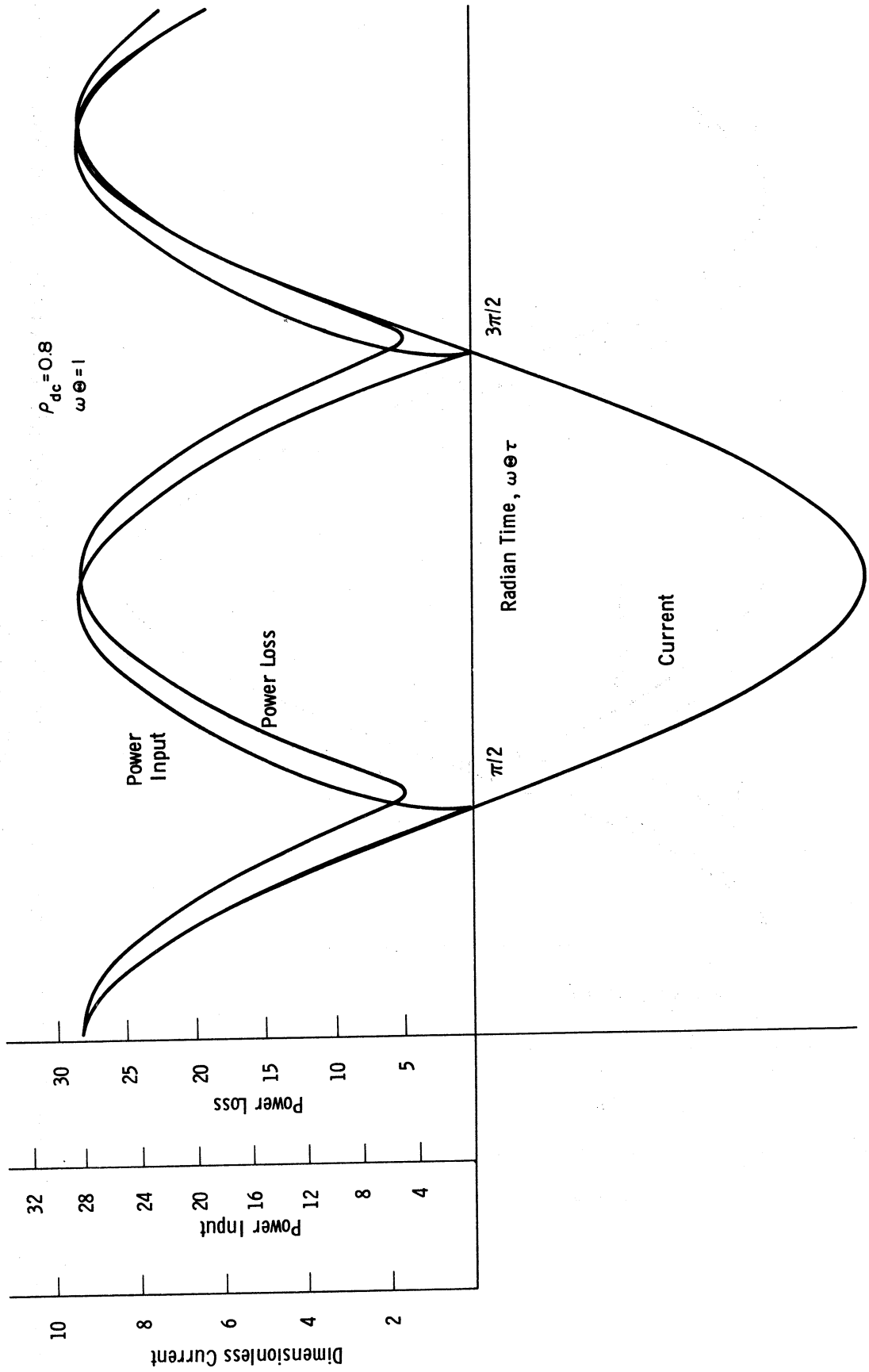

Figure 23. Theoretical Waveforms of Power Input, Power Loss, and Dimensionless Current for $\omega\Theta = 1$

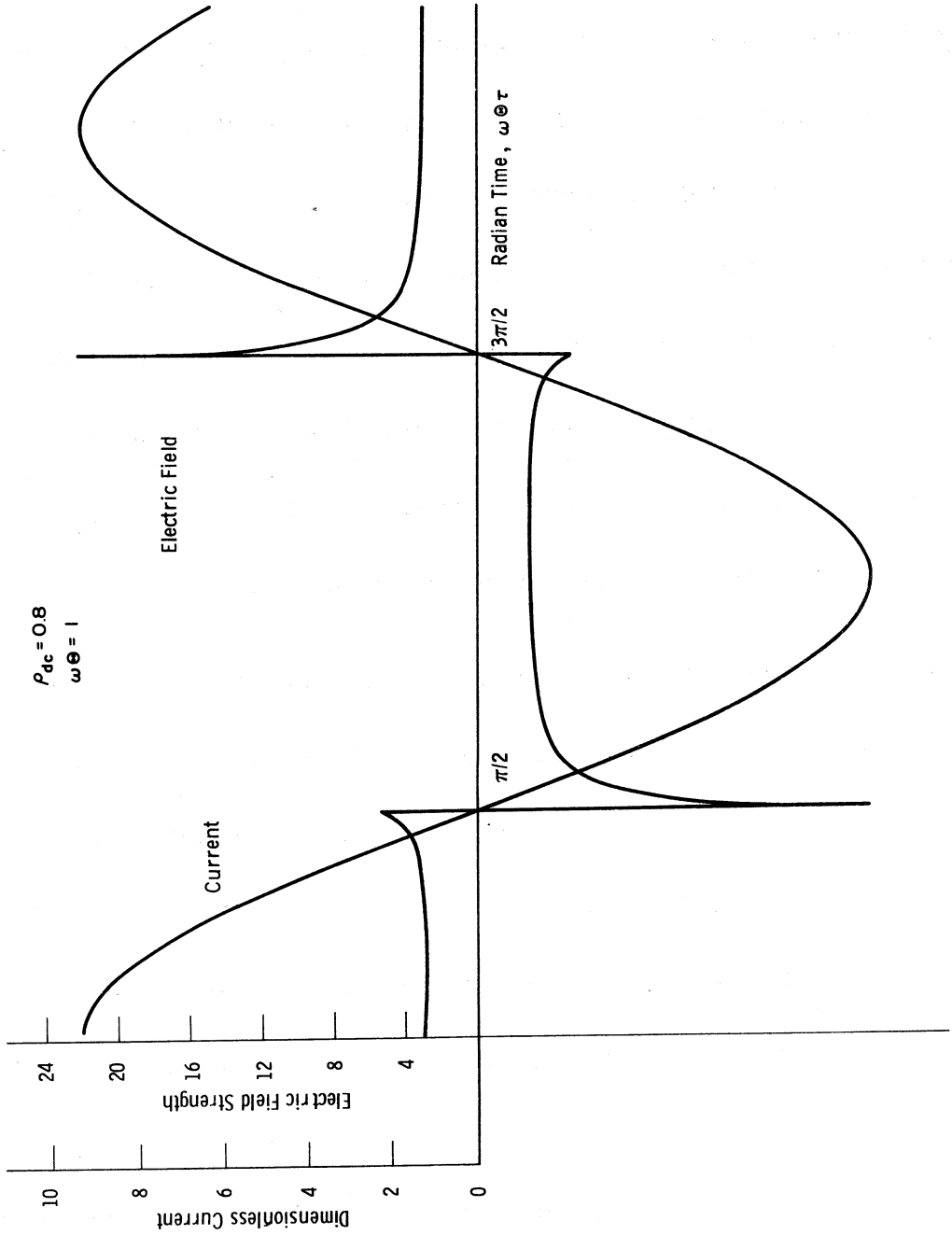

Figure 24. Theoretical Waveforms of Electric Field Strength and Dimensionless Current for $\omega\Theta = 1$

followed. From the DC solution found in the previous section one can construct such a characteristic as well as a curve that relates ρ_{dc} to I_m. The behavior of these variables is shown in Figs. 15 and 25. During the high current portion of the sine wave input, the arc is operating on the branch of the $\rho_{dc} - I_m$ curve where $d\rho/dI$ is very small. Hence, the flat top for the $\rho(\tau)$ curve. Near current zero, however, the static curve can no longer be followed and the sharply rising and falling portions of the radius curve are dictated by dynamic considerations. On the other hand, the centerline heat flux potential has more nearly the shape of the input current since, at large values of ρ, the DC solution indicates near proportionality between ρ and I.

The input power and power loss functions are shown in Fig. 23, with the former closely resembling the centerline heat flux potential. Again, this is expected because of the low effective frequency of the present example. The power loss function, however, has a much smoother behavior than any of the other thermal variables. No cusps occur at all, and with good reason. From the expression given earlier for $\overline{P}_{out}$, it is evident that only the heat flux potential adjacent to the wall, V_1, and the radius $\rho(\tau)$ enter into its determination. The cusped character of, say, the centerline heat flux potential indicates the presence of very high frequency harmonics in its waveform. It is characteristic of transient heat conduction problems that a heat wave is

dispersed during propagation through the heat conducting medium. In the present problem one can think of the electrically conducting core as a distribution of heat sources having a certain temporal variation. As the heat flows to the cold walls, the high frequency components of the heat generation function are strongly attenuated, meaning that close to the wall only the low frequency behavior appears. Hence, the smoother behavior of the power loss function.

Finally, in Fig. 24, the electric field waveform exhibits some interesting characteristics. Compared to the DC value, there is an immense reignition transient immediately following the zero current passage. The arc suffers a rapid loss in conductance when it is momentarily extinguished so that a large field is required to drive the specified current. As the column gains energy again, from the Joule heating, the field strength drops to a value that is comparable to the DC level and remains nearly constant for over 50% of the half cycle. This plateau behavior is explained by reference to the static characteristic, Fig. 25. Here, one sees that at high current levels the arc voltage varies only slightly with the current. At a low frequency the AC arc can closely follow the static characteristic until, of course, the time comes for current reversal. Then the analogy no longer is valid. At its lowest point the AC arc burns with a voltage somewhat

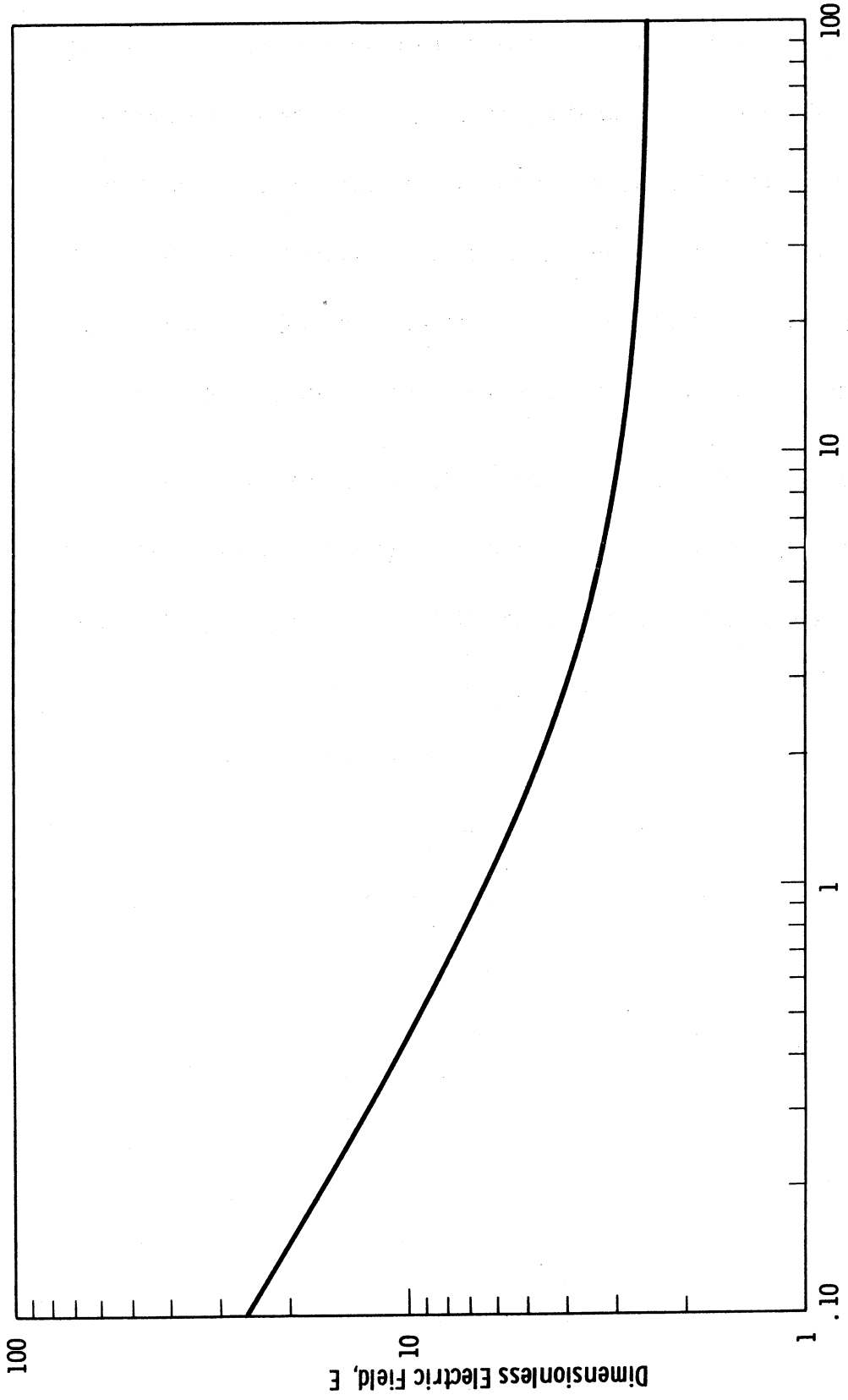

Figure 25. Theoretical Voltage-Current Characteristic for DC Arc

below the corresponding DC level. This is a dynamic effect due to the AC arc actually over ionizing as a result of the initial voltage transient.

The behavior of AC and DC arcs can be clearly shown in a cyclogram or dynamic E-I characteristic. Such a plot appears in Fig. 26, with only the positive half-cycle of the AC arcs being shown. At high frequencies the near-Ohmic, positive characteristic is in evidence, while for $\omega\Theta = 1$ the falling DC characteristic is closely approximated. In fact, this close adherence to the DC curve brings about a voltage rise before current zero passage that has been observed experimentally; it is known as an extinction peak. For the conditions assumed in the present numerical calculations, it appears that $\omega\Theta$ must be less than 1.5 before an extinction peak develops. The presence of an external circuit or of different current magnitudes may alter this conclusion considerably.

Returning to the electric field waveform for the high frequency arc, one sees, by comparison with Fig. 24, that the character has changed from that of a pure sine curve nearly to that of a square wave. The non-linear element, which is the arc, introduces harmonics into a circuit that are not originally there; the current is, after

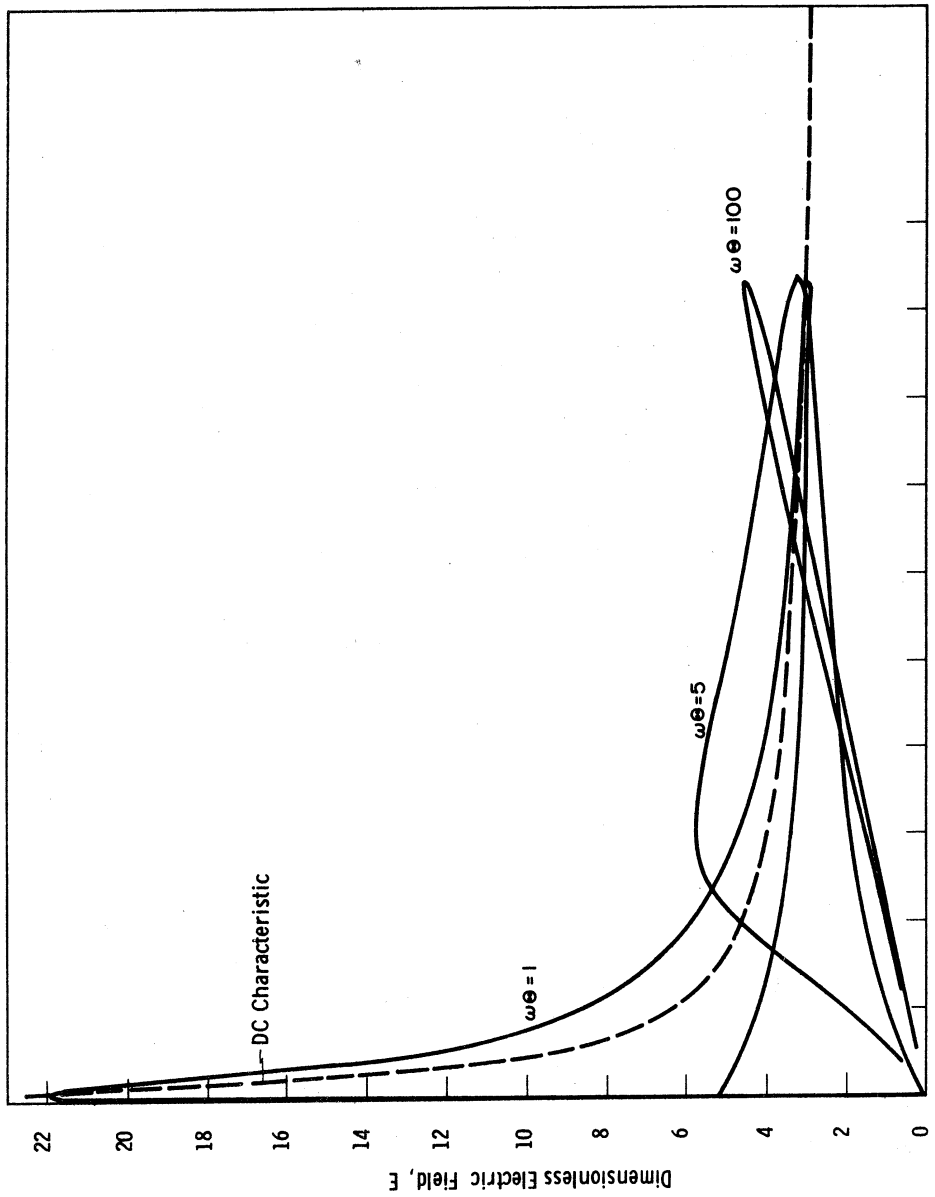

Figure 26. Theoretical Dynamic and Static Arc Characteristics

all, a pure wave form. It is interesting to examine one of the more obvious consequences of the presence of harmonics in a circuit element that are higher than fundamental.

If one retains the usual definition of power factor for a circuit or part circuit, one finds that the power factor for an AC arc carrying a pure sine wave of current can be significantly different from unity. It should be emphasized that this statement applies for the arc alone and not a complete circuit. For the usual AC circuit with linear elements it is easy to understand a non-unity power factor; some amount of the input energy is always stored in a capacitor or inductor. Here, however, all input energy must be dissipated in the arc and to understand the existence of a power factor less than one it is necessary to re-examine the concept of effective or root-mean-squared circuit quantities.

In (44) the special considerations which must be given to the analysis of a circuit that contains non-fundamental harmonics is carefully described. The concept of Fourier decomposition is introduced; any periodic waveform can be represented by a linear superposition of the many frequency components which it comprises. If the average power of a circuit element is defined by

$$W = \frac{1}{T} \int_0^T E \cdot I \, d\tau \quad ,$$

where T is the fundamental period, one can easily show that a value of W, different from zero, is obtained only by the combination of a voltage and current of the same frequency. That is, if E and I are represented by their respective Fourier series, the cross product terms in the above integrand will contribute nothing to the value of the integral, W. In the present case $I(\tau)$ is a pure harmonic with no overtones, so the amplitude of its first and only harmonic is simply I_m. The voltage waveform, however, is rich in higher harmonics, none of which will contribute to the average power. Upon integrating the above expression one obtains

$$W = \frac{1}{2} E_{m1} I_{m1} + \frac{1}{2} E_{m2} I_{m2} + \cdots \quad ,$$

where E_{mi} and I_{mi} are the magnitudes of the various voltage and current harmonics. No phase angle between voltage and current has been assumed to exist, but no generality is lost by this assumption. It is most essential to recognize that since the I_{mi}, $i > 1$, are all zero, the average power is simply given by

$$W = \frac{1}{2} E_{m1} I_m$$

On the other hand, the usual definition of effective voltage requires that

$$E_{eff} = \frac{\sqrt{2}}{2} \sqrt{E_{m1}^2 + E_{m2}^2 + \cdots} \quad .$$

As usual, $I_{eff} = (\sqrt{2}/2)\, I_m$ and it is easy to see that if the voltage wave has a non-fundamental harmonic of even the most minute magnitude, the power factor of the arc, $W/(I_{eff} \cdot E_{ff})$, cannot be precisely one. Physically, the large arc voltage that is required to overcome the high resistance that follows extinction is ineffectively used to produce power. The current is very low at this point and the power added to the arc is trivial compared to that potentially obtainable from a situation where the voltage and the current have the same harmonic content. In Fig. 27 the variation in arc power factor with the effective frequency, $\omega\Theta$, is shown. When one is trying to dissipate power by means of an AC arc it is clear that the higher the value of $\omega\Theta$, the more efficient the utilization of the available power supply. This non-linear effect, therefore, is definitely penalizing to the arc heater designer who uses AC power.

Another consequence of the presence of overtones in the electric field waveform is that the possibility arises of non-equilibrium effects occurring. Not only is the reignition transient of a much higher

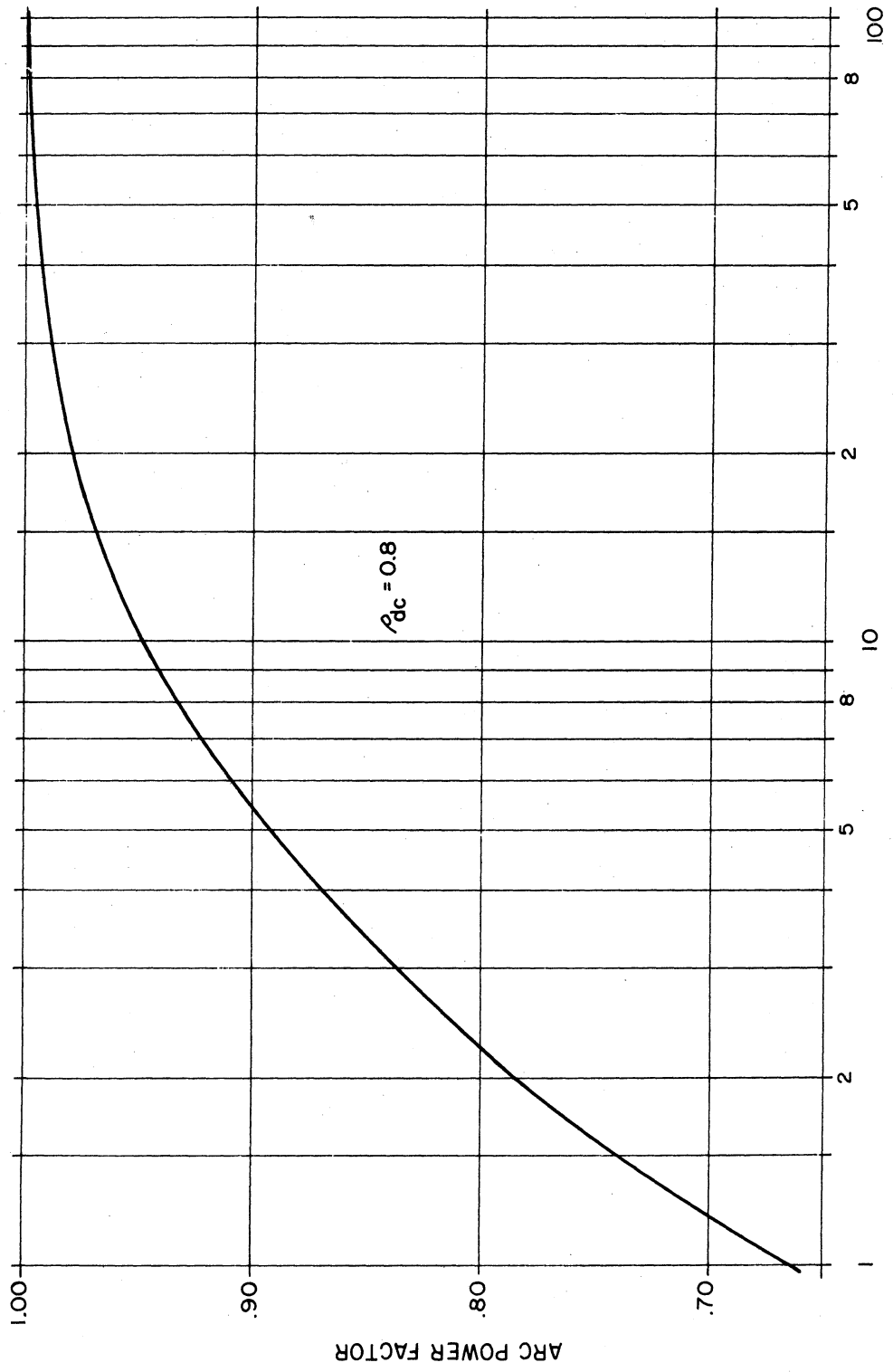

Figure 27. Theoretical Power Factor vs. $\omega\Theta$ for an Isolated AC Arc

frequency than the fundamental, but, in addition, it is due to a very rich harmonic. The result is that the arc voltage momentarily rises to a value that, in the case $\omega\Theta = 1$, is about 8 times higher than the plateau level. While this voltage spike is applied to the arc, the probability of the electron gas having a higher local temperature than the ion and atom gas is large. Furthermore, the frequency at which the transient field is applied to the column is at least an order of magnitude greater than the fundamental frequency, an apparent violation of the assumptions made at the outset of this study. Closer scrutiny indicates, however, that is not the case.

Chemical non-equilibrium is brought about by overly rapid changes in the gas temperature or, what is the same here, the heat flux potential. While the steep voltage rise causes the power input to increase more rapidly than normal, the effect on reaction times is not large. Since the reignition transient quickly disappears, the slopes of the power input and heat flux waveforms soon return to allowable values. Thus, the only significant effect of the abnormally high field strength could be to cause the electron gas to be greatly out of equilibrium with the heavier parent gas particles. Again, however, this effect would only last as long as the reignition spike itself unless, after the voltage is back to normal, the equilibration time between the two gases is very long. It was pointed out earlier, however, that the time

required for this type of equilibration, under the conditions of interest here, is of the order of a microsecond. This is three orders of magnitude lower than the minimum period allowed under the present analysis. It is not likely, therefore, that the reignition transient will cause a significant deviation from the predicted equilibrium conditions. It is of interest, however, to estimate by how much the electron temperature could possibly deviate from the parent gas temperature.

If one compares the energy gained by electrons moving in the existing electric field with that lost to the heavy particles during collisions, the following relation is obtained as a criterion for testing the existence of kinetic thermal equilibrium:

$$\frac{T_e - T_g}{T_g} = \frac{e^2E^2}{3fm\nu_e^2 k T_g} \ll 1$$

Here T_e and T_g are the electron and gas temperatures, respectively, e is the electronic charge, f is the fraction of electron energy transferred per collision to a heavy particle, ν_e is the collision frequency and k is the Boltzmann constant. The above expression is simple to derive and may be found in (45) or (46). Using values that are appropriate to an atmospheric pressure nitrogen arc with a centerline temperature of about $10,000^{\circ}K$, it is possible to obtain a rough estimate of the

degree of non-equilibrium which might exist between the electron and heavy particle gases. According to (45), f can be taken as 10^{-3} since some fraction of the collisions that take place are inelastic. Taking $\nu_e = 5 \times 10^{11}$, according to (47), and $T_g = 10,000^{\circ}K$, one finds

$$\frac{(T_e - T_g)}{T_g} = 2.72 \times 10^{-6} E^2 \quad ,$$

if E is in volts/cm. For the nitrogen arcs that have been operated in this laboratory, a reignition spike as high as 100 v/cm has been observed. Under these conditions, the electron temperature can be about $270^{\circ}K$ higher than the parent gas. The plateau voltage, however, is about 40 v/cm, in which case the degree of kinetic non-equilibrium is trivial. Since the spike rapidly disappears, the two gases will quickly equilibrate; no important effects due to electric fields are anticipated.

Finally, to complete this section, a few heat flux potential and temperature profiles that result from the numerical computations are presented. For the high frequency arc there is virtually no deviation from the mean value profile, which in turn closely resembles the DC structure. The latter is shown in Fig. 28 for an initial dimensionless arc radius of 0.8. There, also, is shown an intermediate profile for the

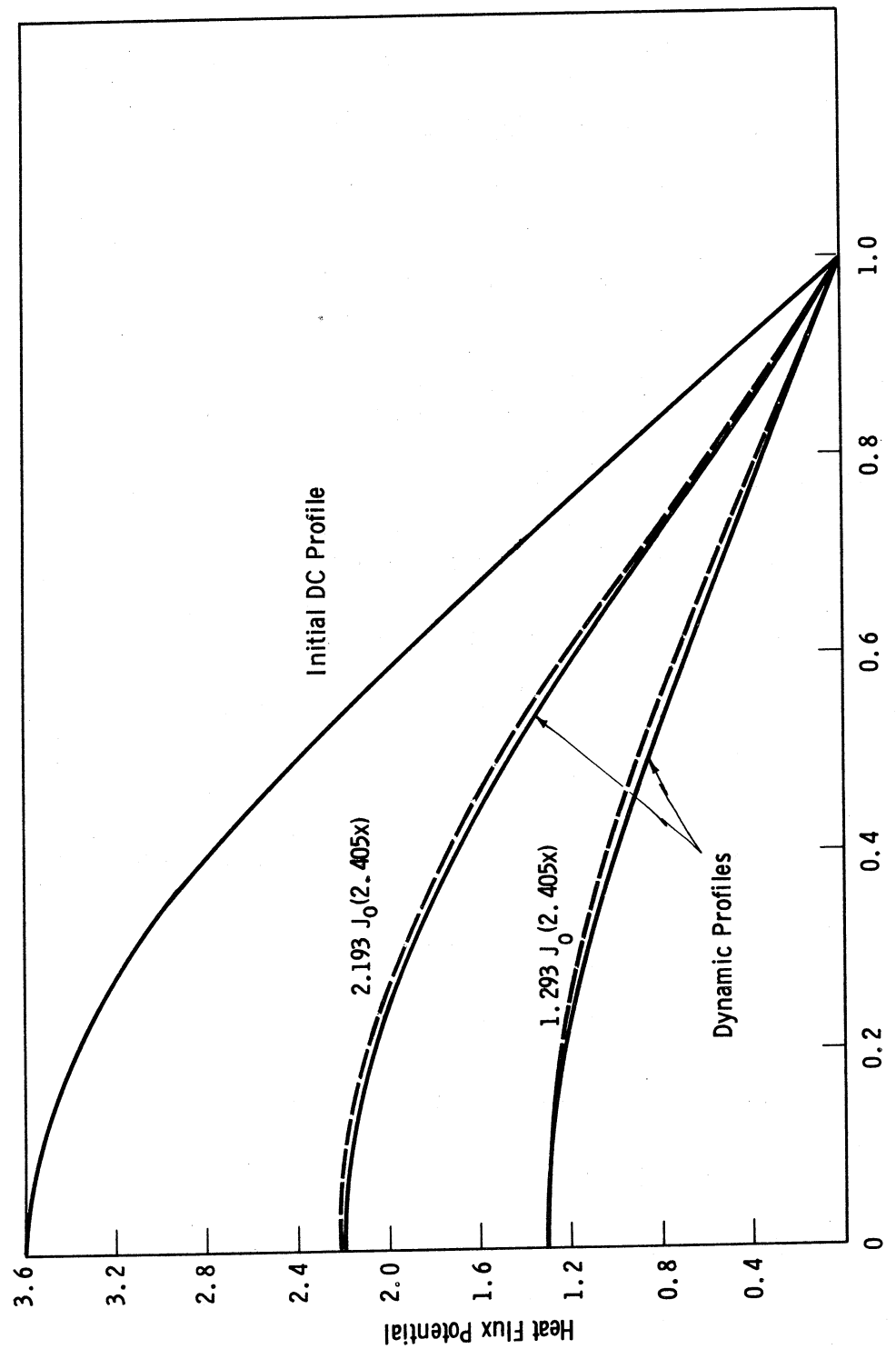

Figure 28. Theoretical Heat Flux Potential Profiles for the Electrically Conducting Region of an AC Arc

$\omega\Theta = 1$ case, as well as the heat flux potential cross-section at the lowest point in the cycle. Bessel function profiles, appropriate to DC only, are included for comparison. It is seen that the dynamic effects of the AC arc do not cause significant deviation from these curves.

In Fig. 29 temperature profiles for nitrogen are shown, with the thermal conductivity data being due to Avco (26). At a high current (and hence high temperatures) the hot core characteristic of molecular gases is in evidence. As the current passes through zero the temperature profile becomes very flat, with a steep gradient near the tube wall. Nothing untoward or unexpected, however, is displayed by these profiles.

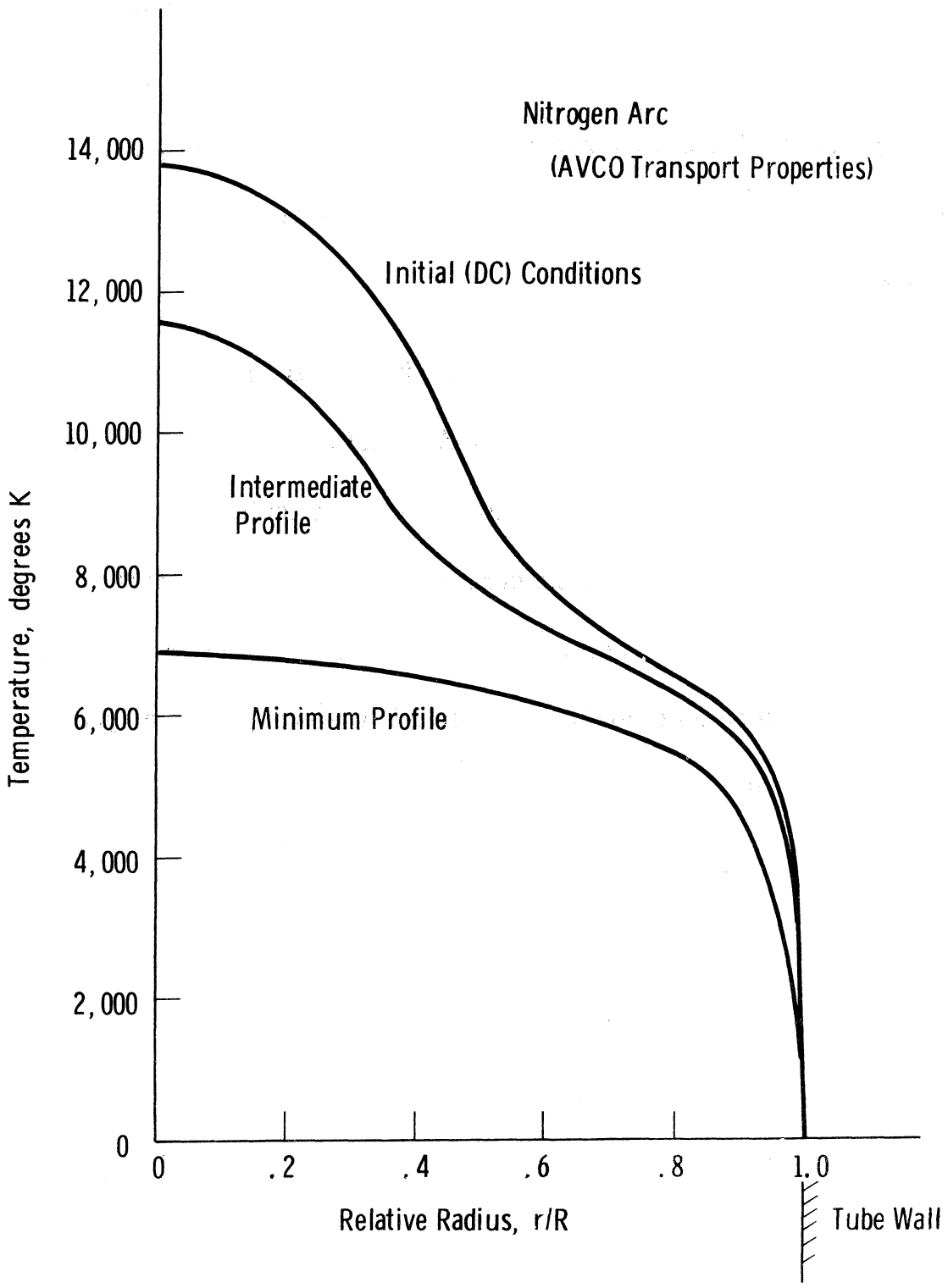

Figure 29. Theoretical Temperature Profiles for a Nitrogen AC Arc

6. THE EXPERIMENTAL DETERMINATION OF AC ARC CHARACTERISTICS

6.1 The Alternating Current Cascade Arc

The measurements of the properties and characteristics of AC arc columns that are reported in the literature have all been made under poorly known and poorly controlled conditions. For the most part, measurements have been made on free burning arcs, where the effects of natural convection are not accurately known. By way of contrast, there are some excellent and carefully taken measurements on DC columns that have been reported in recent years. These have been made possible by the use of a device first reported by Maecker (24) in 1960. This is the cascade arc, so-named because the arc is forced to strike through holes drilled in a series of copper disks that are electrically and thermally insulated from each other. The effect is to produce a wall stabilized arc in a highly anisotropic tube; it is a good conductor in the radial direction, but has all the properties of an insulator along the tube axis. According to Maecker and others, it is possible to create an extremely steady and reproducible discharge in an apparatus of this sort, with the obvious additional advantage that the arc boundary conditions are known precisely. With this device, Maecker and others have obtained very accurate measurements of DC arc characteristics (E-I curves) and column temperature profiles.

Also, it has been possible to infer from these measurements some transport properties of high temperature gases. If the individual disks are well cooled the tube wall can be held at nearly a constant temperature and, if a portion of the column where no axial gradients exist can be found, one has the experimental counterpart of the cylindrically symmetric wall stabilized arc. As mentioned earlier this arrangement is amenable to analysis.

An additional advantage of the cascade arc is that column potential differences (and hence electric field strength) can be measured directly without the interference of electrode effects. Each copper disk, being electrically isolated from the circuit, acts as a probe; it assumes some potential that is characteristic of the local column properties. A high input impedance instrument can be used to measure the potential difference that exists between any two disks. To be sure, a space charge sheath will form on the inside of the probe (disk) so that absolute potentials cannot be determined in this way. In a fully developed portion of the discharge, however, the sheath effects at any two disks will be comparable. Thus, the potential difference measurement will be accurate.

In order to obtain data for the AC column to compare with the present theoretical work, it was necessary to construct a Maecker-like

cascade arc. The use of AC power with such a device, however, presents one or two problems that are not present in the DC counterpart.

It is conceivable that the stack of disks, insulated one from the other, can act as a shunting capacitor to the arc column, thereby changing its characteristics. It was necessary to verify that this was not the case, since only pure arc behavior was desired. First, the capacitance of the device with no arc present was measured directly with an impedance bridge and was found to be 20 pf. In addition, with the arc burning, a varying amount of shunt capacitance, up to 12 μf, was purposely added to the circuit to determine at what value the arc waveform was noticeably changed. There was no observable effect for the range of operating conditions that prevailed. Physically, one would not expect the capacitance to play a large role unless the maximum energy it could store were comparable to the arc energy. A comparison of typical values indicated that the cascade capacitance should be of no consequence.

A second problem peculiar to AC cascade operation is due to a power supply imposed limitation. Since the arc voltage rises to large values after the current zero passage, complete extinction can result unless the available open circuit voltage can overcome this transient. The total reignition voltage is, of course, strongly dependent upon

column length so that with a fixed open circuit voltage it is important to minimize the total arc length. At the same time, however, one must have sufficient length to allow the development of an asymptotic column. While the theoretical problem of the approach to the asymptotic column is very difficult, the apparent success of the Stine and Watson (9) simplified analysis of the DC arc moves one to attempt a similar approach for the AC column. If such a solution could be obtained it would permit one to predict the minimum length required for the establishment of an asymptotic column in cascade type arc heaters.

Following Stine and Watson, it is assumed that the arc has a constant radius; it does not vary with either time or z, the axial distance. All of the simplifications and assumptions listed in Section 2 are in effect here. Thus, the equations for the constant radius AC arc are applicable (Section 4), except for the inclusion of axial transport terms. If, in the energy equation, the transport of heat in the z direction by conduction is neglected compared to that carried by convection, one obtains a soluble partial differential equation. Near $z = 0$ the solution will not be valid, but at a short distance down the column one can show that convection will definitely dominate conduction. This approach has been well verified experimentally, (10). If all variables have their previous definitions and

$$z^* = z\ (W_o \Theta) \quad ,$$

one obtains the following boundary value problem:

$$\frac{1}{x}\frac{\partial}{\partial x}\left(x\frac{\partial U}{\partial x}\right) - \rho^2\frac{\partial U}{\partial z} + \rho^2 E^2 U = \rho^2\frac{\partial U}{\partial \tau}$$

$$(0 \leq x \leq 1) \quad , \quad z > 0 \quad , \quad \tau > 0 \tag{21}$$

$$U_x\ (0, z, \tau) = 0 \quad , \quad U\ (1, z, \tau) = 0 \quad , \quad U\ (x, z, 0) = U_o J_o\ (\beta x)$$

$$U(x, 0, \tau) = 0 \quad , \quad 2\pi\rho^2 E \int_0^1 xU\ (x, z, \tau)\ dx = I(\tau) \quad .$$

Here, W_o is the flow velocity of the gas along the arc column and it is assumed to be constant. Clearly, this crude model of the arc cannot possibly satisfy all conservation equations, nor Maxwell's equations. Nevertheless, some of the salient features of the energy transfer processes should be delineated by this approach. The initial distribution that is assumed is unimportant, since only the steady state is of interest.

Assuming a solution to Eq. 21 of the form

$$U\ (x, z, \tau) = P\ (z, \tau) \cdot X(x) \quad ,$$

one obtains

$$\frac{1}{x}\frac{(xX')'}{X} = \frac{\rho^2}{P}\left(\frac{\partial P}{\partial z} + \frac{\partial P}{\partial \tau}\right) - \rho^2 E^2 = -\beta^2 \quad ,$$

where β^2 is a separation constant and $(\ )' = d/dx$. The above relation yields the following two equations:

$$\begin{aligned} &(xX')' + \beta^2 xX = 0 \\ &\rho^2\left(\frac{\partial P}{\partial z} + \frac{\partial P}{\partial \tau} - E^2 P\right) + \beta^2 P = 0 \quad . \end{aligned} \tag{22}$$

The details of the solution of the separated equation are presented in Appendix B, but, briefly, the procedure is to use the Laplace transform on the $P(z, \tau)$ equation and to investigate the result for large time, i. e., when all effects of the initial condition have died out. The resulting equation is:

$$U(x, z, \tau) = \frac{I_m J_0(\beta x)}{2\sqrt{2}\,\pi\rho J_1(\beta)}\left\{\left[1 - \exp\left(\frac{-2\beta^2 z}{\rho^2}\right)\right]\left[1 + \cos\gamma\cos(2\omega\Theta\tau - \gamma)\right]\right\}^{1/2} \tag{23}$$

For large z the solution given above goes over to the constant radius asymptotic column solution that was discussed earlier. The details of Eq. 23 are not of much interest here, only the rate at which the fully developed column is approached. From Ohm's law

$$E(z, \tau) = \frac{\sqrt{2}\left|\frac{\beta}{\rho}\right| \cos(\omega\Theta\tau)}{\left[1 - \exp\left(\frac{-2\beta^2 z}{\rho^2}\right)\right]^{1/2} \sqrt{1 + \cos\gamma \cos(2\omega\Theta\tau - \gamma)}} \quad , \tag{24}$$

and one sees that the axial behavior of the field strength is contained in the term

$$\left[1 - \exp\left(\frac{-2\beta^2 z}{\rho^2}\right)\right]^{1/2} \quad .$$

An RMS value for the field strength could be obtained, but since magnitude is of no importance, write

$$\overline{E} = \left[1 - \exp\left(\frac{-2\beta^2 z}{\rho^2}\right)\right]^{-1/2} \quad , \tag{25}$$

where $\overline{E}$ is defined so as to include the scale factor for $E(z, \tau)$. From Eq. 30 one finds that $\overline{E}$ is within 7% of its ultimate value when $(2\beta^2/\rho^2)z = 2$.

A dimensionless total column voltage drop can be obtained from

$$\overline{V} = \int_0^z \overline{E}(\alpha)\, d\alpha \quad ,$$

which, when integrated, yields

$$\overline{V} = \frac{\rho^2}{2\beta^2} \ln \left\{ \frac{1 + \left[1 - \exp\left(\frac{-2\beta^2 z}{\rho^2} \right) \right]^{1/2}}{1 - \left[1 - \exp\left(\frac{-2\beta^2 z}{\rho^2} \right) \right]^{1/2}} \right\} .$$

This function is also shown in Fig. 30 where a linear behavior for the voltage drop is seen to begin at about $(2\beta^2/\rho^2)\, z = 2$. Thus, when the design parameters of the cascade arc satisfy the relation

$$\left(\frac{2\beta^2}{\rho^2} \right) z \geq 2 \quad ,$$

one can expect that an asymptotic column will prevail. This criterion can be expressed in terms of dimensional variables as

$$z^* \geq \frac{\rho^2}{\beta^2} \frac{\dot{w}}{\left(\frac{\overline{\kappa}}{C_p} \right)} \quad \text{cm} \quad ,$$

where the total mass flow, $\dot{w}$, is introduced because it is directly measurable. The most unfavorable value of ρ in the above criterion is clearly unity so that in terms of tube diameters one can write

$$\frac{z^*}{2R} \geq 0.055 \frac{\left(\frac{\dot{w}}{2R} \right)}{\left(\frac{\overline{\kappa}}{C_p} \right)} \quad .$$

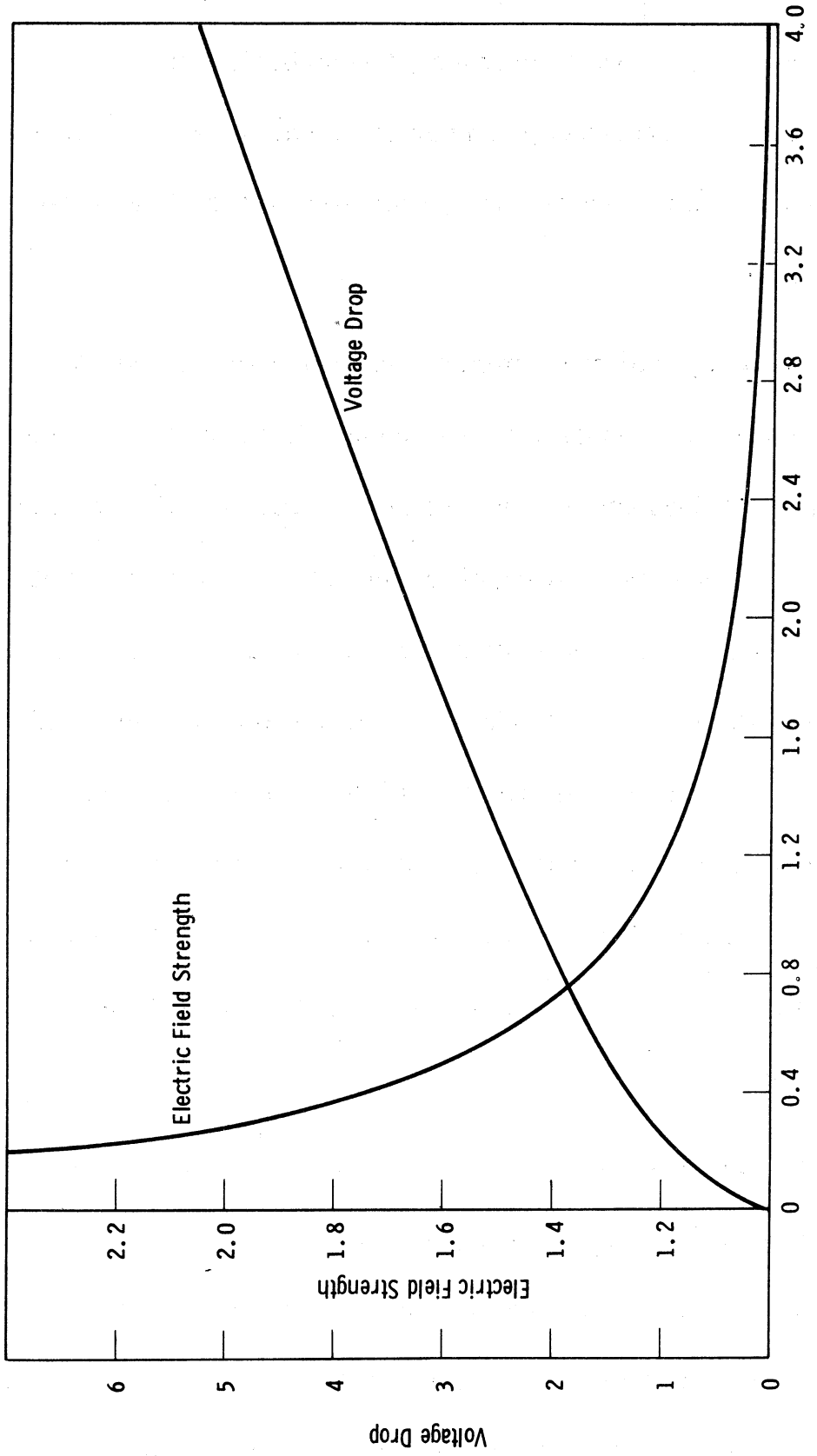

Figure 30. Axial Variation of Electric Field Strength and Voltage Drop Derived from the Approximate Model of the Tube Arc

The maximum value of $(C_p/\overline{\kappa})$ for high temperature nitrogen at 1 atm. is about 10^3 cm-sec/gm. Thus, to insure the establishment of an asymptotic column in a reasonable number of tube diameters, the flow rate of nitrogen should be such that the parameter $\dot{w}/R$ is of the order of 10^{-2} gm/cm-sec.

Guided by this approximate criterion, one can design a cascade arc heater which is long enough to insure the development of an asymptotic column and yet does not tax the voltage capabilities of the available power supply. A schematic drawing of the unit which was finally built is shown in Fig. 31a. It is easily disassembled so that the hole size of the cascade tube can be quickly changed. Uncooled carbon electrodes are used to ease the voltage requirements of the complete arc and to encourage smooth burning. Electrode erosion is slight in view of the fact that they are provided with no cooling. A photograph of the assembled unit is shown in Fig. 31b. Size can be judged by knowing that the device is about 8 in. long.

One of the requirements of the present cascade unit is that the electrodes not influence the behavior of the positive column. Toward this end, the working gas is injected with a slight tangential component at a central position in the tube. The flow divides, with the major portion going toward the hollow electrode. Some (unknown) fraction passes

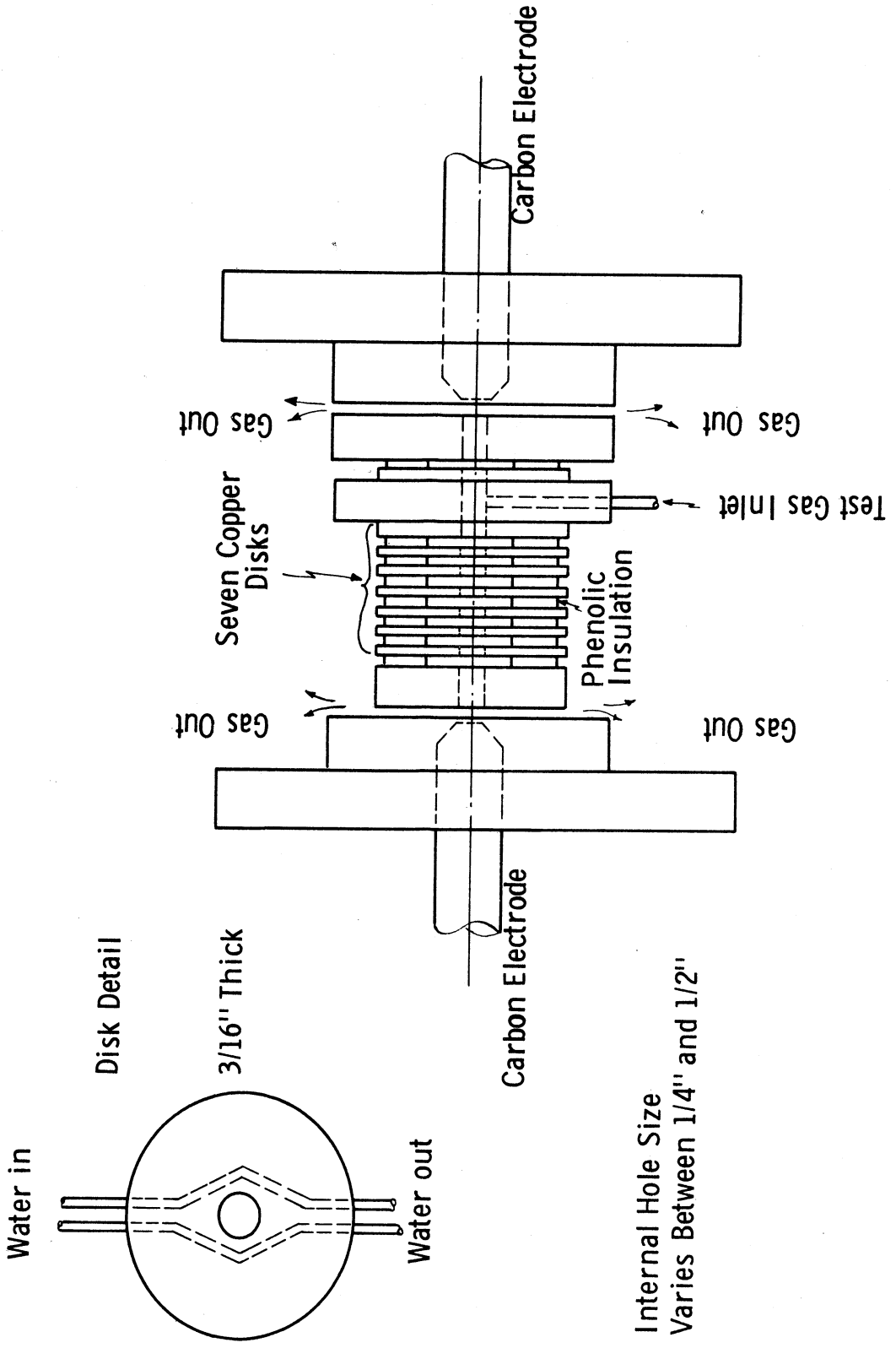

Figure 31a. Schematic Drawing of the Alternating Current Cascade Arc

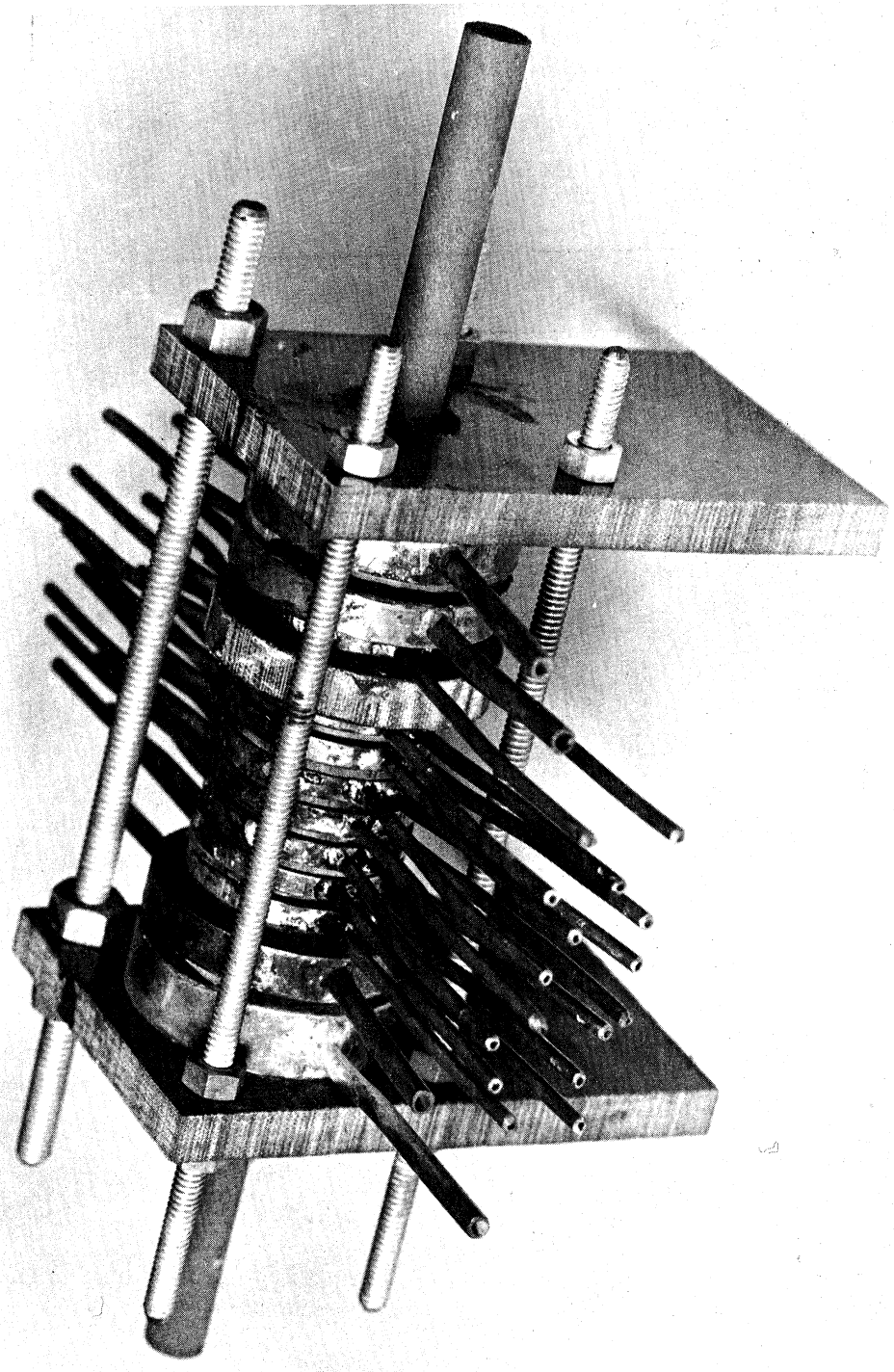

Figure 31b. Photograph of the AC Cascade Arc Unit

through the longer portion of the cascade, where the measurements are made, through the transition section, past the electrode, and exits radially. This flow arrangement is designed to prevent any electrode material from entering the column portion of the arc, thereby changing its chemical composition. There is a threshold flow rate that must be established to achieve this condition since the cathode jet from the momentarily negative electrode can penetrate a substantial distance into the opposing flow. The attainment of this critical flow level can be determined by monitoring the column voltage waveform on an oscilloscope. A marked asymmetry appears when there is a cathode jet injection of carbon into the column since even a small amount of low ionization potential contaminant (about 11 volts for carbon) can profoundly influence the electrical conductivity and hence the arc voltage.

Spectrograms of argon and nitrogen arcs appear in Fig. 32a; the absence of carbon lines attests to the purity of the plasma column. In the nitrogen arc CN bands would be quite intense, even for a small amount of carbon. A particularly strong one would occur at 3883 $\mathring{A}$, but only the 3918 $\mathring{A}$, N_2^+ band appears in this region, indicating the purity of the arc gas. It should also be noticed that the absence of copper lines in both spectra indicates that the cooling of the cascade disks is sufficient to prevent erosion of the exposed surfaces. If

Scale in millimeters. See Fig. 32(b) for conversion to wavelength

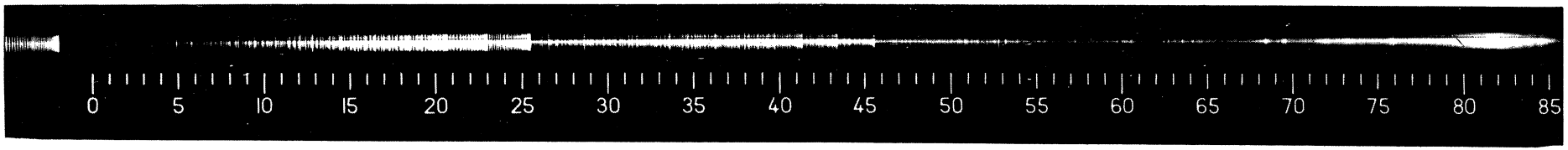

Nitrogen arc spectrum (Argon Reference above and below)

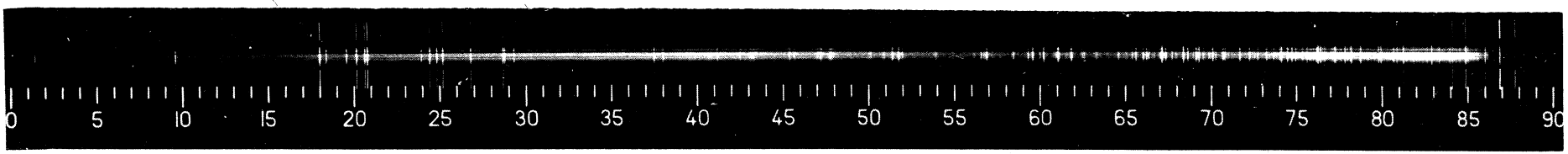

Argon Arc spectrum (Argon Reference above and below)

Figure 32a. Time Resolved Spectra of Nitrogen and Argon Arc Columns

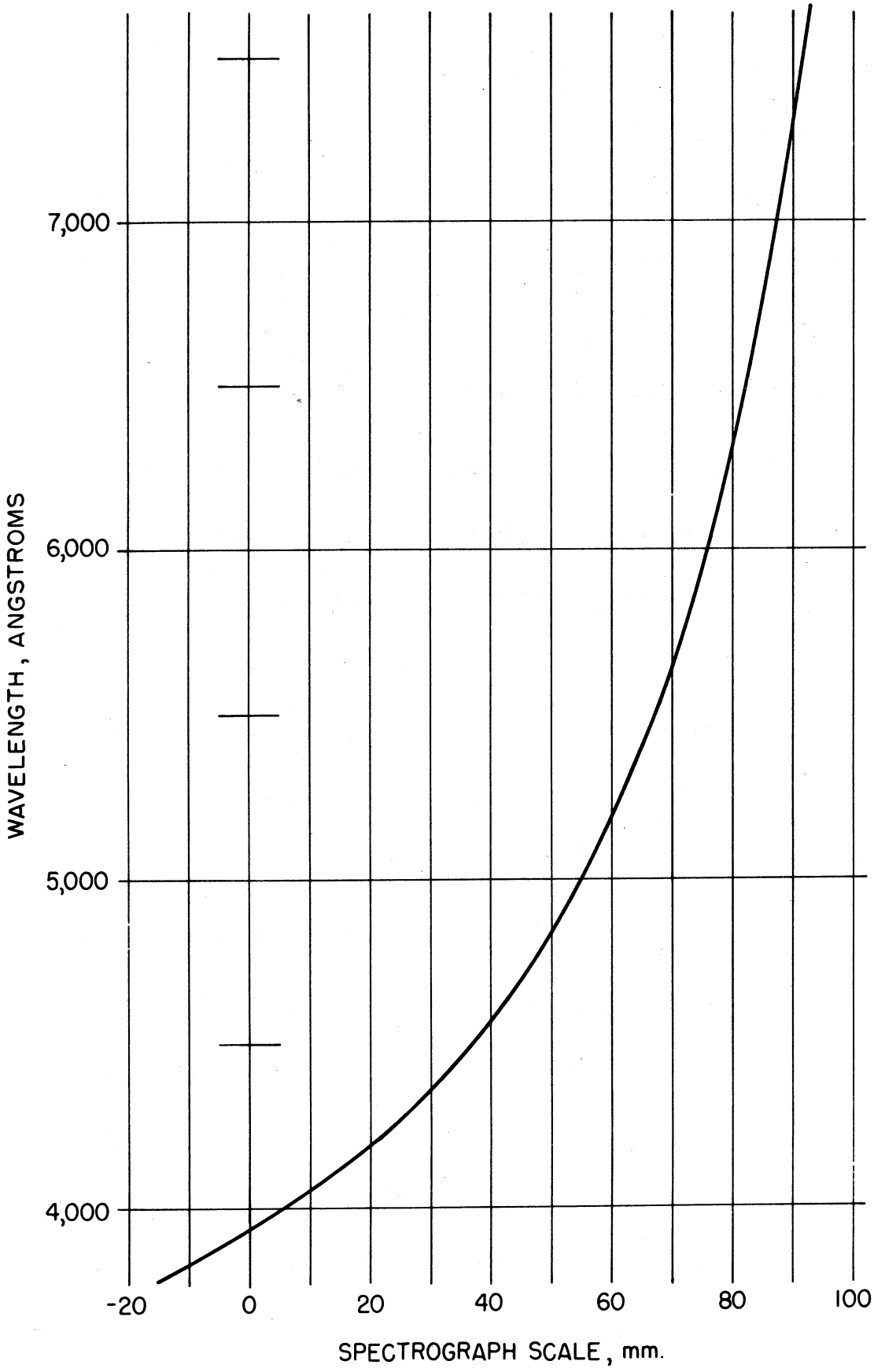

Figure 32b. Wavelength Conversion Scale for Spectra of Figure 32a

copper contamination were present the most dominant lines would occur at 5106 Å and at 5153 Å The spectra were taken through a window in the cascade that was formed by replacing a micarta insulating washer with a .030 in. slice of thin wall Vycor tubing. The glass section held up quite well in spite of the high temperature environment and remained free from discoloration throughout the experimental program.

Other, more qualitative tests were conducted to show that the electrodes have no effect on the positive column. Besides the carbon-carbon electrode pair, which was normally used, a series of other combinations were tried. Carbon-tungsten, carbon-copper, tungsten-tungsten, tungsten-copper, and copper-copper electrode combinations all showed essentially the same behavior; no discernible changes in the column voltage waveform could be detected.

In order to show the existence of an asymptotic column in the device of Figs. 31a and b, two tests were performed. The first involves the measurement of the pressure drop along the left (working) section of the cascade. Each disk was provided with a pressure tap, the line from which was led to a single pole, 6 throw Scanivalve pressure switch. The single outlet from the switch was connected to an inclined manometer that could detect pressure differences of 0.02 in. H_2O. Since one expects a Poiseuille flow to be established in the asymptotic column

portion of the arc, a linear pressure drop indicates the attainment of this condition. Some typical results of the pressure surveys are shown in Fig. 33 for both argon and nitrogen arcs with different total flow rates and constrictor diameters. These results indicate that Poiseuille flow is attained at about disk number 3 which, for the hole sizes used, represents an entry length of about 2 diameters. For the current level that prevailed for these tests, $\rho^2 \cong 0.5$ and $(C_p/\overline{\kappa})$ for nitrogen is of the order of 10^3 cm-sec/gm. The total mass flow was about 2×10^{-1} gm/sec. so the asymptotic column criterion developed above indicates

$$\left(\frac{z^*}{2R}\right) \geq 5.5 \quad .$$

Not all of the measured mass flow, however, passes through the working section of the cascade. If this fact is taken into account, it is seen that the analytical prediction of the location of the fully developed column is at least approximately correct, which is all that was initially anticipated.

Finally, as Fig. 30 indicates, the voltage of an asymptotic column should vary linearly with arc length. By using a vacuum tube voltmeter (with an input impedance of about 10 megohms), it is possible to obtain an RMS measurement of the voltage variation along the column, referred to, say, the first or last disk. A summary of several such measurements

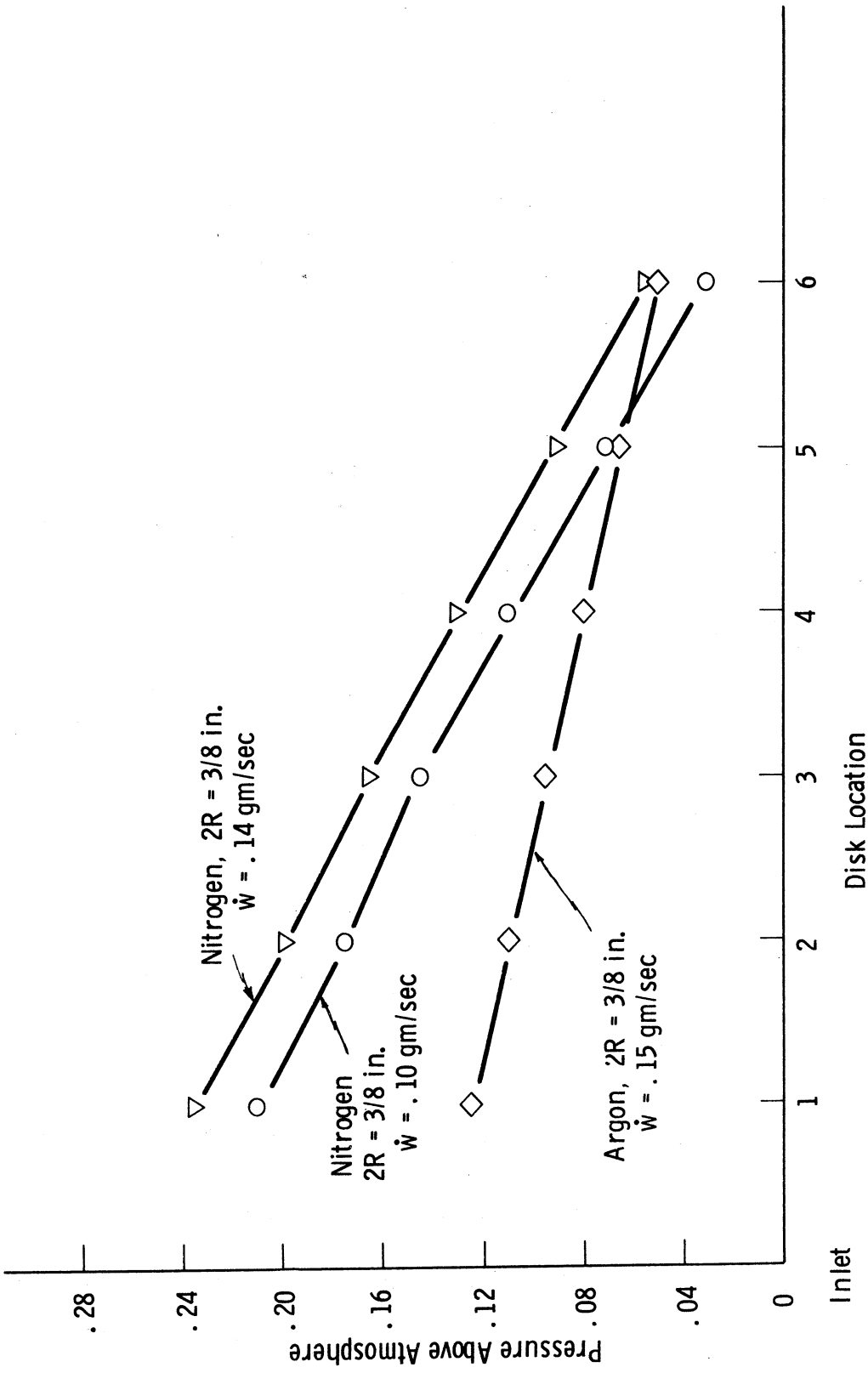

Figure 33. Axial Pressure Surveys from the Cascade Arc Unit

is shown in Fig. 34 where it is seen that, except for the first disk, a straight line can be drawn through the data points. Thus, one concludes that the establishment of an asymptotic column requires between one and two tube diameters, certainly no more than three. It is interesting to examine the behavior with axial distance of the column waveform for a typical cascade operating condition. Such a survey taken in a nitrogen arc is shown in Fig. 35. Going from top to bottom, one can see the evolution of the waveform as the column is sampled at a progressively greater distance from the gas inlet. Finally, the smooth waveform shown in the last trace is obtained; this is typical of the results to be described shortly.

A word or two is certainly in order about the flow regime (laminar or turbulent) in which the cascade operates. The average Reynolds number in the arc column is of the order of 15 to 20 as computed by the best available transport and thermodynamic properties. While this low Reynolds number would ordinarily prompt one to assume that laminar flow exists, such a conclusion might be unwarranted. The stability of plasma flows wherein electric fields exist is not at all understood and furthermore, near the cold tube wall, the Reynolds number will be much higher than the average value since the viscosity is very low. Experimentally, only an aural diagnostic was used to determine

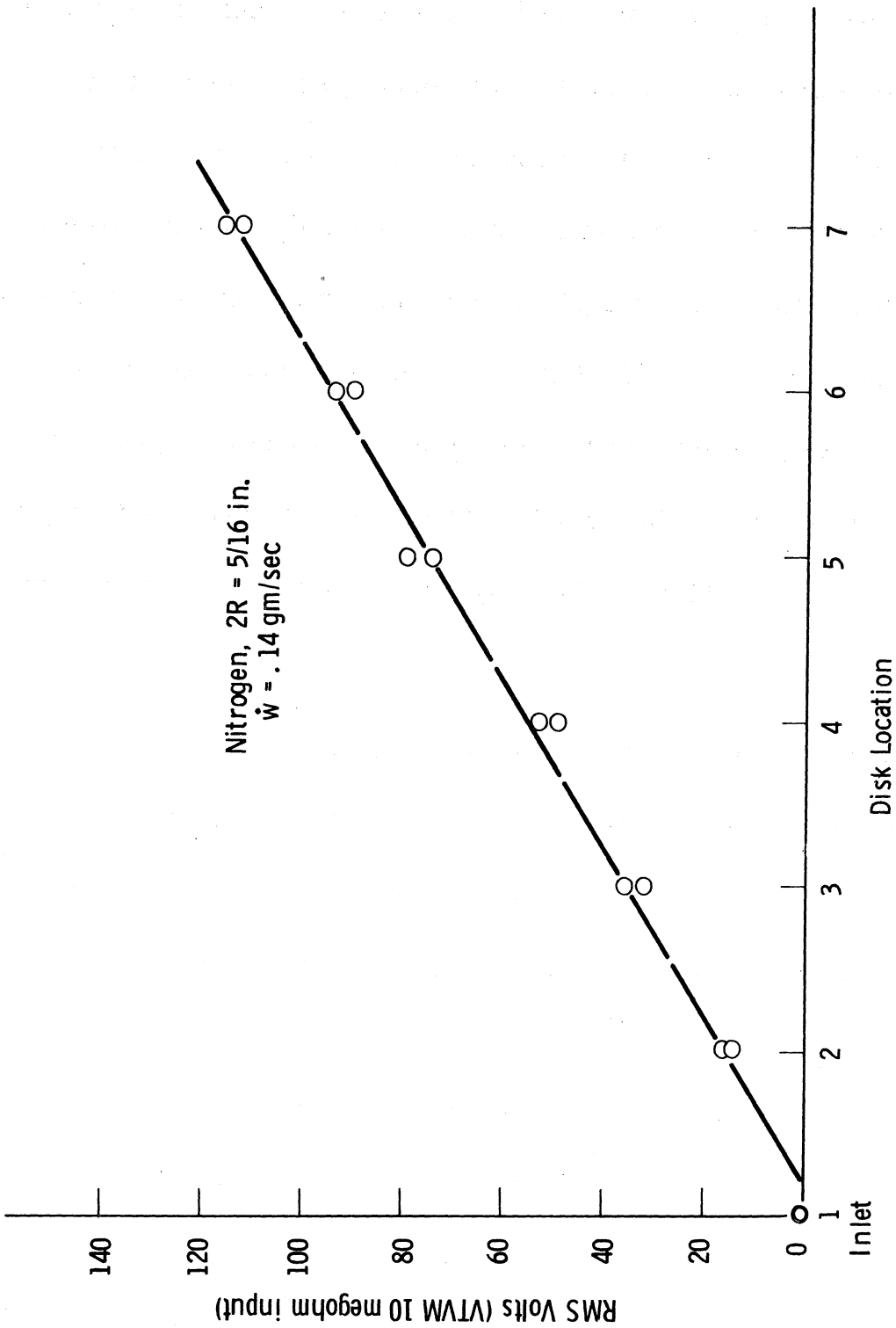

Figure 34. Root-Mean-Squared Arc Voltage Drop Survey from the Cascade Arc Unit

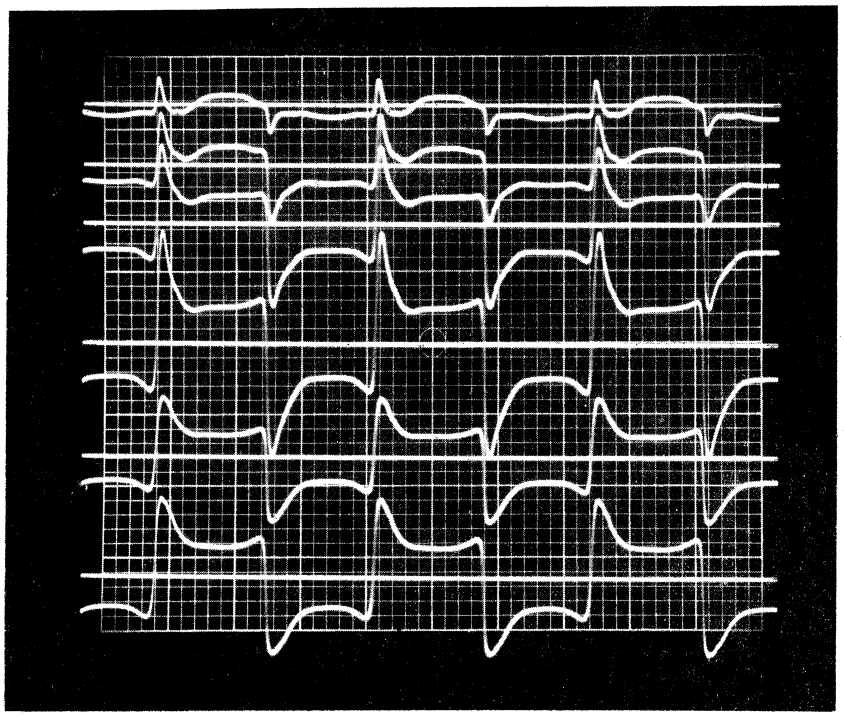

Conditions :
P = 1 ATM, Nitrogen, $\dot{w}$ = .14 gm/sec
2R = 3/8 in. , $I_{rms} \cong$ 22 amps

Sensitivities :
Traces 1-4, 100 volts/cm
Traces 5 and 6, 200 volts/cm

Figure 35. A Survey of Voltage Waveforms Along the AC Arc Column in Nitrogen

whether or not laminar flow (probably) existed. That is, there is a range of flow rates for which the arc operation sounds smooth. Depending upon the gas being used, there is a critical flow rate that, when exceeded, causes the arc to burn with a rough sound. Whether this is due to the onset of turbulence or to some separation phenomenon has not been determined, but smooth, reproducible results can be obtained only when the cascade is operated below this threshold flow rate.

It has also been noted that the voltage waveform of the arc column is quite sensitive to this onset of apparent turbulence, and abruptly changes shape at that point. There is likewise a minimum flow rate that can be tolerated, but this is due to a different phenomenon than the high flow limit. Unless the test gas is introduced into the cascade in excess of some minimum rate, room air can enter the tube and markedly influence the column behavior. This is especially true when argon is the test gas. Since there is nothing in the theory that was developed earlier that could account for turbulent phenomena, one would not expect good agreement with experiment unless laminar flow existed in the cascade tube. In the absence of evidence to the contrary, it was assumed that laminar flow was present.

6.2 Experimental Results

The broad purpose of the experimental program was to obtain measurements that characterized the behavior of the arc column and that could easily be compared with the analytical results of Section 5. Because of the limited capabilities of the AC power supply, the only parameter that could be significantly varied was the dimensionless frequency, $\omega\Theta$. Only 60 cps power was available, however, so parametric changes were effected by varying either the tube radius, R, or, by using different gases, the effective thermal diffusivity, λ. All data were taken from atmospheric pressure arcs that used either argon or nitrogen as the working gas. The primary diagnostic tool was the oscilloscope by which means the electric field and arc current waveforms were obtained. The power supply was a three phase variable transformer (Powerstat), which was capable of supplying about 30 amps, single phase, at 565 volts. The circuit current was limited chiefly by an inductor that provided 15 ohms impedance at 60 cps. For a specific gas, only the constrictor tube radius was varied. The range of variation was from a 1/4 in. to a 1/2 in. diameter, except in the case of nitrogen where an arc could not be sustained in the 1/4 in. tube. Even with a diameter of 5/16 in., the nitrogen arc could barely be sustained, due to its relatively high operating voltage.

Because of its favorable experimental properties, the most conclusive results were obtained in argon and these are presented first. Oscillograms of arc voltage and arc current for tube diameters of 1/4 in., 3/8 in., and 1/2 in., are presented in Figs. 36, 37, and 38, respectively. In all of these cases the current is nearly a perfect sine wave so, in that sense, comparison with the theoretical results should be feasible. Some amount of discretion is necessary in choosing values of S_1, B, and λ in order to interpret the arc data in terms of the dimensionless waveforms in Section 5. The DC solution can be used to guess at a range of values for which linear approximations to the σ - S and F - S curves should be chosen. The data in Section 1 indicate that reasonable values for argon are: B = 1.5 mhos/watt, S_1 = 5 watts/cm, and, since the tube wall is very cold, $S_2 \cong 0$. A linear fit to the F - S curve is somewhat arbitrary, but a selection should be weighted by the average value of heat flux potential that will probably exist in the column. Since the circular frequency corresponding to 60 cps is 377 rad/sec, a particularly simple expression for $\omega\Theta$ results if the reasonable value of 37.7 cm^2/sec is chosen for the thermal diffusivity. Thus, $\omega\Theta = 10\ R^2$, where R is in centimeters.

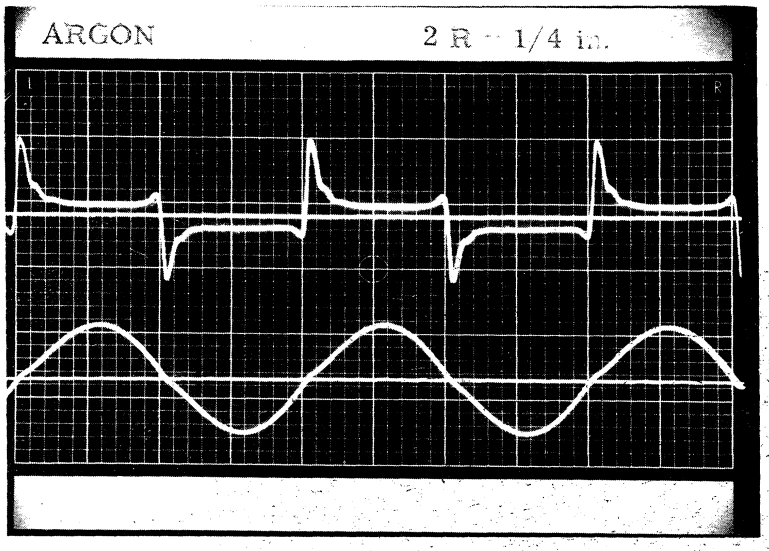

P = 1 ATM, Argon

2R = 1/4 in.

$\omega\Theta \cong 1$

Upper Trace: Arc Voltage
Sensitivity: 50 volts/cm

Lower Trace: Arc Current
Sensitivity: 50 amps/cm

Voltage sampled over ~1.2 cm of arc column

Figure 36. Experimental Voltage and Current Waveforms for an Argon Arc in a 1/4 in. Tube

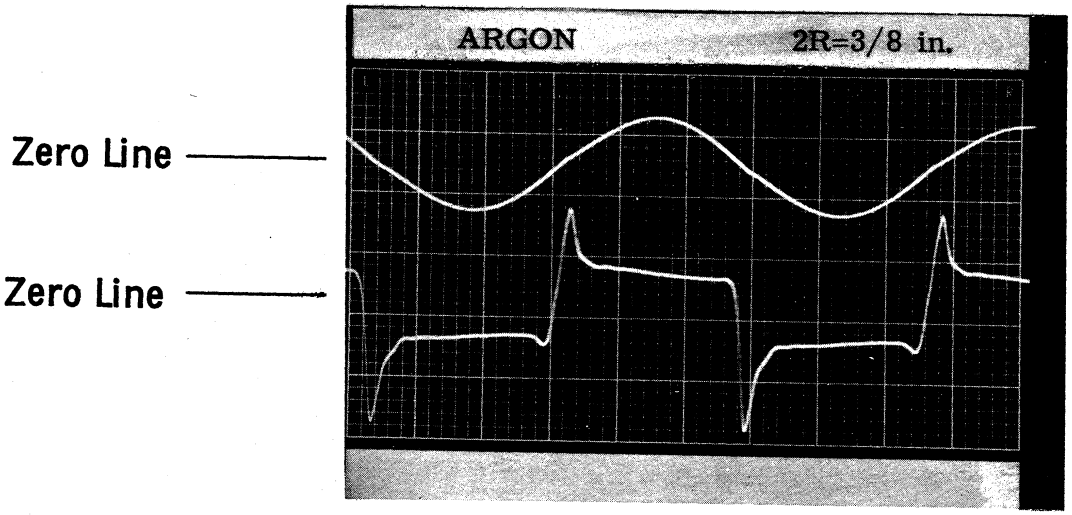

Figure 37. Experimental Voltage and Current Waveforms for an Argon Arc in a 3/8 in. Tube

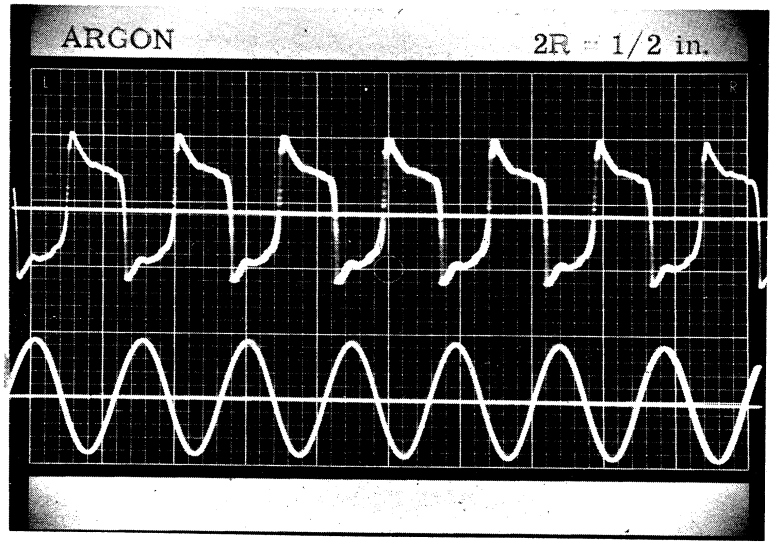

P = 1 ATM, Argon

2R = 1/2 in.
$\omega\Theta \cong 4$
Upper Trace : Arc Voltage
Sensitivity : 5 volts/cm

Lower Trace : Arc Current
Sensitivity : 50 amps/cm

Voltage sampled over~1.2 cm of arc column

Figure 38. Experimental Voltage and Current Waveforms for an Argon Arc in a 1/2 in. Tube

For the 1/4 in. diameter tube R = .3175 cm and $\omega\Theta \cong 1$. For Figs. 37 and 38 the above expression gives $\omega\Theta = 2.25$ and 4, respectively. The waveforms for the 1/2 in. and 1/4 in. tubes should be compared with Figs. 21 and 24 of Section 5. The resemblance as to waveform shape is clear. Theoretical data for the intermediate size were not presented earlier, but a voltage waveform for the case $\omega\Theta = 2.0$ is shown in Fig. 39. The comparison is not as favorable as in the other cases, but the theory nonetheless predicts the trend of the arc dynamic behavior. All of the argon waveforms exhibit slight non-uniformities and asymmetries. It required much effort, however, to obtain data as clean as that shown above and, in view of the complex phenomena occurring in the arc column, they are considered to be good waveforms.

There are several points to consider when comparing the experimental and theoretical results. All the theoretical curves were obtained for a dimensionless current level corresponding to $\rho_{dc} = 0.8$. For the same dimensional current, the three tube diameters that were used correspond fo a conducting zone radius that varies between 0.81 and 0.89. For a fixed value of $\omega\Theta$, a lower dimensionless current causes the arc to behave (in a nonlinear manner) as if it had a lower dimensionless frequency. The magnitude of this effect, however, is not great for high initial values of ρ, such as those that occur here. Also,

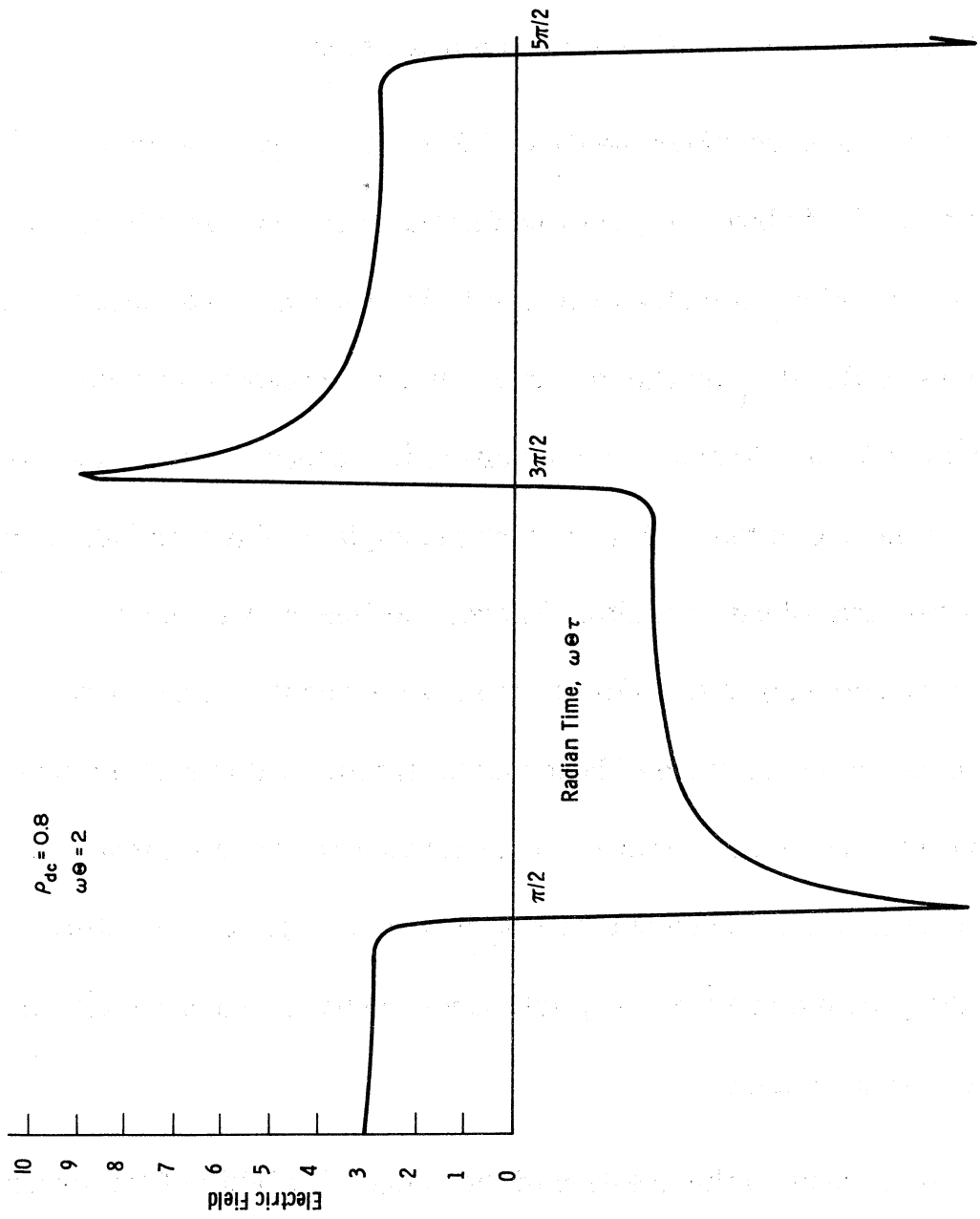

Figure 39. Theoretical Waveforms of Electric Field Strength and Dimensionless Current for $\omega\Theta = 2$

upon examining the transport property plots of Section 1, it is clear that argon, over the appropriate range of heat flux potential, shows a wide variation in possible choices of B. A poorly chosen value of B directly affects the dimensional voltage magnitude.

For example, consider the data of Fig. 36. Here, one finds a reignition peak of about 45 v/cm (the distance between cascade disks is about 1.2 cm) and a plateau value of 5.5 volts/cm. The theory, using the values of B and S_1 indicated above, yields corresponding voltage gradients of 55.5 volts/cm and 7.6 volts/cm, respectively. It is possible that the use of the "filling factor" principle of Maecker (24) could yield better quantitative results. There, the linear fit to the σ - S curve is selected so as to duplicate the area under the actual curve, up to some maximum value of heat flux potential. This principle was developed for DC arcs, however, and only an approximate form of it could be used here. Since only trends in arc behavior are of interest here, the problem of accurate quantitative prediction must be left for a more advanced study.

Finally, there is the question of the range of validity of the linear approximation to the σ - S curve. A glance at the actual variation in electrical conductivity shows that at some (high) value of heat flux potential the slope becomes rather small. This change in slope is

reflected in the E - I characteristic of the DC tube arc as a minimum in the arc voltage. That is, the increase in electrical conductivity with current, which initially is rapid, eventually falls off, so that the field strength begins to increase with current. Results of this type can be found in (23). The point at which the voltage reaches a minimum depends upon the type of gas and the tube radius in which the arc burns. Small tube radii and small values of S_1 move this point to the left in the dimensionless E - I plane. For argon, S_1 is rather small so that, for the 1/4 in. tube, this effect could appear. A further refinement of the theory presented herein could involve approximating the σ - S curve with three straight line segments, or even a power law behavior.

For nitrogen, the situation is more complicated. Voltage waveforms for a nitrogen arc burning in 5/16 in. and 1/2 in. tubes are shown in Figs. 40 and 41, respectively. Their behavior seems to be much smoother, but, of course, their overall voltage level is much higher than for the argon arc. Thus, small irregularities would not appear. The distorted current waveform indicates that the arc constitutes a large part of the circuit impedance. Hence, the results of Section 5 are not directly applicable. However, the entire circuit can be included in the theory so that the reciprocal effect of the arc can be studied. Before presenting results of this type it should be noted

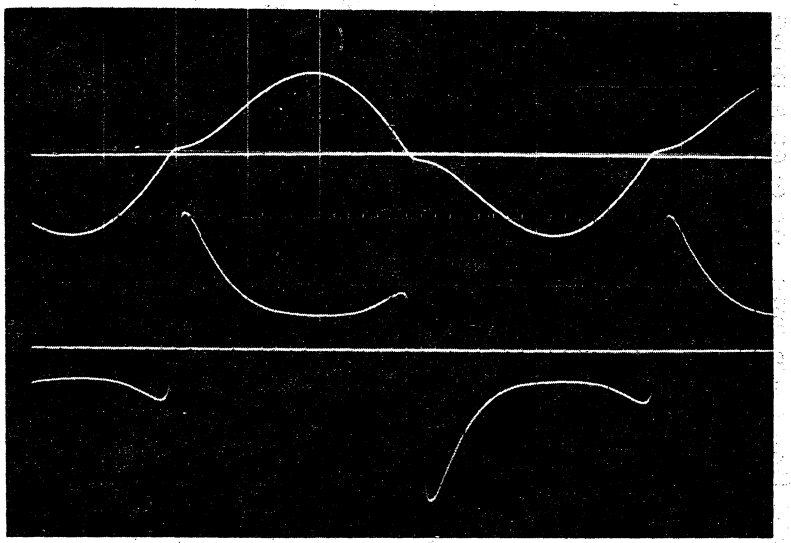

P = 1 ATM, Nitrogen

2R = 5/16 in.
$\omega\Theta \cong 0.5$
Upper Trace : Arc Current
Sensitivity : 28 amps/cm

Lower Trace : Arc Voltage
Sensitivity : 50 volts/cm

Voltage sampled over~1.2 cm of arc column

Figure 40. Experimental Voltage and Current Waveforms for a Nitrogen Arc in a 5/16 in. Tube

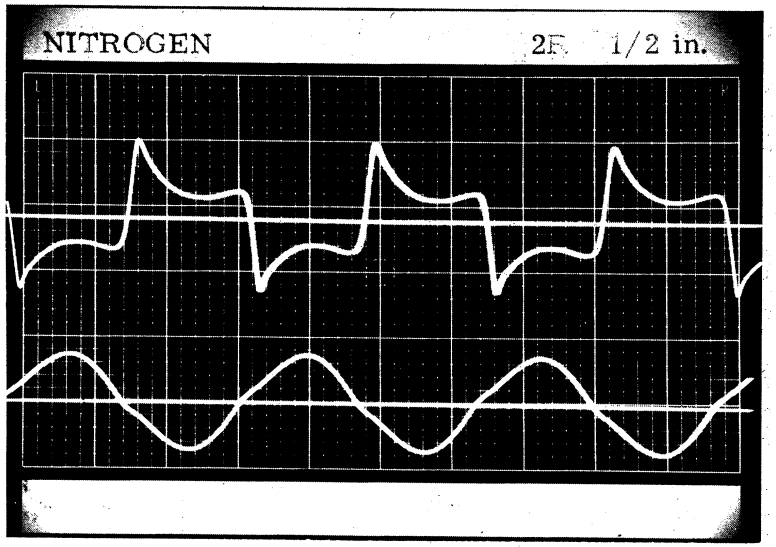

P = 1 ATM, Nitrogen

2R = 1/2 in.
$\omega\Theta \cong 1.25$
Upper Trace : Arc Voltage
Sensitivity : 50 volts/ cm

Lower Trace : Arc Current
Sensitivity : 50 amps/ cm

Voltage sampled over ~1.2 cm of arc column

Figure 41. Experimental Voltage and Current Waveforms for a Nitrogen Arc in a 1/2 in. Tube

from the data that a two and one half-fold change in $\omega\Theta$ does not perceptibly change the character of the voltage waveform. This is understandable when one considers the probable values of $\omega\Theta$ that apply to these situations. From Fig. 4, one obtains $\lambda = 75$ cm^2/sec, indicating a dimensionless frequency of about 0. 5. For the larger diameter this value increases to only 1. 25, still a very low $\omega\Theta$. At the same time, the dimensionless current decreases significantly so the net effect is to keep the voltage waveform looking the same as in the 5/16 in. tube.

Notice that the reignition spike is not as sharp as for the argon arc. This results from the reciprocal effect of the arc on the current waveform. This is evident in Fig. 40 where it is seen that, following current zero passage, the current waveform departs markedly from a sine curve. The high voltage spike has limited the current, which, in turn, limits the height of the reignition peak. The current level subsequently remains low, thereby keeping the voltage high and spreading out the reignition peak over a large portion of the half-cycle. The arc column equations have been solved, in conjunction with the circuit equation given in Section 5, for a set of conditions where the arc has a noticeable effect on the current waveform. The resulting current and voltage waveforms are shown in Fig. 42; the similarity to the experimental data is obvious.

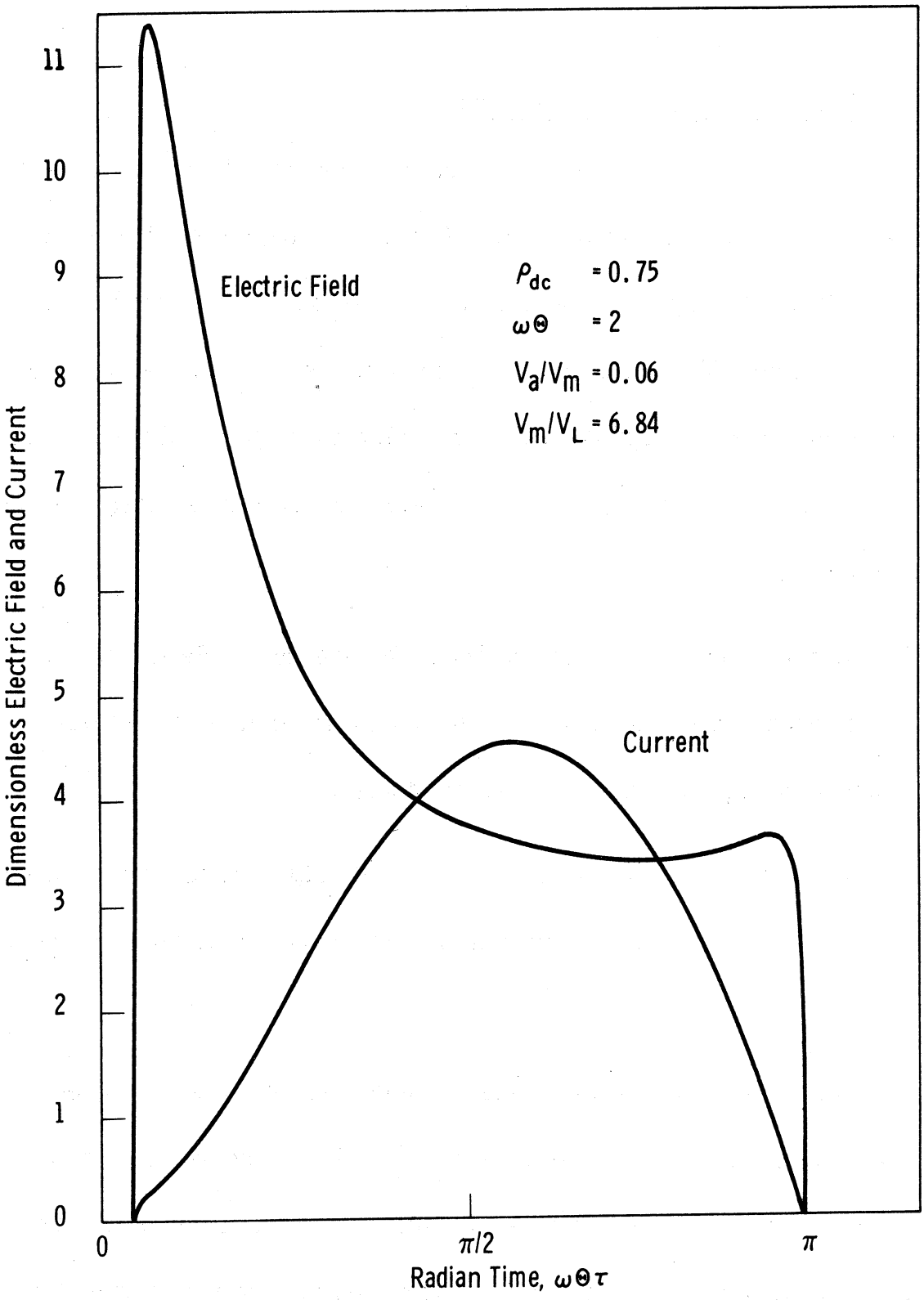

Figure 42. Theoretical Waveforms of Electric Field Strength and Dimensionless Current Including the Effects of an External Circuit

6.3 Suggestions for Future Research

Improvements can be made in both the theoretical and experimental areas of the work reported herein. If a wider range of conditions can be attained, the experimental findings can be made more conclusive and inclusive. This would involve designing a system for bathing the electrodes in an inert gas. Then, the column test gas could be oxidizing or corrosive. Presently, the use of, say, oxygen rapidly destroys the electrodes.

An improved cascade device should be pressurizable and capable of operation in a sub-atmospheric vessel so that column conditions under various pressure levels can be studied.

A power supply with higher current and voltage capabilities should be used, as well as, or in addition to, one that has a variable frequency output.

In a more advanced experimental study, arc parameters other than voltage and current should be monitored. These would include time resolved spectroscopic measurements of emitted radiation, arc power input, and cyclogram area. With the aid of spectroscopy, the actual structure of the column, as well as its temporal variation, can

be studied. Measurement of the cyclogram area (dynamic voltage-current characteristic) could, it appears, lead to a means of inferring the thermal diffusivity of the arc gas, since the included area is a strong function of $\omega\Theta$.

The area of theoretical investigation of AC arc characteristics is by no means closed. There is room for both quantitative and qualitative improvement of the theory of the dynamic arc, even without the added complication of an external circuit. As mentioned earlier, an improved approximation to the σ - S curve should be devised, perhaps with a three-segment polygonal fit. This would still permit the governing equations to be universalized, whereas a non-linear approximation would require that the problem be solved anew for each gas. It may be useful, however, to study the behavior of one particular gas in some detail. For this purpose one would use the best possible approximation, however nonlinear, to its transport and thermodynamic properties, so that accurate quantitative data could be obtained.

The effect of radiative transfer on the column properties should be included in the energy conservation equation so that a wider range of pressures and arc currents can be studied. This would be of special importance if the results were to be used in arc heater design.

Ultimately, one would like to include the effects of an external circuit, and, in so doing, study the stability of the arc-circuit combination. This, too, will be of great interest to the arc heater designer, as will be the effects of mass flow on the column properties.

Finally, when it becomes necessary, the effects of relaxation phenomena will have to be accounted for. It may be that the dynamic arc will provide a means for investigating chemical reaction rates, but, at this point, this is pure conjecture.

7. CONCLUSIONS

It has been possible to simplify the conservation equations that describe the behavior of the alternating current arc column so that only two dimensionless parameters need be specified to obtain a solution. The equations can be solved once and for all for a suitable range of these parameters, and, in this sense, are universal and independent of any type of gas.

The solutions to these equations, while complicated, have the advantage over older theories, (11) and (12), that they can be directly related to measureable or calculable quantities that characterize a particular gas and current level. This relation occurs through the two parameters $\omega\Theta$, and I_m, which determine the arc dynamic behavior and power level, respectively.

Under certain special circumstances, the equations for the dynamic arc can be solved in closed form. This is possible for a high frequency AC arc, $\omega\Theta \geq 10$, and for a DC arc subjected to a step function increase in current.

Based upon experimental findings from a Maecker-like AC cascade arc, it is concluded that the trend in arc behavior with $\omega\Theta$ can be

successfully predicted by the theory mentioned above. From this, one infers that AC arc theory can be treated as a sophisticated heat conduction problem, and that all its salient features can be discovered by such a description.

APPENDIX A

TRANSFORMATION OF THE ARC EQUATIONS TO A FIXED DOMAIN

After one introduces the simplifications and assumptions described in Section 2, the energy equation assumes the form

$$\frac{1}{r}\frac{\partial}{\partial r}\left(r\frac{\partial S}{\partial r}\right) + BE^2 (S - S_1) = \frac{1}{\lambda}\frac{\partial S}{\partial t} \quad , \quad 0 \leq r \leq r_o(t) \quad , \quad t > 0$$

$$\frac{1}{r}\frac{\partial}{\partial r}\left(r\frac{\partial S}{\partial r}\right) = \frac{1}{\lambda}\frac{\partial S}{\partial t} \quad , \quad r_o(t) \leq r \leq R \quad , \quad t > 0$$

$$S_r(0,t) = 0 \quad , \quad S(r_o^-, t) = S_1$$

$$S(r_o^+, t) = S_1 \quad , \quad S(R,t) = S_2$$

$$S_r(r_o^-, t) = S_r(r_o^+, t) \quad .$$

Furthermore,

$$2\pi BE^* \int_0^{r_o(t)} r\,(S - S_1)\,dr = I^*(t) \quad .$$

With the equations in this form, it is difficult to see what role the moving boundary, $r_o(t)$, will play. The problem can be transformed into a fixed domain by non-dimensionalizing the spatial variable with respect to the free boundary. For the region $0 \leq r \leq r_o(t)$, introduce the new variable

$$x = r/r_o(t) \quad .$$

Now, x and t are the new independent variables and derivatives are formed in the following manner:

$$\frac{\partial}{\partial r} = \left(\frac{\partial x}{\partial r}\right)\frac{\partial}{\partial x} \quad , \qquad \frac{\partial}{\partial t} = \left(\frac{\partial x}{\partial t}\right)\frac{\partial}{\partial x} + \frac{\partial}{\partial t} \quad .$$

But

$$\frac{\partial x}{\partial r} = \frac{1}{r_o} \quad \text{and} \quad \frac{\partial x}{\partial t} = -\frac{r}{r_o^2}\left(\frac{dr_o}{dt}\right) \quad ,$$

so

$$\frac{\partial}{\partial r} = \frac{1}{r_o}\frac{\partial}{\partial x} \quad \text{and} \quad \frac{\partial}{\partial t} = \frac{\partial}{\partial t} - \frac{x}{r_o}\left(\frac{dr_o}{dt}\right)\frac{\partial}{\partial x} \quad .$$

In addition,

$$\frac{\partial^2}{\partial r^2} = \frac{1}{r_o^2}\frac{\partial^2}{\partial x^2} \quad .$$

After introducing the dimensionless variables and parameters

$$U(x,t) = \frac{(S - S_1)}{(S_1 - S_2)} \quad , \qquad \rho(t) = \frac{r_o(t)}{R} \quad ,$$

$$E = (B^{1/2} R)\, E^* \quad , \qquad I = \frac{I^*}{B^{1/2} R(S_1 - S_2)} \quad , \qquad \Theta = \frac{R^2}{\lambda} \quad , \qquad \tau = \frac{t}{\Theta} \quad ,$$

it is a straightforward matter to obtain

$$\frac{1}{x}\frac{\partial}{\partial x}\left(x\frac{\partial U}{\partial x}\right) + \frac{1}{2}\frac{dp^2}{d\tau}\left(x\frac{\partial U}{\partial x}\right) + \rho^2 E^2 U = \rho^2\frac{\partial U}{\partial \tau} \quad ,$$

valid in the domain $0 \leq x \leq 1$, $\tau > 0$. The boundary conditions become

$$U_x(0,\tau) = 0 \quad , \quad U(1,\tau) = 0 \quad .$$

In the annular, non-conducting region a different transformation must be introduced to eliminate the free boundary. Here, define

$$y = \frac{R - r}{R - r_o(t)} \quad .$$

The derivatives must again be formed with care since y is a function of both r and t. Here,

$$\frac{\partial y}{\partial r} = -\frac{1}{R - r_o} \quad , \quad \frac{\partial y}{\partial t} = \frac{R - r}{(R - r_o)^2}\left(\frac{dr_o}{dt}\right) \quad ,$$

so

$$\frac{\partial}{\partial r} = -\frac{1}{(R - r_o)}\frac{\partial}{\partial y} \quad , \quad \frac{\partial}{\partial t} = \frac{\partial}{\partial t} + \frac{y}{(R - r_o)}\left(\frac{dr_o}{dt}\right)\frac{\partial}{\partial y} \quad ,$$

and

$$\frac{\partial^2}{\partial r^2} = \frac{1}{(R - r_o)^2}\frac{\partial^2}{\partial y^2} \quad .$$

Again, straightforward manipulation gives

$$\frac{\partial^2 V}{\partial y^2} - \frac{1}{[(1-\rho)^{-1} - y]} \frac{\partial V}{\partial y} - \frac{1}{2} \frac{1-\rho}{\rho} \frac{d\rho^2}{d\tau} \left(y \frac{\partial V}{\partial y} \right) = (1-\rho)^2 \frac{\partial V}{\partial \tau} \quad ,$$

valid for $0 \leq y \leq 1$, $\tau > 0$. Here, $V(y, \tau) = (S_1 - S)/(S_1 - S_2)$, $V(0, \tau) = 1$, and $V(1, \tau) = 0$. The continuity of slope condition, which fixes the boundary position, transforms to

$$U_x(1, \tau) = - \frac{\rho}{1-\rho} V_y(1, \tau) \quad .$$

Finally, Ohm's law becomes

$$2\pi\rho^2 E \int_0^1 xU(x, \tau)\, dx = I(\tau) \quad ,$$

thereby completing the boundary value problem posed in Section 2.

APPENDIX B

THE APPROACH TO THE ASYMPTOTIC COLUMN

In order to estimate what the length of the cascade arc heater must be to insure the development of an asymptotic column, the following boundary value problem was developed:

$$\frac{1}{x}\frac{\partial}{\partial x}\left(x\frac{\partial U}{\partial x}\right) - \rho^2\frac{\partial U}{\partial z} + \rho^2 E^2 U = \rho^2\frac{\partial U}{\partial \tau} \quad ,$$

$$0 \leq x \leq 1 \quad , \quad z > 0 \quad , \quad \tau > 0$$

$$U_x(0, z, \tau) = 0 \quad , \quad U(1, z, \tau) = 0 \quad , \quad U(x, z, 0) = U_o J_o(\beta x)$$

$$U(x, 0, \tau) = 0 \quad , \quad 2\pi\rho^2 E\int_0^1 xU(x, z, \tau)\,dx = I(\tau) \quad .$$

All symbols were defined in the text. As a first step, separation of variables may be applied by assuming a solution of the form

$$U(x, z, \tau) = P(z, \tau)\cdot X(x) \quad .$$

By this method, one obtains two equations

$$\left.\begin{aligned} (xX')' + \beta^2 xX &= 0 \\ \rho^2\left(\frac{\partial P}{\partial z} + \frac{\partial P}{\partial \tau} - E^2 P\right) + \beta^2 P &= 0 \end{aligned}\right\} \qquad \text{(B-1)}$$

where β is a separation constant. The first of these equations is Bessel's differential equation, having the solution

$$X = J_o(\beta x) \quad .$$

Since $U(1, z, \tau) = 0$, $J_o(\beta) = 0$, with $\beta = \beta_1, \beta_2, \ldots \beta_n$, where the β_n are the zeros of the Bessel function. Only the first root is of interest here because the initial distribution is proportional to the first eigen-function.

In order to solve the equation for $P(z, \tau)$, first find from Ohm's law

$$PE^2 = \frac{\beta^2 I^2}{4\pi^2 \rho^4 J_1^2(\beta) \cdot P(z, \tau)} \quad ,$$

since

$$\int_0^1 x J_o(\beta x)\, dx = \frac{1}{\beta} J_1(\beta) \quad .$$

Then, selecting P^2 as the dependent variable, one obtains

$$\frac{\partial P^2}{\partial z} + \frac{\partial P^2}{\partial \tau} + \frac{2\beta^2}{\rho^2} P^2 = \frac{\beta^2 I^2}{2\pi^2 \rho^4 J_1^2(\beta)} \quad . \tag{B-2}$$

The method of the Laplace transform can now be applied to Eq. B-2. If

$$\mathcal{L}\left\{P^2(z, \tau)\right\} = \int_0^\infty e^{-s\tau} \cdot P^2(z, \tau)\, d\tau = y(z, s) \quad ,$$

one can obtain the ordinary differential equation

$$\frac{dy}{dz} + \left(\frac{2\beta^2}{\rho^2} + s\right) y = F(s) + P_o^2 \quad , \tag{B-3}$$

where

$$P_o^2 = P^2(z, 0) \quad \text{and} \quad f(s) = \mathcal{L}\left[\frac{\beta^2 I^2}{2\pi^2 \rho^4 J_1^2(\beta)}\right]$$

With the help of an integrating factor, Eq. B-3 can be solved to yield

$$y(z, s) = \frac{f(s) + P_o^2}{\left(\frac{2\beta^2}{\rho^2} + s\right)} \left\{1 - \exp\left[-\left(\frac{2\beta^2}{\rho^2} + s\right) z\right]\right\} \quad . \tag{B-4}$$

The solution, y (z, s), can be easily inverted with the aid of the convolution integral and a table of Laplace transform pairs. One obtains

$$P^2(z, \tau) = \int_0^\tau f(\alpha) \exp\left[\frac{-2\beta^2}{\rho^2}(\tau - \alpha)\right] d\alpha$$

$$- \exp\left(-\frac{2\beta^2 z}{\rho^2}\right) \int_0^\tau f(\alpha - z) \exp\left[\frac{-2\beta^2}{\rho^2}(\tau - \alpha)\right] d\alpha \tag{B-5}$$

$$+ P_o^2 \exp\left(\frac{-2\beta^2 \tau}{\rho^2}\right)\left[1 - \exp\left(\frac{-2\beta^2 z}{\rho^2}\right) H_z(\tau)\right] \quad ,$$

where $H_z(\tau) = 1$ when $\tau > z$ and vanishes for $\tau < z$. Also, $f(\alpha - z) = 0$ for $\alpha < z$. Notice, that for large τ, the term involving the initial value, P_o^2, will tend to zero, and, since only a periodic, quasi-steady solution is of interest, the effect of the initial distribution will not be important. Furthermore, $\tau \gg z$ so, if one assumes,

$$I(\tau) = I_m \cos(\omega\Theta\tau) \quad ,$$

the complete solution to the original boundary value problem can be written as

$$U(x, z, \tau) = \frac{I_m J_o(\beta x)}{2\sqrt{2}\pi\rho J_1(\beta)} \left\{ \left[1 - \exp\left(\frac{-2\beta^2 z}{\rho_2} \right) \right] \left[1 + \cos\gamma \cos(2\omega\Theta\tau - \gamma) \right] \right\}^{1/2} .$$

REFERENCES

1. Finkelnburg, W., and Maecker, H., "Elektrische Bögen und thermisches Plasma," Handbuch der Physik, 22, Springer-Verlag, 1956.

2. Loh, Otto, "Eine Theorie des Wechselstrom-kreises mit Lichtbogen," Archiv für Elektrotechnik, 44, 4, 203-233, 1959.

3. John, R. R., and Bade, W. L., "Recent Advances in Electric Arc Plasma Generation Technology," ARS Journal, 31, 1, 4-17, 1961.

4. Phillips, R. L., "Fundamental Considerations in the Design of an AC Arc Heater," ARL 64-9, Aerospace Research Laboratories, Wright-Patterson AFB, Ohio, Jan., 1964.

5. Phillips, R. L., et al, "Three-Phase AC Arc Heater," ARL 64-29, Aerospace Research Laboratories, Wright-Patterson AFB, Ohio, Feb., 1964.

6. Uhlenbusch, J., "Zur Theorie und Berechnung stationärer und quasistationärer zylindrischer Lichtbogen," Dissertation, Rhein.-Westf. Technische Hochschule, Aachen, 1962.

7. Skifstad, J. G., "Investigation of Energy Transfer in a Tube Arc Heater," Ph. D. Thesis, Purdue University, 1963.

8. John, R. R., et al, "Energy Addition and Loss Mechanisms in the Thermal Arc Jet Engine," AIAA Reprint 63-022, 1963.

9. Stine, H. A., and Watson, V. R., "The Theoretical Enthalpy Distribution of Air in Steady Flow Along the Axis of a Direct Current Arc," NASA Technical Note D-1331, Aug., 1962.

10. Cann, G. L., et al, "Basic Performance Limits of Coaxial Arc Gas Heaters," Research Rept. RR-18, Electro-Optical Systems, Inc., Pasadena, Calif., Nov., 1963.

11. Cassie, A. M., "Arc Rupture and Circuit Severity: A New Theory," Conference Internationale des Grands Réseaux Electriques à Haute Tension, (Paris, France), pp. 1-14, 1932.

12. Mayr, O., "Beiträge zur Theorie des statischen und des dynamischen Lichtbogens" Archiv für Elektrotechnik, 37, 12, 588-608, 1943.

REFERENCES (cont.)

13. Bishop, D. O., "A Method of Determining the Dynamic Characteristics of Electric Arcs," Proc. Inst. Electr. Eng., 101, 6, 18-26, 1954.

14. Nöske, H., "Zum Stabilitätsproblem beim Abschalten kleiner induktiver Ströme mit Hochspannungsschaltern," Archiv fur Electrotechnik, 43, 2, 114-133, 1957.

15. Edels, H., and Ettinger, Y., "Arc Interruption and Thermal Reignition," Proc. Inst. Electr. Eng., 109A, 2, 89-98, 1962.

16. Hirschfelder, J. O., Curtiss, C. F., and Bird, R. B., Molecular Theory of Gases and Liquids, John Wiley and Sons, Inc., 1954.

17. Cann, G. L., "Energy Transfer Processes in a Partially Ionized Gas," Memorandum No. 61, Guggenheim Aero. Lab., Calif. Inst. of Tech., June 15, 1961.

18. Wu, C. S., "On the Energy Equation in Magnetogasdynamics," Technical Report No. 32-2, Jet Propulsion Lab., Calif. Inst. of Tech., Jan. 7, 1960.

19. Peters, Th., "Characteristics of Cylindrical Arcs at High Temperatures," AGARD Report 325, Advisory Group for Aeronautical Res. and Dev., Paris, Sept., 1959.

20. Penner, S. S., Introduction to the Study of Chemical Reactions in Flow Systems, AGARDograph No. 7, Butterworths Scientific Publications, London, 1955.

21. Hilsenrath, J., and Klein, M., "Tables of Thermodynamic Properties of Nitrogen in Chemical Equilibrium Including Second Virial Corrections from 2000°K to 15,000°K," Tech. Doc. Rept. No. AEDC-TDR-63-162, Arnold Eng. Dev. Ctr., Tullahoma, Tenn., March, 1964.

22. Wray, K. L., "Chemical Kinetics of High Temperature Air," Research Report 104, Avco-Everett Research Lab., Everett, Mass., June, 1961.

REFERENCES (cont.)

23. Schmitz, G., Patt, H. J., and Uhlenbusch, J., "Eigenschaften und Parameterabhängigkeit der Temperaturverteilung und der Charakteristik eines zylindersymmetrischen Stickstoffbogens," Zeitschrift für Physik, 173, 552-567, 1963.

24. Maecker, H., "Messung und Auswertung von Bogencharakteristiken (Ar, N_2)," Zeitschrift für Physik, 158, 392-404, 1960.

25. Schmitz, G., "Zur Theorie der wandstabilisieren Bogensaule," zeit. Naturforschung, 5a, 571, 1950.

26. John, R. R., et al, "Theoretical and Experimental Investigation of Arc Plasma-Generation Technology," Part II, Vol. 2, Tech. Doc. Report No. ASD TDR-62-729, Air Force Materials Lab., Aeronautical Systems Div., Wright Patterson AFB, Ohio, Jan., 1963.

27. Marlotte, G. L., Electro-Optical Systems, Inc., Pasadena, Calif., Private communication.

28. Drellishak, K. S., Aeschliman, D. P., and Cambel, A. B., "Tables of Thermodynamic Properties of Argon, Nitrogen, and Oxygen Plasmas," Tech. Doc. Rept. No. AEDC-TDR-64-12, Arnold Engineering Dev. Ctr., Tullahoma, Tenn., Jan., 1964.

29. Wienecke, R., "Über das Verhalten abgeschalteter Lichtbögen hoher Stromstärke," Zeit. für Physik, 143, 118, 1955.

30. Frind, G., "Uber das Abklingen von Lichtbögen," Zeit. für angew. Physik, 12, 5, 231-237, 1960.

31. Yoon, K. H., and Spindle, H. E., "A Study of the Dynamic Response of Arcs in Various Gases," Trans. Am. Inst. Elect. Engrs., 77, 2, 1634-1640, 1959.

32. Carslaw, H. S., and Jaeger, J. C., Conduction of Heat in Solids, 2nd ed., Oxford, 1959.

33. Slater, L. J., Confluent Hypergeometric Functions, Cambridge, 1960.

34. Miller, J. C. P., "Note on the General Solution of the Confluent Hypergeometric Equation," Math. Tables and Aids to Comp., 58, 97-99, 1957.

REFERENCES (cont.)

35. von Engel, A., and Steenbeck, M., Elektrische Gasentladungen, ihre Physik und Technik, Julius Springer, Berlin, 1932.

36. Weizel, W., and Rompe, R., Theorie elektrischer Lichtbogen and Funken, J. A. Barth, Leipzig, 1949.

37. Frie, W., "Über den Wechselstromwiderstand eines elektrischen Bogens," Zeit. für angew. Physik, 13, 2, 99-102, 1961.

38. Forsythe, G. E., and Wasow, W. R., Finite-Difference Methods for Partial Differential Equations, John Wiley and Sons, New York, 1960.

39. Fox, L., Numerical Solution of Ordinary and Partial Differential Equations, Addison-Wesley Publishing Co., Reading, Mass., 1962.

40. MacKay, D. M., and Fisher, M. E., Analogue Computing at Ultra-High Speed, Chapman and Hall, Ltd., London, 1962.

41. Howe, R. M., "Solution of Partial Differential Equations," Class Notes, Dept. Aero and Astro Eng., Univ. of Michigan, 1961.

42. Albrecht, R. F., "Approximation to the Solution of Partial Differential-Equations by the Solutions of Ordinary Differential-Equations," Numerische Mathematik, 2, 245-262, 1960.

43. Salvadori, M. G., and Baron, M. L., Numerical Methods in Engineering, 2nd ed., Prentice-Hall, Inc., Englewood Cliffs, New Jersey, 1961.

44. Stout, M. B., Analysis of AC Circuits, Ulrich's Book Store, Ann Arbor, Mich., 1952.

45. Bowen, S. W., et al, "Theoretical and Experimental Investigation of Microwave Scattering from a Cylindrical Plasma," ARL 63-159, Aerospace Research Labs., Wright Patterson AFB, Ohio, Sept. 1963.

46. Olsen, H. N., "Thermal and Electrical Properties of an Argon Plasma," Physics of Fluids, 2, 6, 614, 1959.

47. Shkarofsky, I. P., Bachynski, M. P., and Johnston, T. W., "Collision Frequency Associated with High Temperature Air and Scattering Cross-Sections of the Constituents," Research Rept. No. 7-801, 5, RCA Victor, Ltd., Montreal, 1959.